THE UNIVERSITY
of EDINBURGH

Regeneration of Dopaminergic Neurons and Other Neuronal Cell Types in Zebrafish

Lindsey J. Caldwell

Doctor of Philosophy

The University of Edinburgh

2018

Statement of Original Contribution

I declare that this thesis was composed by myself, that the work contained herein is my own except where explicitly stated otherwise in the text. The work contained in this thesis has not been submitted for any other degree or professional qualification, except as specified. Parts of this work appear in the open access preprint repository bioRxiv in the following entry:

Caldwell, L.J.*, Davies, N.O.* et al. 2018. Regeneration of dopaminergic neurons in adult zebrafish depends on immune system activation and differs for distinct populations. *bioRxiv*, p.367151.

* Co-first authors

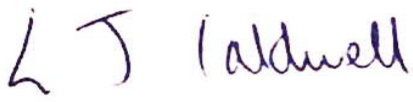

27th August 2018

Abstract

Unlike mammals, zebrafish have a remarkable capacity to regenerate the central nervous system. Following neuronal loss by physical injury or chemical ablation zebrafish are capable of replacing neurons through increased neurogenesis, resulting in functional recovery.

In the adult zebrafish brain, certain populations of dopaminergic and noradrenergic neurons, identified by immunohistochemistry for tyrosine hydroxylase (Th^+), are regenerated after ablation with 6-hydroxydopamine (6OHDA), an analogue of dopamine commonly used to specifically ablate these neurons. Here I ask where these newly formed Th^+ neurons originate and which signals are involved in their regeneration.

In the adult zebrafish new neurons are derived from progenitor cells, the soma of which form part of the ependyma and which have radial processes extending to the pial surface, termed ependymo-radial glial cells (ERGs). In this thesis I show that ERGs lining the diencephalic ventricle are a heterogeneous population in terms of expression of *her4*, *gfap*, and *olig2*. Using genetic lineage tracing and proliferation analysis I demonstrate that regenerated Th^+ neurons are derived from specific ERGs at the diencephalic ventricle.

In contrast to mammals, Th^+ neurons are constantly generated in the adult zebrafish brain. Here I show that injection of 6OHDA elicits an immune response, and that inhibiting this immune response with the artificial glucocorticoid dexamethasone attenuates proliferation of ERGs and neurogenesis of Th^+ neurons to control levels. Although stimulating an immune response increases proliferation of ERGs, an immune response is not sufficient to increase Th^+ neurogenesis. This demonstrates

that an immune response is necessary but not sufficient for the regeneration of Th^+ neurons in the adult zebrafish brain.

Following a spinal cord lesion, both larvae and adult zebrafish are capable of functional regeneration. Spinal cord regeneration has been shown to involve increased neurogenesis of motor neurons; however, the extent to which other neuronal populations are regenerated has not been fully elucidated. Here I show that glutamatergic neurons are regenerated after a spinal cord lesion in larvae, and GABAergic neurons are regenerated in both larvae and adults.

Taken together, these results provide new insights into the regeneration of the central nervous system in zebrafish. I identify populations of neurons which are regenerated, progenitor cells that give rise to regenerated neurons, and I demonstrate the pivotal role of the immune response in modulating regeneration. These results could ultimately inform future attempts to promote neuroregeneration in mammals.

Lay Summary

In adult mammals, including humans, new nerve cells (neurons) are very rarely produced in the brain and spinal cord. When neurons die, for example as a result of an injury or a neurodegenerative disease (e.g. Parkinson's disease), these cells are not replaced. This leads to lifelong debilitating conditions with little chance of improvement. In contrast, zebrafish are able to regenerate neurons in the brain and spinal cord even into adulthood.

Parkinson's disease is caused by the death of a specific type of neuron called dopaminergic neurons. In zebrafish, we can kill dopaminergic neurons by injecting a toxin into the brain. In some areas of the brain, these neurons are then replaced. In this thesis I show where these new neurons come from, identifying a specific type of cell in a particular area of the brain.

Injection of the toxin elicits a response from the immune system. Inhibiting this immune response reduces the number of new dopaminergic neurons formed. Unlike mammals, zebrafish are constantly producing new dopaminergic neurons, but stimulating an immune response did not increase the number of new dopaminergic neurons formed above the normal levels. This means that activation of the immune system is necessary for the replacement of dopaminergic neurons, but stimulating the immune system alone, without killing neurons, is not enough to increase the production of dopaminergic neurons in the brain. Hence, additional signals are needed for successful regeneration.

In mammals, spinal cord injury can lead to permanent paralysis. However, zebrafish are able to repair their spinal cord and regain normal swimming capacity. Repairing the spinal cord involves the replacement of neurons which have been lost; however, it is not known whether all the different types of neurons in the spinal cord can be

replaced. Here I show that two types of neurons (glutamatergic neurons and GABAergic neurons) are both replaced after a spinal cord lesion.

Taken together, these results provide new insights into the regeneration of the brain and spinal cord in zebrafish. I demonstrate the types of neurons which can be replaced, where new dopaminergic neurons come from in the brain, and the pivotal role of the immune system in the replacement of dopaminergic neurons. These results could ultimately inform future attempts to promote brain and spinal cord repair in mammals.

Acknowledgements

First and foremost I would like to thank my PhD supervisors Catherina and Thomas Becker for their help and guidance throughout my time in their group, and for the many scientific discussions.

I am grateful to the BBSRC for their funding through the Eastbio Doctoral Training Partnership. I am also appreciative of the many opportunities for personal and professional development, in particular my internship at the Association of the British Pharmaceutical Industry (ABPI), as well as all of the friends I have made through the programme.

I would like to acknowledge the past and present members of our research group who have contributed to the work presented in this thesis. The help and guidance from Nick Davies was invaluable in learning the techniques I have used throughout the thesis, including surgical procedures on adult zebrafish and histology. I am grateful to Leonardo Cavone for his assistance with drug administrations and quantitative RT-PCR, and for his support and guidance. I would like to thank Karolina Mysiak for working together with me on the investigation into LTC4 and *irf8*$^{-/-}$ fish. Thank you also to Silvère Santos and Joly Ghanawi for the excellent job they have done keeping the fish in the best condition possible.

Thank you to all of the members of the Becker group, past and present, who have helped to create a friendly and co-operative environment to work in during my time in Edinburgh. A special thanks goes to the three other PhD students, Hannah Smith, Tess M^{c}Cann, and Themis Tsarouchas, who I have shared this experience with over the past four years. Without you I am sure this PhD would have been a very different experience.

Last but not least I would like to thank my Mum, Dad, Hannah, Katrina, and Will for their constant support over the course of this PhD. I am forever grateful to you all.

Abbreviations

µL	Microlitre(s)
µM	Micromolar
µm	Micrometre(s)
4OHT	4-hydroxytamoxifen
6OHDA	6-hydroxydopamine
CNS	Central nervous system
Dex	Dexamethasone
DMSO	Dimethyl sulfoxide
dpf	Days post fertilisation
dpi	Days post injection
dpl	Days post lesion
EdU	Ethynyl-deoxyuridine
ERG	Ependymo-radial glial cell
GABA	γ-amino butyric acid
Gad	Glutamate decarboxylase
GFAP	Glial fibrillary acidic protein
GFP	Green fluorescent protein
Her4	Hairy-related 4
hpf	Hours post fertilisation
L	Litre(s)

LTC4	Leukotriene C4
M	Molar
mg	Milligram(s)
ml	Millilitre(s)
mM	Millimolar
MS222	aminobenzoic acid ethylmethylester
MPP^+	N-methyl-4-phenylpyridine
MPTP	1-methyl-1,2,3,6-tetrahydropyridine
Mtz	Metronidazole
NTR	Nitroreductase
Olig2	Oligodendrocyte transcription factor 2
Otp	orthopedia homeobox
PBS	Phosphate buffered saline
PBSTx	PBS containing Triton X-100
PFA	Paraformaldehyde
pink1	PTEN-induced putative kinase 1
PTEN	Phosphatase and tensin homolog
RFP	Red fluorescent protein
Th	Tyrosine hydroxylase
Vglut	Vesicular glutamate transporter
Zy	Zymosan

Table of Contents

Chapter One: General Introduction

1.1 The scope of the study

The mammalian central nervous system has a remarkably poor natural ability to repair and regenerate (Gage & Temple 2013). Through the investigation of successful regeneration in other species, such as zebrafish, we can gain insights into how neurons can be replaced in the adult brain and spinal cord (Kaslin et al. 2008; Zupanc 2009; Sîrbulescu & Zupanc 2011; Becker & Becker 2015).

In the adult zebrafish brain, certain populations of dopaminergic neurons, identified by immunohistochemistry for tyrosine hydroxylase (Th^+), are regenerated after ablation (Vijayanathan et al. 2017; Caldwell et al. 2018). In addition, both larval and adult zebrafish are capable of regeneration following a spinal cord lesion, and this involves the replacement of lost neurons through neurogenesis (Becker et al. 2004; Reimer et al. 2008; Ohnmacht et al. 2016).

In this thesis I investigate the source of newly generated Th^+ neurons in the adult zebrafish brain and the signalling mechanisms involved in their regeneration. I then investigate a number of different methods used to ablate dopaminergic neurons and evaluate their success in ablating Th^+ populations in the zebrafish brain. Lastly, I investigate the extent to which glutamatergic and GABAergic neurons in the spinal cord are regenerated following a spinal cord lesion.

In order to achieve this, in chapter 3 I investigate the origin of newly generated Th^+ neurons in the adult zebrafish brain. I describe the heterogeneity of cells lining the diencephalic ventricle and use genetic lineage tracing to show that new Th^+ neurons are derived from a subpopulation of these cells.

In chapter 4 I investigate the signalling pathways involved in the regeneration of Th^+ neurons. I show that the ablation of Th^+ neurons elicits an immune response. I then ask whether this immune response is necessary and/or sufficient for the successful regeneration of Th^+ neurons. Furthermore, I investigate the involvement of particular signalling molecules in the regeneration of Th^+ neurons, including leukotriene C4, tnf-α, and dopamine.

Thirdly, in chapter 5 I investigate three methods to ablate Th^+ neurons. I evaluate the extent of Th^+ cell loss in *pink1*$^{-/-}$ zebrafish compared to wildtype fish, in chemogenetic ablation of dopaminergic neurons, and in fish injected with MPTP and MPP^+.

Chapter 6 focusses on the regeneration of interneurons following a spinal cord lesion. I investigate whether glutamatergic and GABAergic neurons are replaced following a lesion in both larval and adult zebrafish by comparing the levels of neurogenesis in unlesioned fish to lesioned fish.

In summary, I demonstrate which populations of neurons are capable of being regenerated in the zebrafish central nervous system, which cells give rise to regenerated neurons, and the signalling pathways involved in their regeneration. These results could ultimately inform future attempts to promote neuroregeneration in mammals.

1.2 The regenerative capacity of the mammalian central nervous system

In mammals, the natural capacity for regeneration of the central nervous system (CNS) is relatively poor when compared to other vertebrates (Gage & Temple 2013). This means that neurons lost as a result of disease or damage to the CNS are not replaced, leading to lifelong impairments. In particular, in this thesis I will focus on dopaminergic neurons in the brain and glutamatergic and GABAergic neurons in the spinal cord.

The successful regeneration of these neurons in humans would revolutionise the treatment of diseases and injuries concerning the brain and spinal cord (Barker et al. 2018).

1.2.1 Cell replacement therapies improve functional recovery in Parkinson's disease and after spinal cord injury

Parkinson's disease is the second most common neurodegenerative disease, affecting an estimated 1% of the world's population over 60 years of age (de Lau & Breteler 2006). The disease is characterised by a selective loss of dopaminergic neurons in the substantia nigra, which are progressively lost and not replaced (Fearnley & Lees 1991; Cheng et al. 2010). This causes a dopamine deficiency in the basal ganglia, leading to debilitating motor and non-motor symptoms (Kalia & Lang 2015). The treatment options for Parkinson's disease are focussed on symptom management rather than disease modification. Current treatments are not effective in all patients and prolonged treatment leads to a loss of efficacy (Connolly & Lang 2014; Toda et al. 2016).

A number of pioneering cell replacement techniques have been trialled in patients with Parkinson's disease, as neuronal loss is largely limited to one neuronal subtype in one location (Barker et al. 2015). Developing midbrain dopaminergic neurons extracted from human foetal ventral midbrain can be transplanted into the brains of patients. These trials have delivered highly variable results, but significant improvements have been reported in patients at several different centres (Li et al. 2016; Kefalopoulou et al. 2014; Hauser et al. 1999). This demonstrates a proof of concept that replacing the lost dopaminergic neurons can provide long-lasting benefits to patients. However, the use of foetal tissue carries a number of technical and ethical limitations (Turner & Kearney 1993), not least because the demand for tissue far outweighs the supply.

Recent advances in protocols to differentiate human embryonic stem cells and induced pluripotent stem cells into midbrain dopaminergic neurons have provided a readily available, robust source of cells for transplantation (Steinbeck & Studer 2015). Transplantation of these cells into rodent and non-human primate models of Parkinson's disease demonstrated their ability to survive and innervate the correct target structures (Kriks et al. 2011; Grealish et al. 2014; Kikuchi et al. 2017). Importantly, the cells integrate into the existing neuronal circuitry (Grealish et al. 2015), and have been shown to improve the animal's performance in motor tasks, demonstrating functional recovery (Kriks et al. 2011; Steinbeck & Studer 2015). As a result, a number of clinical trials are currently ongoing and planned for the near future to determine whether the transplantation of these cells offers an efficacious and safe treatment for Parkinson's disease.

Despite the advancement in cell replacement therapies, there are limitations associated with the transplantation of cells into the brain. Human foetal neurons and human embryonic stem cells both have the disadvantage that they can lead to transplant rejection, and there are ethical concerns attached to the use of human embryonic tissue (Stoker et al. 2017; Turner & Kearney 1993). On the other hand, the variability in the response of each individual cell line to differentiation protocols means that each graft of patient-specific induced pluripotent stem cells would be subject to regulatory approval, resulting in a likely prohibitive financial hurdle for a large-scale treatment (Stoker et al. 2017). An alternative to these approaches is to use fibroblasts which have been directly reprogrammed to dopaminergic neuron-like cells, minimising the risk of the transplanted cells developing into tumours by avoiding the pluripotent stage (Marro et al. 2011, Parmer et al. 2018). Although this is a promising new approach, there is a lack of studies showing the long-term survival of these neurons and the extent to which they can re-innervate the striatum, and a risk that these

transplants could contain unwanted cell types (Parmer et al., 2018). Hence, there is significant interest in promoting the production of new dopaminergic cells from endogenous neural progenitor cells in the brain, thus harnessing the intrinsic neurogenic potential of the human brain for a possible treatment for Parkinson's disease (Lamm et al. 2014).

Spinal cord injuries can result in severe and lifelong disabilities, dramatically reducing quality of life. At present, treatment options are primarily physiotherapy, surgical procedures to stabilise the spinal cord, and the anti-inflammatory drug methylprednisolone (Silva et al. 2014; Baptiste & Fehlings 2007). However, these interventions offer limited hope for functional recovery (Silva et al. 2014; Baptiste & Fehlings 2007).

Spinal cord injuries cause neuronal death, and in the mammalian spinal cord these cells are not replaced, despite the presence of neural stem cells which can be propagated *in vitro* (Weiss et al. 1996; Shihabuddin et al. 1997; Meletis et al. 2008). Transplantation of stem cells into the injured rodent spinal cord has been shown to improve functional recovery (Hofstetter et al. 2005; Ogawa et al. 2002), partly due to the replacement of cells which have been lost as a result of the injury (Meletis et al. 2008; Ogawa et al. 2002). It is therefore of interest to investigate how endogenous stem cells might be used to replace neurons in order to develop new therapies for humans with spinal cord injuries.

1.3 Zebrafish as a model for successful regeneration of the CNS

Unlike mammals, zebrafish have a remarkable capacity for CNS regeneration (Reimer et al. 2008; Ogai et al. 2014; Ming & Song 2011; Goldshmit et al. 2012; Becker & Becker 2008; Becker & Becker 2015; Gemberling et al. 2013; Ghosh & Hui 2016). Neurons lost in the retina as a result of cytotoxic, mechanical, or light-induced

lesions can be regenerated, including all major retinal cell types (Goldman 2014). After a stab lesion to the telencephalon or injection of neurotoxic substances into the brain constitutive neurogenesis is significantly increased to replace the neurons which have been lost (Kroehne et al. 2011; Kyritsis et al. 2012; Skaggs et al. 2014; Bhattarai et al. 2017). Following a spinal cord injury motor neurons, pax2 expressing interneurons, V2 interneurons, and serotonergic interneurons are all replaced as a result of injury-induced neurogenesis (Reimer et al. 2008; Kuscha, Barreiro-Iglesias, et al. 2012; Kuscha, Frazer, et al. 2012; Hui et al. 2010). This ability to regenerate neurons in all regions of the CNS after a variety of different insults has inspired research into the mechanisms involved in the successful regeneration of the zebrafish CNS.

In addition to their capacity of CNS regeneration, zebrafish have become a commonly used model to study regeneration of the nervous system for a number of reasons. Firstly, zebrafish are vertebrates and therefore share more similarities with mammals than invertebrate model organisms with high regenerative capacity, such as planarians (Orii et al. 2005). The processes which regulate development of the nervous system are highly conserved among vertebrates (Lieschke & Currie 2007), and CNS regeneration in zebrafish has been shown to recapitulate some of the processes which occur during development (Becker & Becker 2015). Furthermore, the value of zebrafish as a tool for developing new therapeutic strategies for the human CNS has precedent. A chemical screen in zebrafish identified compounds which have subsequently been taken forward into clinical trials in patients with Dravet syndrome, a severe childhood epilepsy, and these trials have so far reported promising results (Griffin et al. 2017). Therefore investigations into the successful regeneration of the zebrafish CNS could provide insights which lead to new strategies for improving regeneration of the mammalian CNS.

Secondly, the zebrafish genome has been sequenced completely and published as a well-annotated reference genome. The genetic accessibility of zebrafish means that targeted mutagenesis techniques such as Tol2 mutagenesis and CRISPR/Cas9 can be employed to precisely manipulate particular genes. This can be used to investigate the role of particular genes in neuroregeneration by assessing the consequences of underexpression or overexpression of genes of interest (Simone et al. 2018; Auer & Del Bene 2014; Halpern et al. 2008; Hans et al. 2009; Kwan et al. 2007).

Furthermore, zebrafish lay clutches with up to several hundred offspring, increasing the sample size and improving the robustness of results in experiments using embryos and larvae. This has led to the development of medium throughput screening technologies, where hundreds of zebrafish can be imaged automatically within a few hours (Hao et al. 2010; Hong 2009; Pfriem et al. 2012; Spomer et al. 2012).

Moreover, there are a large number of fluorescent reporter lines available, and new transgenic reporter fish can be easily created. Developing zebrafish are translucent up to a few days post fertilisation, and their size means the entire brain or spinal cord can be observed in reasonable detail when placed under a microscope. This obviates the need for sectioning and thus makes developing zebrafish particularly amenable to live imaging (Higashijima et al. 2003; Feierstein et al. 2015). This is an invaluable tool in investigating the dynamic processes involved in regeneration of the CNS. Furthermore, the size of the adult brain renders it relatively accessible for live imaging, and this has already led to new insights into stem cells in the adult brain (Dray et al. 2015; Barbosa et al. 2015a).

1.4 Neurogenesis in the adult zebrafish CNS in comparison to the mammalian CNS

Regeneration of the CNS is a complex process involving clearance of dead and damaged cells, the replacement of neurons, and the regrowth of severed axons and re-innervation of their target structures, culminating in functional recovery (Zupanc 2009; Zupanc 2001; Becker & Becker 2015; Sofroniew 2018). In this thesis I focus on increased neurogenesis in the damaged CNS, a mechanism to replace neurons which have been ablated or lost as a result of injury.

The production of new neurons, neurogenesis, occurs in the intact adult CNS, albeit to a vastly different degree depending on the species (Kaslin et al. 2008; Grandel & Brand 2013; Gage & Temple 2013; Zupanc & Sîrbulescu 2011). It has been suggested that the success of CNS regeneration in a species correlates to the number of proliferative zones present in the CNS (Grandel et al. 2006). Progenitor cells in these zones proliferate to generate new cells, which can differentiate into neurons, migrate away from the proliferative zone, and integrate into the existing circuitry.

In the human CNS neurogenesis is believed to be confined to two regions of the brain: the subventricular zone (SVZ) of the lateral ventricles in the telencephalon and the subgranular zone (SGZ) of the dentate gyrus in the hippocampus (Eriksson et al. 1998; Bergmann et al. 2015). However, even the production of new neurons in these two areas remains controversial due to the limitations of working with human subjects (Sorrells et al. 2018; Lee et al 2018).

Although the existence and extent of adult neurogenesis in humans is still a matter of debate, there is a substantial amount of literature identifying new neurons in other mammals (Ming and Song 2011; Bergmann et al. 2015). In rodents, neurogenesis has been detected in the SVZ, SGZ, and the olfactory bulb in adulthood (Altman &

Das 1965; Altman 1969; Bergmann et al. 2015). Newly generated cells in the SVZ migrate along the rostral migratory stream to the olfactory bulb where they contribute to the constant turnover of interneurons in the olfactory bulb (Merkle et al. 2007). The majority of neuroblasts in the SVZ do not mature into differentiated neurons, and only a small percentage integrate into the circuitry of the olfactory bulb (Biebl et al. 2000; Winner et al. 2002). Newly generated cells in the SGZ migrate the relatively short distance to the granular cell of the dentate gyrus, where they integrate into the existing circuitry and show functional electrophysiological properties (Cameron et al. 1993; Seri et al. 2001; Seri et al. 2004; van Praag et al. 2002).

Analysis of the proliferative zones in the adult zebrafish brain identified 16 distinct zones with constitutive proliferation, and these domains were located along the entire rostral-caudal axis, including in the telencephalon, preoptic region, thalamus, hypothalamus, midbrain and cerebellum (Grandel et al. 2006). These zones contained label-retaining cells at the ventricle, and the majority of the progeny generated from these cells differentiate into neurons (Zupanc et al. 2005; Grandel et al. 2006), indicating that these are self-renewing neural progenitor cells. At least in the telencephalon these cells are the source of a number of different neuronal subtypes, including GABAergic neurons, dopaminergic neurons, and parvalbuminergic neurons (Adolf et al. 2006; Grandel et al. 2006; Skaggs et al. 2014).

Comparing the numbers of cells labelled with the thymidine analogue BrdU (5-bromo-2'-deoxyuridine) as provided quantitative comparisons between the numbers of cells generated in the adult rodent brain and the zebrafish brain. BrdU intercalates into DNA during S phase, labelling proliferating cells and their progeny. The number of $BrdU^+$ cells indicate that the level of cell proliferation in the zebrafish CNS is at least one, potentially two, orders of magnitude greater than the adult rodent CNS (Zupanc & Sîrbulescu 2011).

However, it should also be noted that there are also examples of regions of the CNS which can successfully regenerate in some species, but which have little or no constitutive neurogenesis. Examples include the adult zebrafish spinal cord and the salamander midbrain (Becker et al. 2004, Berg et al. 2010). This demonstrates that although there may be a correlation between the number of proliferation zones and the regenerative ability of the CNS in a species, constitutive proliferation of progenitor cells is not a prerequisite to neuroregeneration.

1.5 Regeneration of dopaminergic neurons in the adult zebrafish brain

As discussed previously, Parkinson's disease is characterised by a selective loss of dopaminergic neurons which are never replaced. This has inspired research into the regenerative capacity of dopaminergic neurons specifically in animals with a higher regenerative capacity than mammals, including zebrafish.

1.5.1 Dopaminergic neuron populations in the adult zebrafish brain

Tyrosine hydroxylase (Th) catalyses the rate limiting step in the synthesis of catecholamines, and therefore serves as a reliable marker of dopaminergic and noradrenergic cells (Pickel et al. 1975; Hökfelt et al. 1976). The Th antibody used to identify Th^+ neurons throughout this thesis has been found to be highly specific (Chen et al. 2009).

The adult zebrafish brain contains 17 distinct populations of dopaminergic and noradrenergic neurons (Figure 1. 1). Throughout this thesis I will refer to the Th^+ populations in the zebrafish brain by the nomenclature suggested by Sallinen et al. (Sallinen et al. 2009), which numbers Th^+ populations according to their rostral-caudal position in the brain.

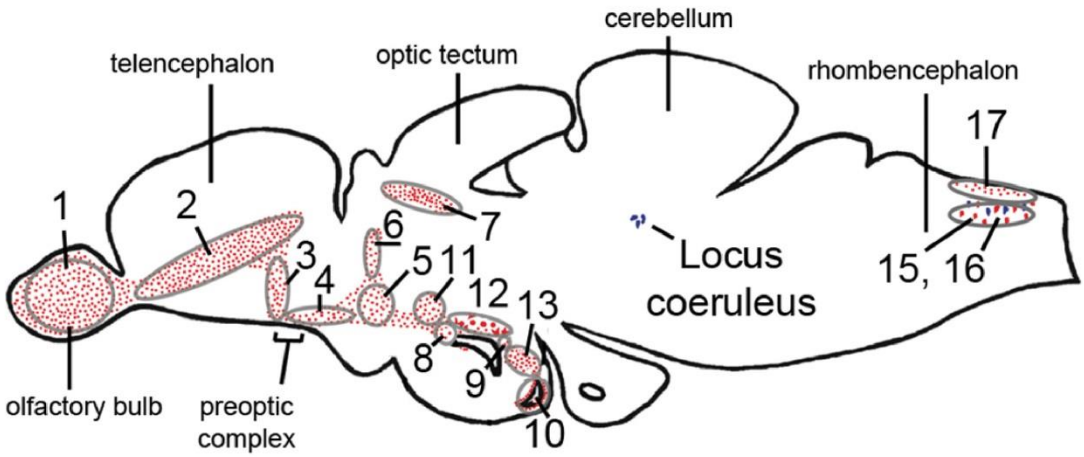

Population of Th^+ cells (Sallinen et al. 2009)	Location
1	Olfactory bulb
2	Telencephalon
3/4	Preoptic area/suprachiarmatic nucleus
5/6	Postoptic/ thalamic nuclei
7	Periventricular pretectal nucleus
8	Anterior paraventricular organ
9	Posterior paraventricular organ
10	Hypothalamus
11	Periventricular nucleus of the posterior tuberculum
12	Posterior tuberal nucleus, periventricular nucleus of the posterior tuberculum
13	Periventricular hypothalamus
14	Locus coeruleus
15/16	Internal reticular formation/vagal lobe (medulla oblongata)
17	Area postrema

Figure 1. 1 Schematic illustrating the 17 distinct populations of Th^+ neurons in the adult zebrafish brain, using the nomenclature suggested by Sallinen et al. 2009. Noradrenergic cells are indicated in blue (in the locus coeruleus and population 15/16), while dopaminergic neurons are indicated in red (all populations listed except the locus coeruleus).

Notably, there are no dopaminergic neurons in the zebrafish midbrain. However, tracer studies have shown that the ascending projections of population 11 in the ventral diencephalon project to the subpallium of the telencephalon, suggesting that these projections are equivalent to the nigrostriatal pathway in mammals. Therefore, population 11 is the strongest candidate population of Th^+ cells for a zebrafish homologue to the substantia nigra (Kaslin and Panula 2001; Rink and Wullimann 2001).

1.5.2 6-hydroxydopamine-induced ablation of Th^+ neurons in the adult zebrafish brain

In order to study the regeneration of Th^+ neurons a method is required to specifically ablate these neurons in the otherwise intact brain. 6-hydroxydopamine (6OHDA) is one of the most commonly used methods to ablate dopaminergic neurons. Injection of 6OHDA has been used since the 1960s (Ungerstedt 1968) to successfully ablate dopaminergic neurons in the adult brain in non-human primates (Eslamboli 2005), rodents (Deumens et al. 2002), amphibians (Berg et al. 2010), planarians (Nishimura et al. 2011) and zebrafish (Matsui et al. 2017; Vijayanathan et al. 2017; Caldwell and Davies et al. 2018).

6OHDA is a structural homologue of catecholamines dopamine and noradrenaline, and as such can enter cells via the dopamine transporter (dat) and the noradrenaline transporter (nat) (Van Kampen et al. 2000; Jackson-Lewis et al. 2012; Bové & Perier 2012). Once inside these cells, 6OHDA undergoes auto-oxidation generating cytotoxic species including H_2O_2, reactive oxygen species (ROS), and catecholamine quinones (Padiglia et al. 1997; Palumbo et al. 1999). Cytotoxic species are also produced in part through oxidation by monoamine oxidase (MAO-A), generating hydrogen peroxide, H_2O_2, which triggers the production of oxygen radicals (Cohen 1984). Hence, 6OHDA-mediated neurotoxicity is a result of oxidative stress (Simola et al. 2007).

In the adult zebrafish brain, our group and others have shown that a single injection of 6OHDA is sufficient to ablate dopaminergic neurons (Caldwell and Davies et al. 2018; Vijayanathan et al. 2017; Matsui et al. 2017). A previous PhD student in our group, Nick Davies, compared the numbers of Th^+ profiles in fish injected with 6OHDA to sham injected controls. He found a 51% reduction in the number of Th^+ neurons in population 5/6, 19% in population 11, and 96% in population 12, as well as a complete

loss of Th$^+$ neurons in the locus coeruleus (LC) after 6OHDA (Figure 1. 2B, (Caldwell and Davies et al. 2018)). Two other studies also reported a 6OHDA-induced reduction in the number of Th$^+$ neurons in the posterior tuberculum (populations 11 and 12) and locus coeruleus (Matsui et al. 2017; Vijayanathan et al. 2017).

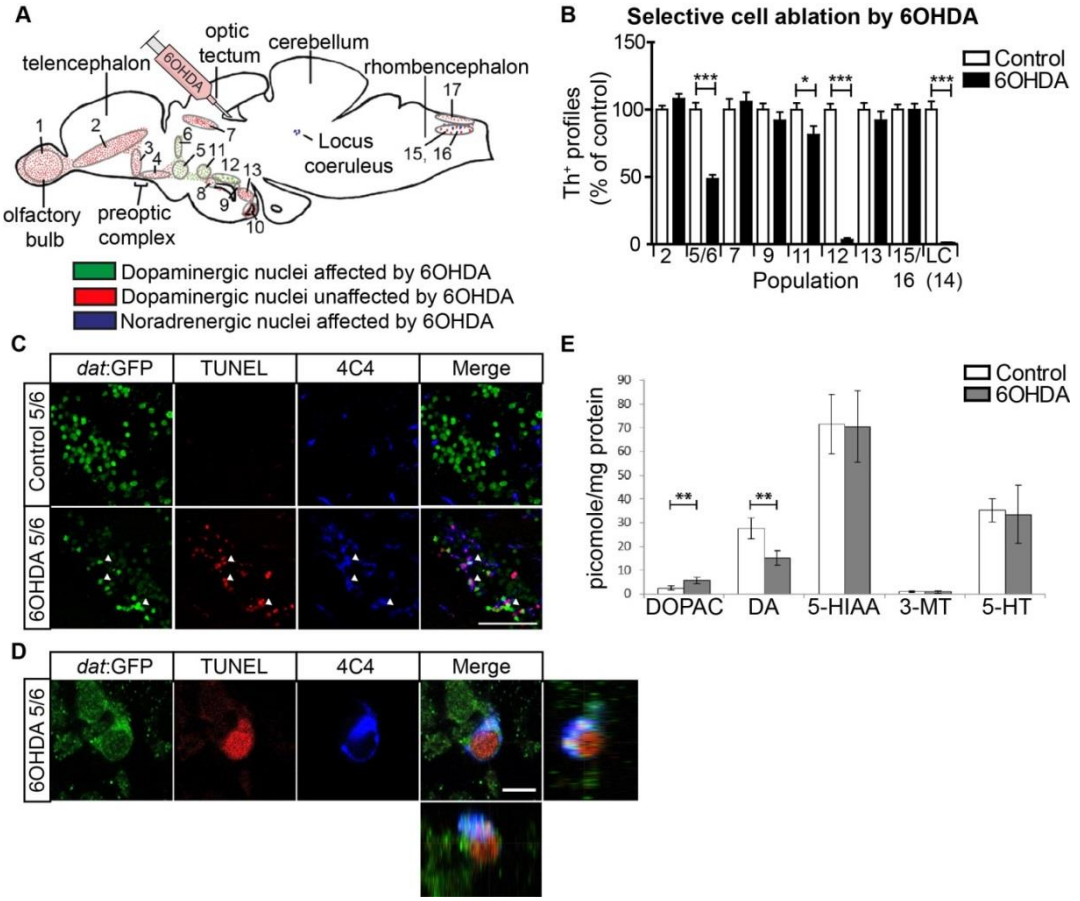

Figure 1. 2 Specific populations of Th$^+$ neurons are ablated by 6OHDA. A: A schematic sagittal section of the adult brain is shown with the 6OHDA resistant dopaminergic cell populations (red) and the vulnerable dopaminergic (green) and noradrenergic populations (purple) in relation to the injection site in the third ventricle indicated. B: Quantification of cell loss after toxin injection at 2 dpi is shown. C: Sagittal sections of population 5/6 are shown in a *dat*:GFP transgenic fish. This shows elevated local TUNEL and microglia labelling in population 5/6 after ablation. Some microglial cells that have engulfed TUNEL and GFP positive cell fragments are depicted by arrowheads. D: A high magnification is shown of a TUNEL$^+$/*dat*:GFP$^+$ and orthogonal views). E: Injection of the toxin decreases levels of dopamine (DA), increases levels of the metabolite DOPAC, but leaves serotonin (5-HT) and metabolites (5-HIAA, 3-MT) unaffected, as shown by HPLC. Student's T- test (with Welch's correction for heteroscedastic data) and Mann Whitney-U tests were used for pairwise comparisons in B and D (*p < 0.05; ** p < 0.01; *** p < 0.001). Bar in C = 50 µm, in D = 5 µm. Figure is reproduced from (Caldwell and Davies et al. 2018)**.**

In line with a reduction in the number of Th$^+$ neurons, we found that 6OHDA induced cell death of Th$^+$ neurons, demonstrated by TUNEL$^+$ cells in a fluorescent reporter fish

for dopaminergic neurons, *Tg(slc6a3:EGFP)*, abbreviated to *dat*:GFP (Xi et al. 2011) (Figure 1. 2C and D, (Caldwell and Davies et al. 2018)). Double positive $TUNEL^{+}/GFP^{+}$ cells were observed only in ablated populations and only in areas labelled by the transgene. This was accompanied by a 45% reduction in the level of dopamine, but not serotonin or its metabolites, in the brain after 6OHDA injection (Figure 1. 2E, (Caldwell and Davies et al. 2018)).

1.5.3 Th^{+} neurons are replaced as a result of increased neurogenesis

The numbers of Th^{+} neurons in populations affected by 6OHDA were counted at several time points after 6OHDA injection. The number of Th^{+} profiles in population 5/6 was increased at 42 dpi compared to 2 dpi, and had returned to control levels by 180 dpi (Figure 1. 3, (Caldwell and Davies et al. 2018)). Despite a transient increase, the numbers of Th^{+} profiles in population 12 and the locus coeruleus never fully recovered, indicating a differential potential for cell replacement among Th^{+} populations in the adult zebrafish brain. Similarly, the axonal projections of population 12 and the locus coeruleus to the spinal cord were never recovered following 6OHDA-induced ablation, even at 540 dpi (Caldwell and Davies et al. 2018). The projections from neurons in these two populations comprise the Th^{+} innervation of the spinal cord, so an absence of Th^{+} axons in the spinal cord can be used as an indication of successful ablation at any time point after 6OHDA injection.

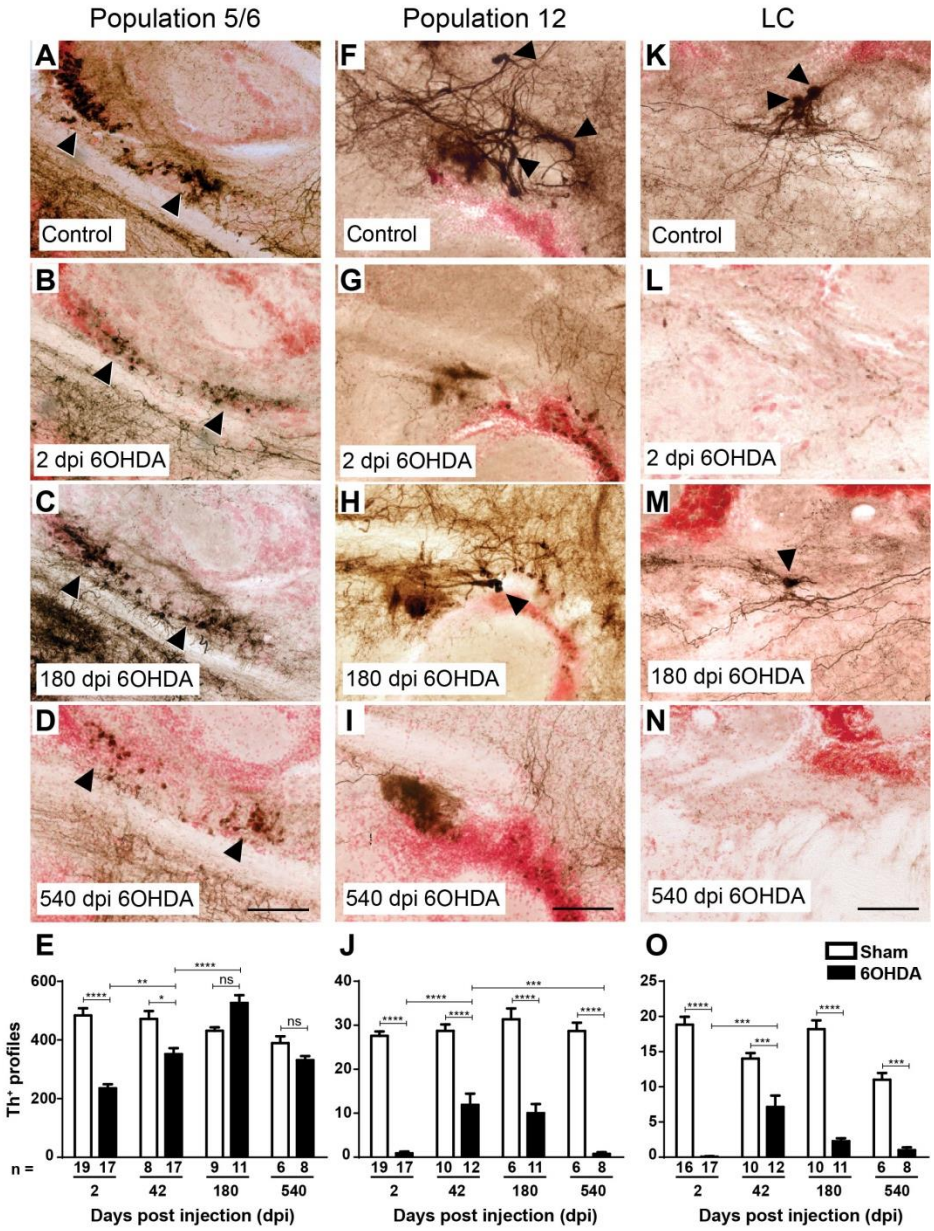

Figure 1. 3 Replacement of Th⁺ neurons differs between brain nuclei. Sagittal brain sections are shown; dorsal is up, rostral is left. Some Th⁺ cell bodies are indicated by arrowheads. A-E: In population 5/6 the number of Th⁺ cells is reduced after toxin-induced ablation and back to levels seen in controls without ablation by 180 dpi. F-J: In population 12, a partial and transient recovery in the number of Th⁺ cells was observed at 42 dpl. K-O: In the LC there was also a partial and transient recovery of Th⁺ cell number. Two-way ANOVA ($p < 0.0001$) with Bonferroni post-hoc test (*$p < 0.05$, **$p < 0.01$, ***$p < 0.001$, ****$p < 0.0001$) for E, J, and O. Bars = 50 µm. Figure is reproduced from (Caldwell and Davies et al. 2018)**.**

Th⁺ neurons are constantly generated in the adult zebrafish brain, as demonstrated previously by the presence of Th⁺/BrdU⁺ cells in the intact adult zebrafish brain 46

days post BrdU injection (Grandel et al. 2006). To determine whether Th^+ cell numbers recovered as a result of increased neurogenesis, Nick Davies examined the number of new Th^+ neurons in 6OHDA-injected fish compared to sham-injected fish. EdU was injected daily for seven consecutive days after 6OHDA injection, and the number of Th^+/EdU^+ cells was counted at 42 days post injection of 6OHDA. Double labelled cells were observed in sham injected fish in populations 5/6, 8, and 11, demonstrating that neurons in these populations are constitutively generated (Figure 1. 4, (Caldwell and Davies et al. 2018)). A 4.9 fold increase was found in the number of newly generated Th^+ neurons in population 5/6 after 6OHDA injection. Meanwhile, no Th^+/EdU^+ cells were observed in population 12 and the locus coeruleus, either in control or 6OHDA-injected fish. Therefore the differences in Th^+ neuron replacement capacity between Th^+ populations correlate with constitutive neurogenesis.

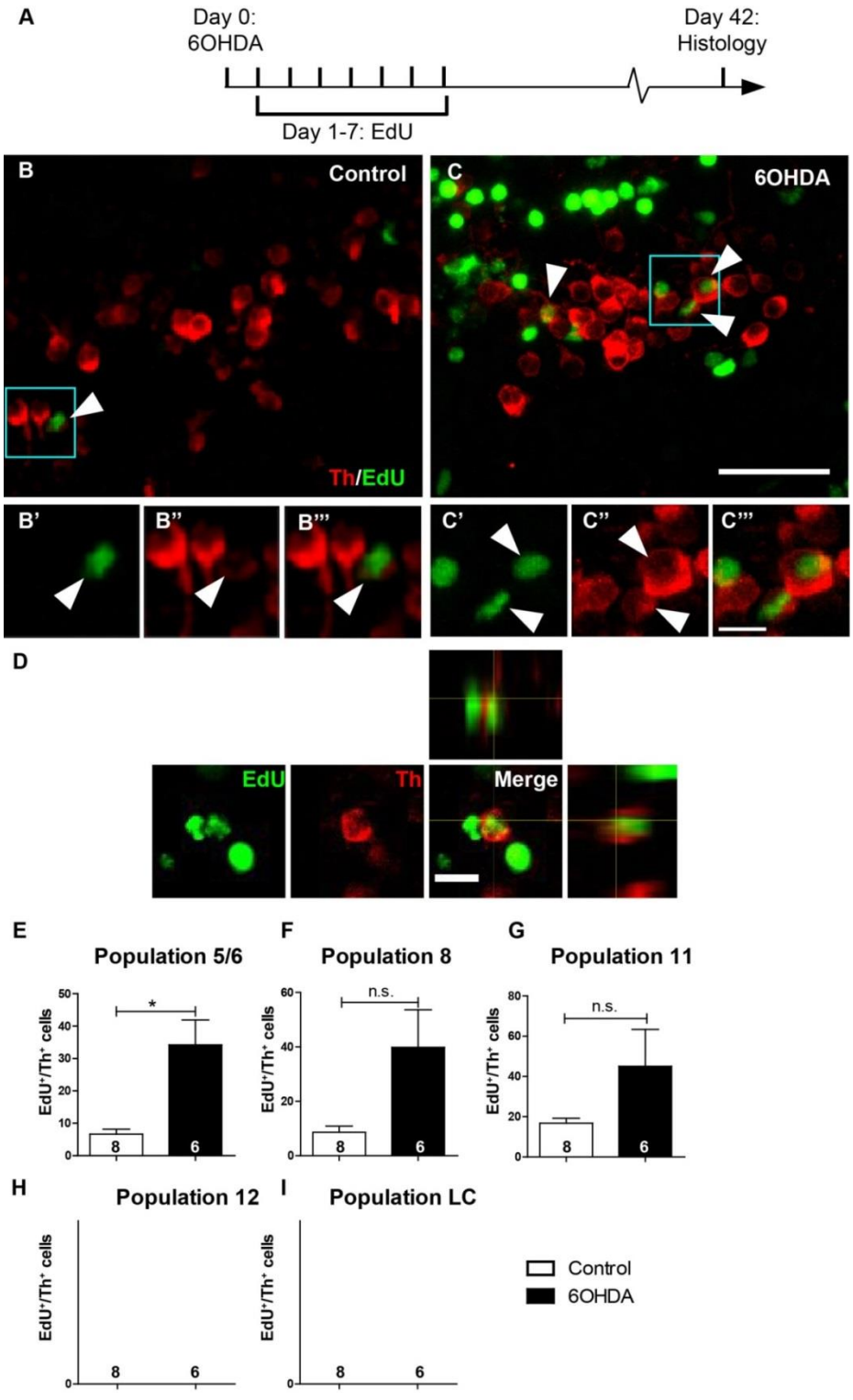

Figure 1. 4 Generation of new Th$^+$ cells is enhanced by prior ablation only in dopaminergic populations showing constitutive neurogenesis. A: The experimental timeline is given. B,C: In sagittal sections of population 5/6 (rostral left; dorsal up), EdU and Th double-labelled cells can be detected. Boxed areas are shown in higher magnifications in B'-C''', indicating cells with an EdU labelled nucleus, which is surrounded by a Th$^+$ cytoplasm (arrowheads). D: A high magnification and orthogonal views of an EdU$^+$/Th$^+$ cell after 6OHDA treatment is shown. E-I: Quantifications indicate the presence of newly generated Th$^+$ cells in specific dopaminergic brain

nuclei (E-G). After 6OHDA treatment, a statistically significant increase in the number of these cells was observed for population 5/6. Note that population 12 and LC showed no constitutive or ablation-induced EdU labelled Th$^+$ cells (H, I). (Student's T-tests with Welch's correction, *p <0.05,). Bar in C = 20 µm for A,B; bar in C''' = 5 µm for B'- C''', bar in D = 10µm. Figure is reproduced from (Caldwell and Davies et al. 2018)**.**

1.6 Successful regeneration of the zebrafish spinal cord

Following complete transection of the spinal cord adult zebrafish are able to recover function and regain normal swimming capacity by six weeks post lesion (Becker et al. 2004; Reimer et al. 2008). Regeneration of the spinal cord involves the replacement of lost neurons and the regrowth of severed axons across the lesion site. In the unlesioned spinal cord, progenitor cells are essentially quiescent, demonstrated by very low numbers of PCNA$^+$ and BrdU$^+$ cells around the central canal (Reimer et al. 2008). However, a spinal cord lesion induces a substantial increase in cellular proliferation in cells around the central canal (Takeda et al. 2008; Reimer et al. 2008). These proliferating cells include neural progenitor cells proximal to the lesion site, shown by an increase in PCNA$^+$ and BrdU$^+$ cells at the ventricle from 3 -14 dpl (Reimer et al. 2008). By 14 dpl new motor neurons can be found close to the site of injury (Reimer et al. 2008). At this time point there is also a 24-fold increase in the number of vsx1$^+$ interneurons and a 3-fold increase in the number of 5-HT interneurons, in comparison to the unlesioned spinal cord (Kuscha, Barreiro-Iglesias, et al. 2012).

Spinal cord regeneration can also be observed in larval zebrafish (Briona & Dorsky 2014a; Ohnmacht et al. 2016). This system recapitulates aspects of the adult zebrafish spinal cord lesion, but on a shorter time scale. Larval zebrafish lesioned at 3 days post fertilisation (dpf) can regenerate their spinal cord and recover normal swimming behaviour by 2 dpl (Ohnmacht et al. 2016). The number of newly generated motor neurons is increased at 2 dpl compared to unlesioned age-matched controls (Ohnmacht et al. 2016), demonstrating that there is a lesion-induced increase in neurogenesis in order to replace neurons which have been lost.

1.7 Statement of aims

- To investigate the origin of new Th^+ neurons in the adult zebrafish brain
- To investigate the signalling pathways involved in the regeneration of Th^+ neurons
- To investigate alternative methods of Th^+ neuron ablation
- To investigate the regeneration of glutamatergic and GABAergic neurons in the spinal cord

Chapter Two: Materials and Methods

2.1 Zebrafish husbandry and lines

Zebrafish (*Danio rerio*) were housed under standard conditions (Westerfield 2000) including a 14/10 hour light/dark cycle, with their water carefully monitored to maintain a constant temperature, salinity, and pH. Embryos were collected within 2 hours of fertilisation and raised in fish water with 0.00001% methylene blue at 28.5°C until 5 dpf. All experimental procedures were approved by the British Home Office.

The fish lines I used were: wild type (WIK and TL, as indicated); *Tg(gfap:GFP),* abbreviated as *gfap*:GFP (Bernardos & Raymond 2006); *Tg(olig2:DsRed2)*, abbreviated as *olig2*:DsRed (Kucenas et al. 2008); *Tg(her4.3:EGFP),* abbreviated as *her4*:GFP (Yeo et al. 2007); *Tg(her4.1:TETA-GBD-2A-mCherry),* abbreviated as *her4*:mCherry (Knopf et al. 2010); *irf8*$^{st95/st95}$, abbreviated as *irf8*$^{-/-}$ (Shiau et al. 2015); *Tg(pink1*$^{sh391:sh397}$*),* abbreviated as *pink1*$^{-/-}$ (Flinn et al. 2013); *Tg(otpb.A:nfsB–egfp),* abbreviated as *otpb*:NTR-GFP (Lambert et al. 2012); *Tg(gad1b:loxP-RFP-loxP-EGFP),* abbreviated as *gad1b*:RFP (Satou et al. 2013); *Tg(vglut2a:loxP-RFP-loxP-EGFP)*, abbreviated as *vglut2a*:GFP (Satou et al. 2013). For genetic lineage tracing I used *Tg(-3her4.3:Cre-ERT2)* (Boniface et al. 2009) crossed with *Tg(actb2:LOXP-mCherry-LOXP-EGFP)* (Ramachandran et al. 2010), as previously described (Skaggs et al. 2014). Note that zebrafish nomenclature treats *her4.1* and *her4.3* as synonymous (https://zfin.org/ZDB-TGCONSTRCT-110825-6).

2.2 Drug administration

2.2.1 Intraperitoneal injections

Fish were anaesthetised by immersion in 0.02% MS222 in PBS and placed on a cooled surface. Using a 30 ½ G needle 25 µl was injected into the peritoneum on the left side. 4-hydroxytamoxifen (4OHT) was injected at a concentration of 0.5 mg/ml dissolved in dH_2O. EdU was injected at a concentration of 4.11 mg/ml dissolved in 0.3 x Danieau's solution with 15% DMSO. Haloperidol was injected at a concentration of 80 µg/ml dissolved in PBS. Haloperidol decanoate was injected at a concentration of 20 mg/kg. Metronidazole was injected at a concentration of 5mg/ml dissolved in PBS. MPTP was injected at concentrations of 2 mg/ml and 3 mg/ml dissolved in PBS. Sham injected animals were injected with vehicle solutions.

2.2.2 Cerebroventricular injections

Fish were anaesthetised by immersion in in 0.02% MS222 in PBS and mounted in a wet sponge surrounded by ice water. A small hole was created in the skull directly above the left optic tectum using sharp forceps. A glass capillary needle was inserted into this hole at a 45° angle from the caudal edge of the tectum into the third ventricle. A pressure injector (IM-300 microinjector, Narishige International, Inc. USA) was used to inject 0.5 to 1.0 µL of solution containing 0.12% fluorescent dextran-conjugate, thus distribution of the solution throughout the ventricular system could be verified under a fluorescence-equipped stereo-microscope. 6-hydroxydopamine hydrobromide (6OHDA) was injected at a concentration of 10 mM dissolved in PBS. Leukotriene C4 (LTC4) was injected at a concentration of 500 ng/ml in 0.45% ethanol in H_2O. MPP^+ was injected at concentrations ranging between 1 and 10 mM dissolved in PBS. Zymosan was injected at a concentration of 10 mg/ml dissolved in PBS. Sham injected animals were injected with vehicle solutions.

2.2.3 Immersion

Adult fish were transferred into tanks containing drug in 1 L system water. Fish were transferred into fresh drug/vehicle every other day. When photosensitive chemicals were used tanks were protected from light. 4-hydroxytamoxifen (4OHT) was used at a concentration of 1 µM solution of 4OHT in system water. Dexamethasone was used at a concentration of 15 mg/L in system water with 0.06% DMSO. Metronidazole was used at a concentration of 10 mM in system water with 0.1% DMSO. Pomalidomide was used at a concentration of 100 nM in system water with 0.1% DMSO). Control animals were immersed in vehicle solution. Larvae were immersed in 100 µM EdU in 1% DMSO in conditioned water, covered in foil, and incubated at 28.5°C.

2.3 Spinal cord injuries

Adult spinal cord lesions were performed by Dr. Thomas Becker as described previously (Becker et al. 1997). Briefly, fish were anaesthetised by immersion in 0.02% MS222 in PBS and placed on a cool surface. A longitudinal incision was made to expose the vertebral column, equidistant from the operculum and the dorsal fin, and the spinal cord was completely transected under visual control.

Larval spinal cord lesions were performed as described previously (Ohnmacht et al. 2016). Briefly, at 3 dpf larvae were anaesthetised by immersion in 0.02% MS222 and transferred onto 4% agarose at room temperature in a lateral position. A 30½ G needle was used to make a dorsal incision transecting the entire spinal cord at the level of the 15th myotome, whilst ensuring the notochord remained intact. Sham lesioned fish were anaesthetised but not lesioned.

2.4 Histology

2.4.1 Perfusion and fixation of adult tissue

Fish were terminally anaesthetised by immersion in 0.1% MS222 in PBS. A 30 ½ G needle was inserted into the heart and used to perfuse the fish with PBS followed by 4% PFA. The fish were stored in 4% PFA at 4°C overnight. Brains and spinal cords were carefully extracted, washed briefly in PBS, and embedded in 4% agar in PBS. A vibrating blade microtome (Leica VT1200S) was used to cut 50 µm sections.

2.4.2 EdU detection in larval zebrafish

Larvae were fixed in 4% PFA at 4°C overnight. The following day they were washed three times in 0.1% PBSTx for 5 minutes each before being transferred into 100% methanol for 5 minutes. This was then replaced with fresh methanol and the larvae were kept at -20°C for at least 2 hours. The larvae were gradually rehydrated in 75% methanol/PBS, 50% methanol/PBS, and 25% methanol/PBS, followed by three five minutes washes in 0.1% PBSTx. The yolk and head of each larva was removed manually and larvae were incubated with 10 µg/ml proteinase K in 0.1% PBSTx at room temperature for 45 minutes. Larvae were placed in 4% PFA for 15 minutes at room temperature, washed three times in 0.1% PBSTx for five minutes each, and then incubated in 1% DMSO/0.5% PBSTx for 20 minutes at room temperature. After another wash with 0.1% PBSTx as much PBSTx was removed as possible and the larvae were transferred into freshly prepared Click-iT^{TM} reaction mix (Invitrogen, C10340, Table 2. 1).

Reaction component	Per 100 µl Reaction Mix
Reaction buffer (10X)	8.6 µl
H_2O	77.2 µl
$CuSO_4$	4 µl
Alexa Fluor 647	0.2 µl
Buffer additive (1X)	10 µl
Total	100 µl

Table 2. 1 EdU Click-iT Reaction Mix

Larvae were protected from light and incubated for two hours at room temperature on a shaker before three five minute washes in 0.1% PBSTx. Immunohistochemistry was then performed as described below.

2.4.3 EdU detection in adult zebrafish

Floating sections of adult brains and spinal cords were washed twice in 0.5% PBSTx for five minutes. The sections were then incubated in freshly prepared Click-iT™ reaction mix (Invitrogen, C10340, Table 2. 1) at room temperature for three hours whilst protected from light on a gentle shaker. Sections were then washed three times with 0.3% PBSTx, for 10 minutes each, followed by a fifteen minute wash with 1 x PBS.

When EdU labelling was combined with immunohistochemistry, sections were then transferred into blocking solution. For EdU detection only, sections were then transferred to 70% glycerol and mounted.

2.4.4 Immunohistochemistry on adult sections

Floating sections were washed in PBS followed by a 10 minute wash in 0.1% PBSTx at room temperature. Sections were incubated with 15% normal donkey serum in

0.1% PBSTx for 30 minutes at room temperature and incubated with primary antibody overnight at 4°C. Following 3 x 15 minute 0.1% PBStx washes at room temperature, sections were protected from light whilst incubated in secondary antibody at room temperature for 45 minutes. Sections were washed in 0.1% PBStx for 2 x 15 minutes, followed by a 1 x 15 minute wash with PBS. Sections were then transferred to 70% glycerol before being mounted onto Superfrost slides. Cover slips were sealed with nail varnish and slides were stored at 4°C until imaged.

2.4.5 Tissue clearing of adult spinal cord

For tissue clearing, the spinal cord was extracted and embedded in ice cold hydrogel Clarity Solution 1 (see buffers section for details). The tube containing the sample was protected from light and stored at 4ºC for 1-2 days to allow for diffusion of the hydrogel into the tissue. The oxygen in the tube was then replaced with nitrogen gas, and the tube was incubated at 37ºC for 3 hours. The tissue was then extracted from the hydrogel and washed with Clarity Solution 2 at 37ºC on a shaker. The solution was replaced with fresh Clarity Solution 2 daily for two weeks. The spinal cord was then mounted in 87% glycerol for imaging.

2.5 Molecular Biology

2.5.1 Quantitative RT-PCR

Adult zebrafish were terminally anaesthetised by immersion in 0.1% MS222 in PBS. The brain was extracted and embedded into 4% agar and sectioned horizontally. A section of 200 µm at the location used for analysis of progenitor cells around the ventricle was collected. The RNeasy® Mini Kit (QIAGEN, 74106) was used to extract RNA following the kit's instructions. Briefly, samples were dissolved in 350 µl RLT buffer and stored at -20°C if required. 350 µl 70% ethanol was added and the samples were centrifuged, then washed with buffers and eluted in 30 µl Nuclease-free H_2O.

cDNA synthesis was performed using the iScript™ cDNA Synthesis Kit (Bio-Rad, 1708891). For each sample, a reaction mix was prepared containing 4 µl 5X Reaction Mix + 1 µl Enzyme + 15 µl RNA template, for a total volume of 20 µl per sample. Samples were then transferred into a PCR machine (programme: 5 min at 25°C, 20 min at 46°C, 1 min at 95°C). SsoAdvanced™ Universal SYBR® Green Supermix (Bio-Rad, 172-5271) was used for the quantitative RT- PCR. Samples were prepared in 96-well plates at a volume of 20 µl per well, and each sample was tested in duplicate. The following primers were used: *18S*: FW: 5'- TCGCTAGTTGGCATCGTTTATG-3', RV: 5'- CGGAGGTTCGAAGACGATCA-3', *tnf-α*: FW: 5'-TCACGCTCCATAAGACCCAG-3', RV: 5'-GATGTGCAAAGACACCTGGC-3', *il-1β*: FW: 5'-ATGGCGAACGTCATCCAAGA-3', RV: 5'-GAGACCCGCTGATCTCCTTG-3'.

2.5.2 Genotyping

Adult *pink1*$^{-/-}$ and *pink1*$^{+/+}$ fish were anaesthetised by immersion in 0.02% MS222 in PBS and a small fin clip was cut. The tissue was dissolved with 100 µl 5 mM NaOH at 95 ºC for 1 hour and vortexing. 10 µl 1M Tris (pH8) was added and the sample was centrifuged at 1000 rpm for 2 minutes. The area of interest of the *pink1* gene was amplified by PCR (forward primer sequence: 5'-TAGGTGTCCATGGCAGTG-3', reverse primer sequence: 5'-CTGGTAACTCCGACTCTC-3', PCR programme: 30 seconds at 94ºC, 40 seconds at 50ºC, 40 seconds at 72ºC, 35 cycles). The PCR product was run on an agarose gel and extracted from the gel using the QIAquick Gel Extraction Kit (QIAGEN, 28706X4). Purified PCR products were sent for sequencing at Source Bioscience Sequencing (forward primer sequence: 5'-TAGGTGTCCATGGCAGTG-3', reverse primer sequence: 5'-CTGGTAACTCCGACTCTC-3').

2.6 Image Acquisition and Analysis

Fluorescent images were obtained using a Zeiss LSM 710 confocal microscope. Images were analysed using Fiji (Schindelin et al. 2012). Figures were prepared using Adobe Photoshop CS3 and Adobe Illustrator CS6.

2.6.1 Cell counting

Wholemount larvae or 50 µm sections were imaged as z stacks, and cell counts were performed manually by going through the stack and counting the number of cells in a stereological fashion. For adult spinal cords, the number of cells was counted in three randomly selected sections from up to 750 µm rostral to the lesion site and three randomly selected sections 750 µm caudal to the lesion site. These counts were then used to calculate the number of cells around the lesion site. The numbers of EdU^+ ERGs at the ventricle were counted in three 50 µm horizontal sections and summed together to give the total number per fish. Within each round of experiments, each fish was normalised to the average value of the sham fish for that round.

2.6.2 4C4 immunoreactivity

To assess the level of 4C4 immunoreactivity maximum projections were created and analysed using Fiji. The ratio of immunolabelling compared to the background signal was calculated for each section by dividing the mean grey value of the area around the ventricle by the mean grey value of the tissue background. Percentage covered was obtained by converting maximum projection images into binary images and using the “measure” function in Fiji to find the percentage area covered.

2.7 Statistics

Animals were randomly assigned to experimental groups and all quantifications were performed with the observer blinded to the experimental condition. Where a sample

of spinal cord sections was analysed the sections were selected at random by assigning each section a number and using a random number generator.

Statistical analyses were performed using GraphPad Prism and SPSS. Quantitative data were tested for normality (Shapiro-Wilk test) and heteroscedasticity (Levene's test) before selecting the appropriate statistical tests, which are described in figure legends. Variability of values is always given as the standard error of the mean (SEM), and n numbers on the graphs represent the number of animals used in the experiment. Power analyses were performed using G*Power3 (Faul et al. 2007).

2.8 Materials

2.8.1 Buffers

- Blocking buffer for wholemount immunohistochemistry

    1 x PBS

    1% DMSO

    1% BSA

    1% normal donkey serum

    0.7% Triton™X-100

- Clarity Solution 1

    10 ml Acrilamide; Bis-Acrilamide 30%

    0.75g VA-044 thermal initiator

    50 ml 8% PFA

    10 ml 10 x PBS

30 ml dH_2O

- Clarity Solution 2

8.68 g boric acid

20 g sodium dodecyl sulfate

400 ml dH_2O

Adjust to pH 8.5 with NaOH

- Paraformaldehyde (PFA) solution 4% (for fixation)

16g paraformaldehyde

40 ml 10 x PBS

Complete with dH_2O up to 400ml

- Phosphate buffered saline (PBS), 10X, pH 7.4

160 g NaCl

28.3 g Na_2HPO_4

4 g KCl

4.8 g KH_2PO_4

2 L dH_2O

2.8.2 Primary antibodies

Antibody	Host species	Dilution	Supplier
α-tyrosine hydroxylase	Mouse	1:1000	Millipore, MAB318
α-GFP	Chicken	1:1000	Abcam, ab13970
α-RFP	Rabbit	1:500	Invitrogen, R10367
4C4	Mouse	1:50	HPC Cell Cultures, 92092321

2.8.3 Secondary antibodies

Antibody	Dilution	Supplier
Cy3 Donkey α-mouse	1:200	JacksonImmunoResearch, 715-165-150
Alexa 488 Donkey α-chicken	1:200	JacksonImmunoResearch, 715-545-150
Alexa 647 Donkey α-mouse	1:200	JacksonImmunoResearch, 715-605-150
Cy3 Donkey α-rabbit	1:200	JacksonImmunoResearch, 711-165-152

2.8.4 List of Materials

Name	Catalogue Number	Supplier
4-hydroxytamoxifen (4OHT)	H6278	Sigma-Aldrich

5’Ethynyl-2’ deoxyuridine (EdU)	A10044	Invitrogen
6-hydroxydopamine hydrobromide (6OHDA)	H116	Sigma-Aldrich
Agar (purified)	LP0028	Oxoid
Aminobenzoic acid ethylmethylester (MS222)	A5040	Sigma-Aldrich
Bovine Serum Albumin (BSA)	A3912	Sigma-Aldrich
Collagenase	C9891	Sigma-Aldrich
Copper (II) Sulfate	451657	Sigma-Aldrich
Dexamethasone	D1756	Sigma-Aldrich
Dimethyl sulfoxide, sterile (DMSO)	D8418	Sigma-Aldrich
Ethanol	E7023	Sigma-Aldrich
Formamide	47670	Sigma-Aldrich
Glycerol	G5516	Sigma-Aldrich
Haloperidol	H1512	Sigma-Aldrich
Haloperidol Decanoate	H0100100	Sigma-Aldrich
Histoacryl Tissue Seal	9381104	B. Braun
Hydrochloric acid, HCl	320331	Sigma-Aldrich
Isopropanol	I9516	Sigma-Aldrich
Leukotriene C4	20210	Cayman Chemical
Lithium Chloride	LX026	Sigma-Aldrich
Magnesium Chloride	31413	Sigma-Aldrich

Methylene Blue	3470.0025	VWR International
Metronidazole	M1547	Sigma-Aldrich
MPP^+	D048	Sigma-Aldrich
MPTP	M0896	Sigma-Aldrich
Normal donkey serum	S30	Millipore
Paraformaldehyde (PFA)	P6148	Sigma-Aldrich
Pomalidomide	19877	Cayman Chemicals
Potassium Chloride	P5404	Sigma-Aldrich
Potassium dihydrogen phosphate (KH_2PO_4)	60218	Sigma-Aldrich
Proteinase K	3115801	Roche
RNAse Zap	R2020	Sigma-Aldrich
Sodium Chloride	S7653	Sigma-Aldrich
Sodium hydroxide, NaOH	S5881	Sigma-Aldrich
Superfrost coated glass slides	48311-703	VWR International
Torula yeast tRNA	R6625	Sigma-Aldrich
Triton X-100	93426	Sigma-Aldrich
Tween 20	P1379	Sigma-Aldrich
Zymosan A	Z23373	Life Technologies

Chapter Three: Investigating the Origin of New Th^+ Neurons in the Adult Zebrafish Brain

3.1 Introduction

The identification of newly generated Th^+ neurons in the adult zebrafish brain (Figure 1.4, (Grandel et al. 2006; Skaggs et al. 2014)) raises the question of where these new neurons originate from. In this chapter I describe a heterogeneous population of neural progenitor cells around the diencephalic ventricle in the adult zebrafish brain. I demonstrate using genetic lineage tracing that Th^+ neurons formed after 6OHDA injection can be derived from a specific subset of these cells.

3.1.1 New neurons are generated throughout the adult zebrafish brain

In contrast to the comparatively few neurogenic niches identified in the adult mammalian brain (Eriksson et al. 1998; Ming & Song 2011), proliferative zones in the adult zebrafish brain are found all along the rostral-caudal axis (Grandel et al. 2006). A combination of immunohistochemistry for proliferating cell nuclear antigen (PCNA) and BrdU shortly after injection have revealed the location of numerous proliferative zones (Zupanc et al. 2005; Grandel et al. 2006; Adolf et al. 2006). Longer post-injection times with BrdU have demonstrated that BrdU-labelled cells can migrate away from the proliferative zones and go on to become neurons, as shown by co-labelling with pan-neuronal marker HuC and markers of specific neuronal subtypes (Zupanc et al. 2005; Grandel et al. 2006; Adolf et al. 2006). Immunohistochemistry for the postsynaptic protein SV2 suggests that these neurons make synaptic contacts,

indicating that they are able to integrate into the existing neuronal circuitry (Rothenaigner et al. 2011).

3.1.2 Neural progenitor cells in the adult zebrafish brain

In adult zebrafish (and other anamniotes) new neurons are derived from progenitor cells called ependymo-radial glial cells (ERGs) (Becker & Becker 2015). These cells have a distinctive morphology, with a soma which forms part of the ependyma and radial processes extending across the entire span of the brain to the pial surface (Berg et al. 2011; Dirian et al. 2014). Evidence from clonal analysis using viral vectors (Rothenaigner et al. 2011) and repeated imaging of labelled ERGs in the adult zebrafish telencephalon (Barbosa et al. 2015b; Dray et al. 2015) demonstrates that these cells are self-renewing and generate multiple neuronal subtypes, two seminal characteristics of neural stem cells.

In addition, ERGs express *sox2*, a marker of neural stem cells (Ogai et al. 2014). ERGs can also be identified by their expression of genes such as *glial fibrillary acidic protein* (*gfap*), *aquaporin 4*, *vimentin*, *s100β*, *brain lipid binding protein (BLBP)*, *olig2*, *glutamine synthase*, and *her4* (Kroehne et al. 2011; Ganz et al. 2010; Jung et al. 2012; Chapouton et al. 2011).

In this chapter I focus on three genes expressed by ERGs which have been shown to generate new neurons in the adult zebrafish CNS, namely *gfap*, *olig2*, and *her4*. Due to the absence of astrocyte-like cells in the zebrafish, expression of *gfap* in the CNS is restricted to ERGs, and *gfap*:GFP^{+} cells in the optic tectum have been shown to act as proliferative neural progenitor cells (Jung et al. 2012). Oligodendrocyte lineage transcription factor 2 (*olig2)* is expressed by ERGs in the telencephalon of adult zebrafish (Adolf et al. 2006), as well as ERGs in the ventral spinal cord which have been shown to give rise to motor neurons after a spinal cord lesion (Reimer et al.

2008). Hairy-related gene 4 (*her4*) is expressed by ERGs in the telencephalon. These ERGs have been shown to increase neurogenesis after a stab lesion or excitotoxic injection (Kroehne et al. 2011; Skaggs et al. 2014), and *her4*$^+$ ERGs are the source of a diverse range of neuronal subtypes (Skaggs et al. 2014). Similarly, in the injured retina *her4*$^+$ progenitor cells produce a variety of different neuronal subtypes, including amacrine, bipolar, and horizontal cells, as well as Müller glia (Wilson et al. 2016).

3.1.3 Investigating where new Th$^+$ neurons originate from in the adult zebrafish brain

Given the high number and widespread locations of Th$^+$ populations (Figure 1.1) and neural progenitor cells ((Grandel et al. 2006)) in the adult zebrafish brain, I decided to limit my search for ERGs producing new Th$^+$ neurons to the population with the highest regenerative capacity, which is population 5/6 (Figure 1.3, Figure 1.4). Compared to other Th$^+$ populations, population 5/6 has a high number of new Th$^+$ cells, demonstrated by the number of Th$^+$ cells that had incorporated EdU (Figure 1.4), and so there is a relatively high chance of detecting new Th$^+$ neurons in this population.

3.1.4 Genetic Lineage Tracing

There are several different approaches used to determine which population of cells gives rise to another population. Parent populations can be labelled by injecting dyes, electroporating plasmids encoding fluorescent reporters, or by genetic means.

Here I have adopted a commonly used technique for genetic lineage tracing using the Cre-loxP system. Cre recombinase is expressed under the control of a cell type-specific promoter to target its expression to a specific cell type. Separately, transgenic animals are generated containing a cassette with loxP target sequences flanking a fluorescent reporter, STOP sequence, or other marker. When animals are crossed together and express the two transgenes, Cre recombinase specifically cuts at the

loxP sites, removing the flanked gene from the cell's genome. This system has been adapted to allow for temporal control. A modified Cre recombinase is fused to the human oestrogen receptor ERT2 (Feil et al. 1997). In the absence of tamoxifen or its active metabolite 4-hydroxytamoxifen (4OHT) the Cre resides in the cytoplasm of the cell, tethered to heat shock proteins, and insensitive to the endogenous ligand 17β-oestradiol (Indra et al. 1999). Upon application of a ligand, the enzyme undergoes a conformational change allowing it be released from heat shock proteins and translocate to the nucleus when it becomes activated and enters the nucleus where it can induce recombination.

The Cre/loxP method has been successfully used to trace the lineage of cells in the adult zebrafish, including those in the retina (Ramachandran et al. 2010), cornea (Pan et al. 2013), and the telencephalon (Kroehne et al. 2011; Skaggs et al. 2014).

3.1.4.1 Genetic lineage tracing of her4$^+$ ERGs using Tg(her4:CreERT2;β-actin:loxP-mCherry-loxP-EGFP) zebrafish

Genetic lineage tracing of *her4*$^+$ cells is possible using existing models using the Cre/loxP system. The 3.4kb promoter of *her4* (Yeo et al. 2007) has been used to drive the tamoxifen-inducible CreERT2 (Boniface et al. 2009). A separate transgenic line exists where the ubiquitously expressed *β-actin2* promoter drives expression of the fluorescent reporter mCherry (Ramachandran et al. 2010), and so every cell is mCherry$^+$ in the absence of tamoxifen. The mCherry sequence is flanked by two loxP sites and followed by an out of frame *EGFP* sequence. Upon activation, CreERT2 translocates to the nucleus and specifically recognises the loxP sites, excising mCherry from the genome and bringing the *GFP* sequence into frame. This means cells which are her4$^+$ at the time of 4OHT application, and all of their progeny, become permanently labelled with GFP (Figure 3. 1). These two transgenic lines have been successfully used in combination with immunohistochemistry for neuronal markers to

identify new cells which have been derived from her4^{+} ERGs since the application of 4OHT(Skaggs et al. 2014).

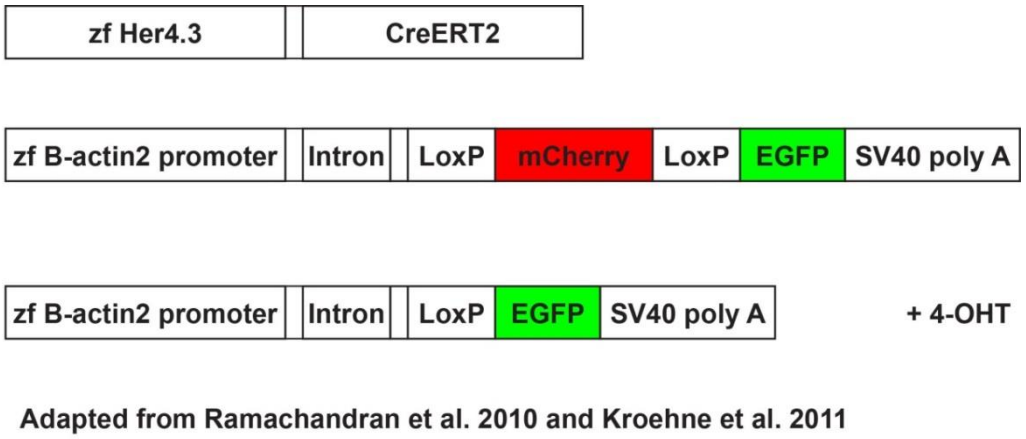

Figure 3. 1 A schematic illustrating the two transgenes in Tg(her4:CreERT2;β-actin:loxP-mCherry-loxP-EGFP) zebrafish. Upon activation with 4OHT, CreERT2 translocates to the nucleus and cuts at loxP sites, excising mCherry from the genome and bringing the EGFP into frame, thus permanently labels her4^{+} cells and their progeny.

3.2 Results

3.2.1 Cells lining the ventricle are a heterogeneous population of ERGs

I used horizontal brain sections of fish with fluorescent reporters driven by three known markers of ERGs to observe the cells lining the diencephalic ventricle. *gfap*:GFP^{+} cells, *olig2*:DsRed^{+}, and *her4*:mCherry^{+} cells are located at the diencephalic ventricle (Figure 3. 2), and exhibit the typical ERG morphology, with their somas contacting the ventricle and long processes extending out towards the pial surface.

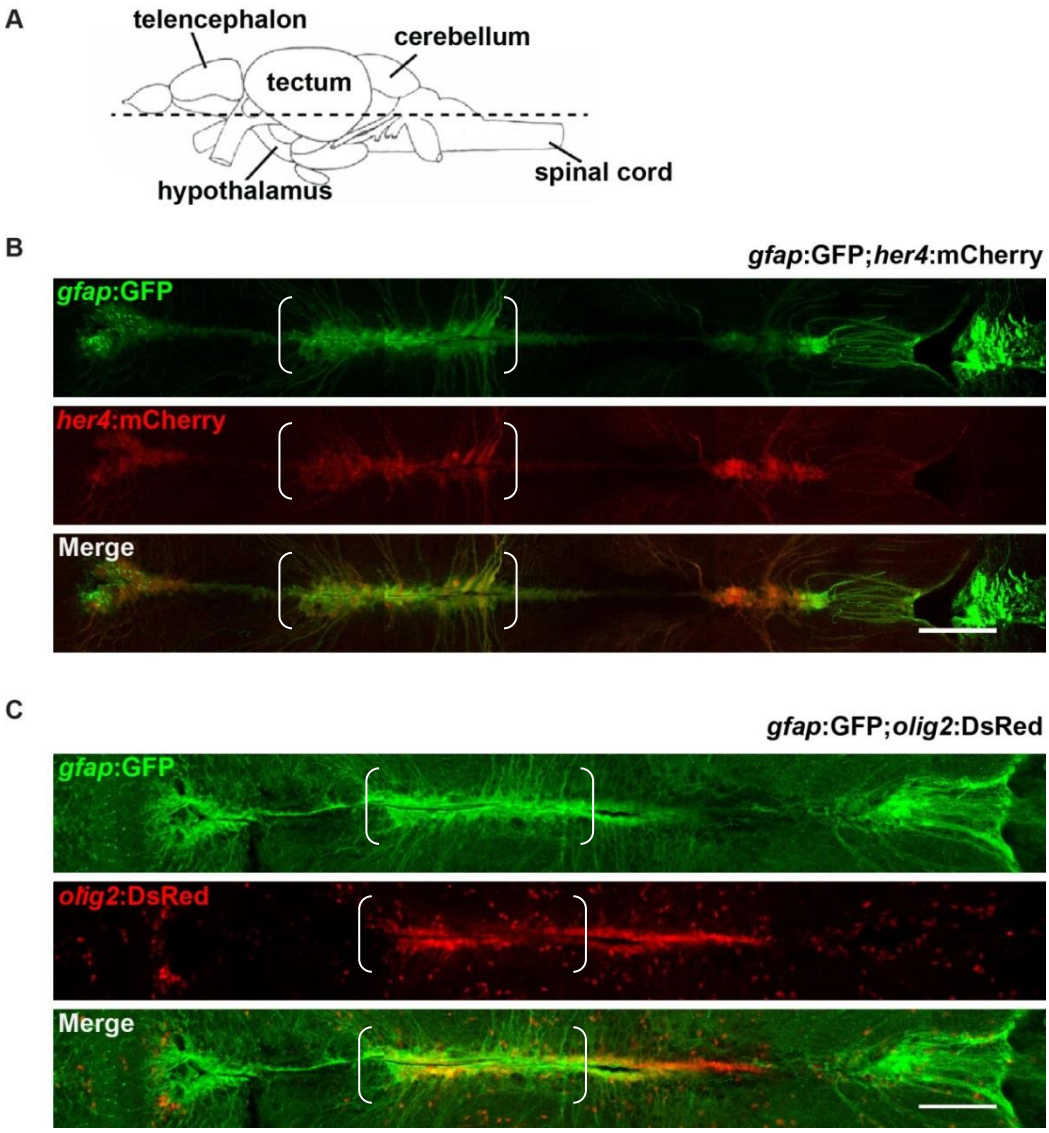

Figure 3. 2 Cells lining the diencephalic ventricle express markers of ERGs and have the typical morphology of ERGs. A: The horizontal plane of sectioning for B and C is marked by the dotted line; rostral is left for all panels. B and C: Maximum projections showing the overlapping but different location of *gfap*:GFP$^+$, *her4:*mCherry$^+$, and *olig2:*DsRed$^+$ ERGs around the diencephalic ventricle, white brackets indicate the approximate location of Th$^+$ cells in population 5/6. Scale bars in B and C = 100µm. A and B are adapted from (Caldwell and Davies et al. 2018).

Olig2:DsRed$^+$ cells can be seen in the parenchyma, and these oligodendrocytes can be distinguished from ERGs by their location and cellular morphology. *gfap*:GFP$^+$ and *her4*:mCherry$^+$ cells were only found lining the ventricle, and all displayed the typical ERG morphology, indicating all of these cells are ERGs.

I observed overlapping but different expression patterns of *gfap*:GFP$^+$, *olig2*:DsRed$^+$, and *her4*:mCherry$^+$ cells at the ventricle. In *gfap*:GFP;*her4*:mCherry double transgenic fish all *her4*:mCherry$^+$ cells were also *gfap*:GFP$^+$, but not all *gfap*:GFP$^+$ cells were *her4*:mCherry$^+$. In *gfap*:GFP/*olig2*:DsRed fish cells were *gfap*:GFP$^+$ only, *olig2*:DsRed$^+$ only, or *gfap*:GFP$^+$/*olig2*:DsRed$^+$. This shows for the first time that there is heterogeneity among these ERGs lining this ventricle.

3.2.2 Regenerated Th$^+$ cells are derived from her4$^+$ ERGs

To specifically induce recombination in her4$^+$ ERGs I immersed adult Tg(*her4*:CreERT2; *β-actin*:LCLG) zebrafish in 4OHT for six days. Fish were injected with 6OHDA on the final day of 4OHT treatment and analysis was performed at 42 dpi. This successfully induced recombination, demonstrated by the presence of GFP$^+$ cells only in 4OHT treated fish (Figure 3. 3). However, I observed different densities of GFP$^+$ cells, indicating variable recombination efficiency among 4OHT-treated fish. The majority of GFP$^+$ cells were ERGs, as indicated by their position lining the ventricle and their distinctive radial morphology. Some GFP$^+$ cells were also observed slightly removed from the ventricle, including double-labelled Th$^+$/GFP$^+$ cells (Figure 3. 3). These Th$^+$/GFP$^+$ cells were always observed in proximity to GFP$^+$ ERGs lining the ventricle, strongly suggesting that these Th$^+$ cells are derived from ERGs at the diencephalic ventricle after 6OHDA injection. The number of Th$^+$/GFP$^+$ cells correlated with a qualitative assessment of the recombination efficiency.

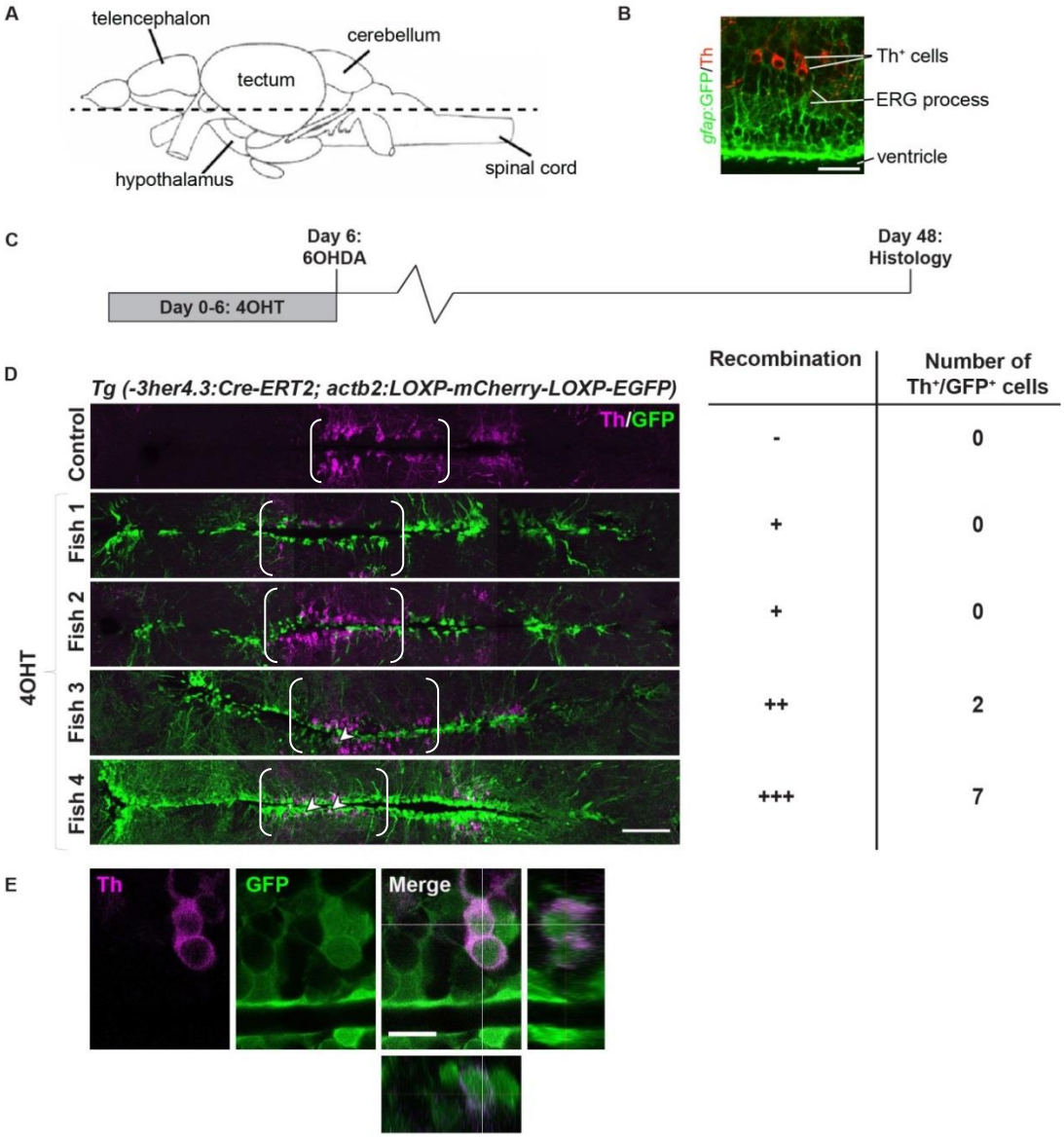

Figure 3. 3 New Th$^+$ cells in the region of the 5/6 population formed after 6OHDA ablation are derived from her4$^+$ ERGs. A: The horizontal plane of sectioning for B, D, and E is marked by the dotted line. B: ERGs are labelled in *gfap*:gfp transgenic fish with their somas at the ventricle and their radial processes alongside Th$^+$ neurons. C: The experimental timeline. D: Maximum projections of horizontal sections (left rostral), white brackets indicate the approximate location of Th$^+$ cells in population 5/6. The number of Th$^+$/GFP$^+$ cells correlates with the observed recombination efficiency. C: High magnification images of double labelled Th$^+$/GFP$^+$ cells, with orthogonal views. Scale bar in B = 25 µm, in D = 100 µm, in E = 10 µm. Figure is adapted from (Caldwell & Davies et al. 2018).

3.3 Discussion

3.3.1 The cells lining the diencephalic ventricle in adult zebrafish are a heterogeneous population of ERGs

Previous descriptions of ependymoradial glial cells in the adult zebrafish brain are largely limited to coronal sections through the brain. Differential expression patterns of genes known to be expressed by ERGs have been reported in the telencephalon (Ganz et al. 2010; Chapouton et al. 2011), the midbrain (Chapouton et al. 2011), and the hypothalamus (Chapouton et al. 2011). However, the diencephalic ventricle extends along the rostral-caudal axis, and this shape has hindered a clear description of the ERGs lining this ventricle in coronal sections. The results presented here provide the first description of the heterogeneity of ERGs around the diencephalic ventricle in the adult zebrafish brain, shown in horizontal sections (Figure 3. 2).

3.3.2 Mapping the expression patterns of genes expressed by ERGs could help identify a Th^+ neuron progenitor domain in the adult zebrafish brain

Analysing the expression of different genes in ERGs can identify pools of progenitor cells programmed to make specific neuronal subtypes. For instance, in the zebrafish spinal cord the expression patterns of various transcription factors have been used to define groups of ERGs which all give rise to a specific neuronal subtype during development (Satou et al. 2012). At least some of these expression patterns persist into adulthood. For example, a motor neuron progenitor domain (pMN), defined by expression of *olig2*, is the source of new motor neurons generated both during development and in the regenerating adult spinal cord (Cheesman et al. 2004; Reimer et al. 2008; Reimer et al. 2009).

The different but overlapping locations of *gfap*:GFP$^+$, *olig2*:DsRed$^+$, and *her4*:mCherry$^+$ ERGs I have described (Figure 3. 2) suggest there may be similar progenitor domains around the diencephalic ventricle. Future experiments could focus on mapping the expression of additional transcription factors expressed by ERGs, particularly those involved in Th$^+$ neurogenesis during development, such as *otpa, otpb, nr4a2a, nr4a2b, lmx1a, lmx1b.1, pitx3,* and *olig2* (Andersson et al. 2006; Filippi et al. 2007; Tay et al. 2011b; Chen et al. 2013; Mahler et al. 2010). This could lead to the identification of a specific pool of ERGs responsible for making new Th$^+$ neurons in the adult brain, similar to the pMN domain described in the spinal cord.

Additionally, genetic lineage tracing with other markers of progenitor cells could elucidate the range of ERGs capable of making Th$^+$ neurons in the adult zebrafish brain. For example, *olig2* has been shown to be involved in neurogenesis of Th$^+$ neurons during development (Mahler et al. 2010), and here I have shown the presence of *olig2*:DsRed$^+$ ERGs at the diencephalic ventricle in a similar location to new Th$^+$ neurons (Figure 3. 2, The *her4* promoter could be replaced with the *olig2* promoter to induce Cre expression in *olig2*$^+$ cells, and this would establish whether ERGs which produce Th$^+$ neurons are also olig2$^+$. Repeating this with other markers of ERGs could develop an expression profile of ERGs which produce Th$^+$ neurons in the adult zebrafish brain, identifying a Th$^+$ neuron progenitor domain analogous to the pMN domain in the lesioned adult spinal cord.

3.3.3 Th$^+$ neurons are derived from her4$^+$ ERGs at the diencephalic ventricle

Here I have demonstrated that in the adult zebrafish brain Th$^+$ neurons formed after 6OHDA injection can be derived from her4$^+$ ERGs at the diencephalic ventricle (Figure 3. 3). This conforms with previously published data showing neurons formed

in the regenerating adult brain after either a stab lesion to the telencephalon (Kroehne et al. 2011) or injection of the excitotoxin quinolinic acid (Skaggs et al. 2014) can be derived from her4$^+$ ERGs.

In the salamander, Th$^+$ neurons formed after 6OHDA ablation are derived from *gfap*$^+$ ERGs, as demonstrated by lineage tracing using *in vivo* electroporation of a plasmid encoding YFP, which specifically labelled *gfap*$^+$ ERGs (Berg et al. 2011). As I found all *her4*:mCherry$^+$ cells around the diencephalic ventricle are also *gfap*:GFP$^+$, this suggests that regenerated Th$^+$ neurons may be derived from ERGs expressing similar markers across species.

The images of GFP$^+$/Th$^+$ cells (Figure 3. 3) show that some of the lineage-traced neurons are catecholaminergic, and in the same location as the dopaminergic 5/6 population. However, the labelled ERGs may not produce Th$^+$ neurons exclusively, as GABAergic and calretinin$^+$ neurons have also been described among the progeny of her4$^+$ ERGs in the telencephalon (Skaggs et al. 2014). Similarly, her4$^+$ progenitor cells in the retina are the source of a wide range of different retinal cells (Wilson et al. 2016), demonstrating that her4$^+$ ERGs are capable of generating multiple neuronal subtypes in the adult zebrafish.

On the other hand, some Th$^+$ neurons formed after ablation may originate from her4$^-$ ERGs. If the recombination efficiency could be improved, perhaps by immersing fish in 4OHT for a longer time period, then future experiments combining genetic lineage tracing with EdU labelling could help to answer this question. If all her4$^+$ cells and their progeny are labelled with GFP before fish are injected with EdU, then any EdU$^+$/Th$^+$/GFP$^-$ cells would be Th$^+$ cells formed from her4$^-$ ERGs.

3.3.4 Future experiments could investigate the cellular dynamics of ERGs at the diencephalic ventricle in the adult zebrafish brain

Following several iterations of a protocol for the administration of 4OHT, I obtained optimal recombination efficiency by immersing fish in 4OHT for six days, as illustrated in the experimental timeline (Figure 3. 3B). However, even with this prolonged exposure to 4OHT the recombination efficiency observed varied between fish (Figure 3. 3). This limits the potential for quantitative analyses, for example comparing the number of new Th^+ cells generated in 6OHDA injected fish with sham injected fish. On the other hand, a lower recombination efficiency of cells lining the diencephalic ventricle could be advantageous for tracking the behaviour of individual ERGs. In the telencephalon, ERGs are located on the outer surface of the brain, and are therefore accessible for live imaging even in adult zebrafish (Dray et al. 2015; Barbosa et al. 2015b). Repetitive imaging of individual ERGs has provided insight into the cellular dynamics underlying self-renewal and neurogenesis, including the identification of neurons formed through the direct conversion of ERGs into neurons, seemingly without proliferation, as well as neurons formed as a result of symmetric and asymmetric cell divisions.

Techniques such as multiphoton microscopy allow for live imaging up to depths of ~2000 µm, which would include a dorsal view of ERGs at the diencephalic ventricle. Therefore, in the future, genetic lineage tracing as described here could be combined with fluorescent reporters of dopaminergic neurons to investigate the cellular dynamics of ERGs at the diencephalic ventricle, and establish which of the methods of neurogenesis described in the telencephalon apply to dopaminergic neurons formed from ERGs around the diencephalic ventricle in the adult brain.

3.4 Conclusions

Cells lining the ventricle display the morphology of ERGs, and express typical markers of progenitor cells *gfap*, *olig2*, and *her4*. There is heterogeneity in the combinations of markers these cells express, and this appears to correlate with the spatial location of the cells around the ventricle. Using genetic lineage tracing, I showed that Th^{+} neurons can be derived from *her4*$^{+}$ ERGs in the adult zebrafish brain.

Chapter Four: Investigating the Signalling Pathways Involved in the Regeneration of Th^+ Neurons

4.1 Introduction

Neurogenesis of Th^+ neurons is increased following ablation with 6OHDA, as demonstrated by an increase in the number of Th^+/EdU^+ cells in population 5/6 (Figure 1.4). In the previous chapter I showed that after ablation, new Th^+ neurons originate from ERGs at the diencephalic ventricle (Figure 3. 3).

Here I investigate the signals involved in the increased Th^+ neurogenesis after ablation of Th^+ neurons. A number of different signalling mechanisms have been shown to mediate neuroregeneration, including the re-deployment of developmental signalling pathways, as well as regeneration specific mechanisms (Becker & Becker 2015; Kizil et al. 2012; Kyritsis et al. 2012; Berg et al. 2011). First I investigate the role of the immune system, which has been implicated in a wide range of regenerative processes across species. I assess the effect of immune activation and immune suppression on ERG proliferation and Th^+ neurogenesis, as well as the effects of modulating specific immune molecules. Secondly, I ask whether ERGs proliferate in response to the reduced levels of dopamine in the brain after a loss of Th^+ neurons (Figure 1.2).

4.1.1 The immune system and regeneration

In the CNS the main mediators of inflammation are resident immune cells called microglia. A significant degree of neuronal cell death in the CNS is likely to elicit an immune response, whether the damage is caused by a mechanical lesion, chemical ablation, or a genetic variant. Hence, microglial activation is a hallmark of many

chronic neurodegenerative diseases, such as Alzheimer's disease (Clayton et al. 2017), Parkinson's disease (Joshi & Singh 2018), and Multiple Sclerosis (Herranz et al. 2016). Similarly, traumatic brain injuries, strokes, and spinal cord injuries elicit a significant immune response (Lehnardt 2009).

The effect of this immune reaction on the process of regeneration appears to be multifaceted, and the overall influence of an immune reaction on the extent and speed of repair varies depending on the timing and magnitude of the immune reaction, the type of insult, the area of the CNS affected, and the species being investigated (DiSabato et al. 2016). Immune cells can perform positive functions such as clearing dying cells and debris, abating infection, and even producing pro-regenerative molecules (Kyritsis et al. 2012; Bhattarai et al. 2016). If delivered with the appropriate timing and measure, promoting an immune response has been shown to accelerate regeneration (Tsarouchas et al. 2018).

4.1.1.1 The immune system and neuroregeneration of the CNS in zebrafish

Successful neuroregeneration in zebrafish has been studied using a variety of different models. Regardless of the method used to damage the CNS, a response is elicited from the resident immune cells of the CNS, microglia, whether neurons are lost due to a mechanical lesion (Becker & Becker 2001; Kyritsis et al. 2012; Ohnmacht et al. 2016), a (chemo)genetic manipulation (Flinn et al. 2013; Ohnmacht et al. 2016), or injection of a neurotoxic substance (Skaggs et al. 2014; Bhattarai et al. 2016). This correlation between eliciting an immune response and successful regeneration of the CNS has inspired investigations into whether an immune response is necessary and/or sufficient to induce neurogenesis, primarily through pharmacological modulation of the immune response.

In zebrafish larvae, a spinal cord lesion elicits a response from immune cells, including microglia (Ohnmacht et al. 2016; Tsarouchas et al. 2018). Suppression of the lesion-induced immune response with the synthetic glucocorticoid dexamethasone impairs spinal cord regeneration after a lesion, demonstrated by a reduction in neurogenesis of motor neurons (Ohnmacht and Yang et al. 2016) and inhibition of the regeneration of axons crossing the lesion site (Tsarouchas et al. 2018). Conversely, treating lesioned larvae with the immuno-stimulant lipopolysaccharide (LPS) improved axonal regeneration at 24 hours post lesion (Tsarouchas et al. 2018).

Similarly, a stab lesion to the adult telencephalon also leads to the recruitment of microglia/macrophages to the lesion site (Kyritsis et al. 2012). Inhibition of this immune response with dexamethasone treatment reduced the number of proliferating ERGs and the number of newly formed neurons after an injury, indicating that an immune response is necessary for successful neuroregeneration in least some areas of the adult zebrafish brain. Moreover, stimulating an immune response in the absence of a mechanical lesion was shown to be sufficient to increase the neurogenesis. However, the authors did not show any results demonstrating the effect of stimulating the immune system after a physical lesion, in other words, whether immune activation could boost regeneration.

These findings suggest that a response from microglia is required for the successful replacement of neurons after injury of the CNS, and that stimulating the immune system alone can promote neurogenesis in the adult brain. However, the results discussed here are limited to models with physical injury, where a microglial reaction is likely to be more pronounced than other CNS insults due to greater tissue disruption and hence more debris to be cleared. This led us to ask whether the immune system plays a similar role in neuroregeneration when a specific population of neurons is ablated without physical injury.

4.1.1.2 Molecular mechanisms for the interaction between the immune system and neuroregeneration

The discovery of a key role for the immune system in regeneration inspired investigations into molecular signals which may be released from microglia to instruct ERGs to proliferate and increase neurogenesis. In this chapter I have focussed on two molecules which are released by immune cells and have been shown to promote regeneration of the zebrafish CNS.

Leukotrienes are peptide-conjugated lipids and act as pro-inflammatory mediators synthesised and released by microglia in response to stimulation. Expression of the leukotriene receptor gene *cysteinyl leukotriene receptor 1 (cysltr1)* is increased around the ventricle in the lesioned hemisphere after a stab lesion in the adult zebrafish telencephalon, and also when microglia are activated with zymosan in the absence of an injury (Kyritsis et al. 2012). Both a stab lesion and zymosan injection lead to increased proliferation of ERGs, indicating that leukotrienes could be released by activated microglia and increase ERG proliferation.

Injection of leukotriene C4 (LTC4), one of the ligands for cysltr1, increased proliferation of ERGs and increased neurogenesis in the uninjured telencephalon (Kyritsis et al. 2012). On the other hand, the cysltr1 antagonist pranlukast decreased radial glial cell proliferation and neurogenesis in the lesioned telencephalon. This suggests that cysltr1 signalling is both necessary and sufficient for neurogenesis in the adult telencephalon. However, whether this applies to ERGs in other brain areas, such as the diencephalon, and to neurogenesis of dopaminergic neurons, is not known.

The immune response which occurs alongside regeneration of the zebrafish CNS includes upregulation of genes encoding pro-inflammatory cytokines. Expression of

tnf-α and *il-1β* are increased after a stab lesion to the telencephalon (Kyritsis et al. 2012) and a spinal cord lesion in larvae (Tsarouchas et al. 2018). Inhibiting tnf-α signalling, either pharmacologically with pomalidomide or with CRISPR/Cas9 targeted to *tnf-α*, impaired regeneration of the spinal cord in larval zebrafish (Tsarouchas et al. 2018). This demonstrates that tnf-α signalling is necessary for successful neuroregeneration in the zebrafish CNS, but the role of tnf-α in promoting neurogenesis in the adult zebrafish brain is not yet known.

4.1.2 Dopamine as a molecule regulating the neurogenesis of Th$^+$ neurons

The signalling pathways underlying the replacement of neurons in the zebrafish brain have been investigated using models where a general insult is used to induce neuronal cell death, such as mechanical lesions, excitotoxic injury, or injection of cell-penetrating Aβ42 derivatives (Kyritsis et al. 2012; Skaggs et al. 2014; Bhattarai et al. 2016). As cell death is not specifically induced in one particular type of neuron, neurogenesis is measured by counting the numbers of new cells co-labelled with pan neuronal markers such as HuC (Kyritsis et al. 2012; Skaggs et al. 2014; Bhattarai et al. 2016). In contrast, the advantage of our 6OHDA model is that I can investigate the signals involved in specifically replacing one neuronal cell type. It is conceivable that after a selective loss of dopaminergic neurons there may be a specific signalling mechanism in place to sense this loss and instruct neural progenitor cells to generate new dopaminergic neurons, rather than a general signal to increase neurogenesis.

In the salamander, Th$^+$ neurons can be ablated by 6OHDA injection, demonstrated by a 75% reduction in the number of Th$^+$ cells of and the presence of TUNEL$^+$/Th$^+$ cells only in 6OHDA-injected animals (Parish et al. 2007). The number of Th$^+$ cells is recovered by 30 days post 6OHDA injection (Parish et al. 2007). Th$^+$ cell numbers are restored through the recruitment of quiescent progenitor cells, as demonstrated by Th$^+$/BrdU$^+$ cells observed in 6OHDA injected animals at 30 dpi and an absence of

$Th^+/BrdU^+$ cells in sham injected controls (Parish et al. 2007). Lineage tracing by electroporating plasmids encoding fluorescent proteins into ventricular cells revealed that $gfap^+$ ERGs cells give rise to new Th^+ neurons after 6OHDA injection (Berg et al. 2010). Interestingly, the number of proliferating ERGs was dramatically reduced by injection of the dopamine precursor L-DOPA in 6OHDA-injected animals, but not in sham-injected controls, or when cholinergic neurons were ablated instead (Berg et al. 2011). Furthermore, L-DOPA inhibited the recovery of Th^+ neurons after 6OHDA ablation, indicating that an increased level of dopamine in the brain can inhibit regeneration of Th^+ neurons. On the other hand, the dopamine receptor antagonist haloperidol evoked ERG proliferation and Th^+ cell numbers, showing that mimicking the decreased levels of dopamine seen after ablation of Th^+ neurons (Figure 1.2, Thiele et al. 2012; Hoffman et al. 1997) can induce Th^+ neurogenesis. Both D1 and D2 dopamine receptors were found to be expressed by ERGs in the midbrain, but a selective D1 receptor antagonist had no effect on cell cycle re-entry, suggesting the signalling is mediated through D2 receptors. Taken together, these results suggest that the level of dopamine regulates the proliferation of ERGs, thus driving the regeneration of Th^+ neurons after 6OHDA-induced ablation.

Neurotransmitters, including dopamine, have been shown to influence proliferation of ERGs in the zebrafish spinal cord (Reimer et al. 2013; Barreiro-Iglesias et al. 2015). Dopamine regulates neurogenesis during development (Reimer et al. 2013; Ohnmacht et al. 2016), and dopamine signalling after a spinal cord lesion is required and sufficient to induce neurogenesis of motor neurons in adult zebrafish (Reimer et al. 2013). This demonstrates that ERGs in at least some parts of the CNS of adult zebrafish are responsive to dopamine, and that dopamine can affect neurogenesis. However, the effect of dopamine signalling on the neurogenesis of Th^+ neurons in the zebrafish brain is yet to be elucidated.

4.2 Results

4.2.1 Injection of 6OHDA elicits an immune response

Injection of 6OHDA leads to dopaminergic cell death in population 5/6, as shown by the presence of TUNEL$^+$/*dat*:GFP$^+$ cells in 6OHDA injected fish only (Figure 4. 1). At the location of population 5/6, microglia appear more abundant in 6OHDA injected brains compared to sham controls, and in some cases appear to engulf TUNEL$^+$/*dat*:GFP$^+$ cells, indicating activation of these immune cells.

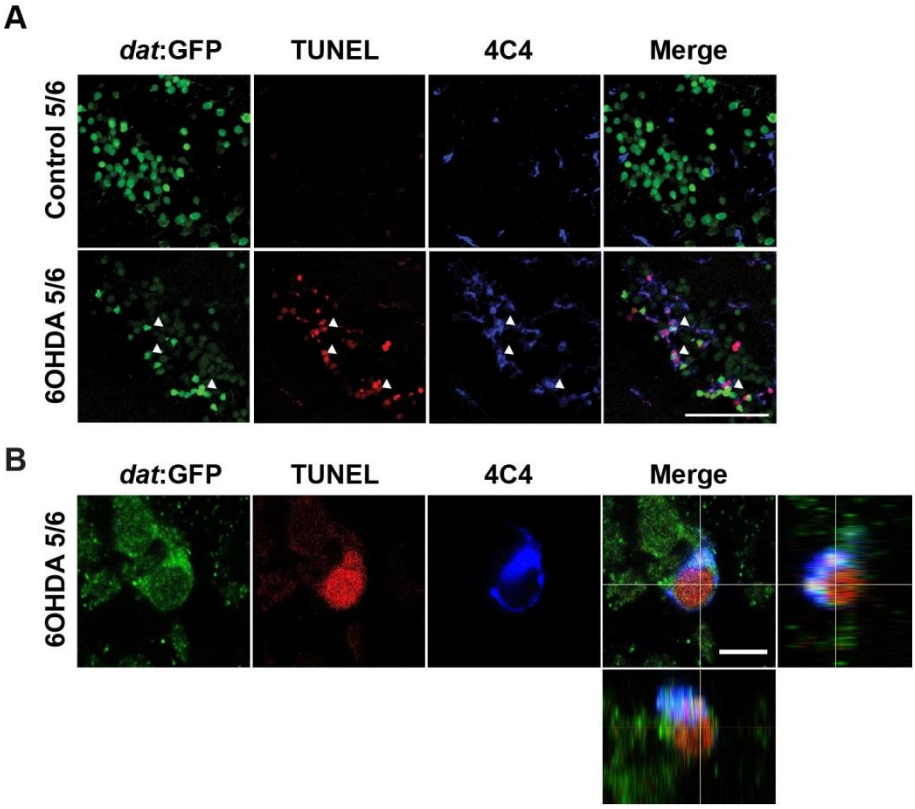

Figure 4. 1 6OHDA elicits an immune response. A: Sagittal sections of population 5/6 in *dat*:GFP fish, showing increased TUNEL and microglia labelling. B: High magnification images with orthogonal views show a GFP$^+$/TUNEL$^+$ neuron engulfed by a microglial cell. Scale bar in A = 50 µm, B = 5 µm. A was performed and imaged by Nick Davies, images in B were taken by myself. Figure is adapted from (Caldwell & Davies et al. 2018).

Together with Leonardo Cavone, a postdoctoral researcher in our group, I assessed the levels of pro-inflammatory cytokines after 6OHDA injection. Fish were injected with 6OHDA and RNA was extracted from a horizontal brain section comprising population 5/6 and the diencephalic ventricle at 3 dpi. Quantitative RT-PCR results

showed a 6OHDA-induced increase in expression of the pro-inflammatory cytokines *tnf-α* and *il-1β* compared to sham injected fish (Figure 4. 2, fold increase in *tnf-α* expression: 5.788 ± 1.398 compared to sham: 1.00 ± 0.00, fold increase in *il-1β* expression: 2.199 ± 0.4399 compared to sham: 1.00 ± 0.00), confirming that there is an immune response to 6OHDA injection. This increase was abolished by immersing the fish in the immunosuppressant dexamethasone (Figure 4. 2, fold increase in *tnf-α* expression: 0.9325 ± 0.3086 compared to sham: 1.00 ± 0.00, fold increase in *il-1β* expression: 0.7868 ± 0.5214 compared to sham: 1.00 ± 0.00). This shows that dexamethasone treatment can reduce the immune response to levels comparable with sham injected fish, and allowed us to investigate whether the 6OHDA-induced immune response is involved in the regeneration of Th^+ neurons.

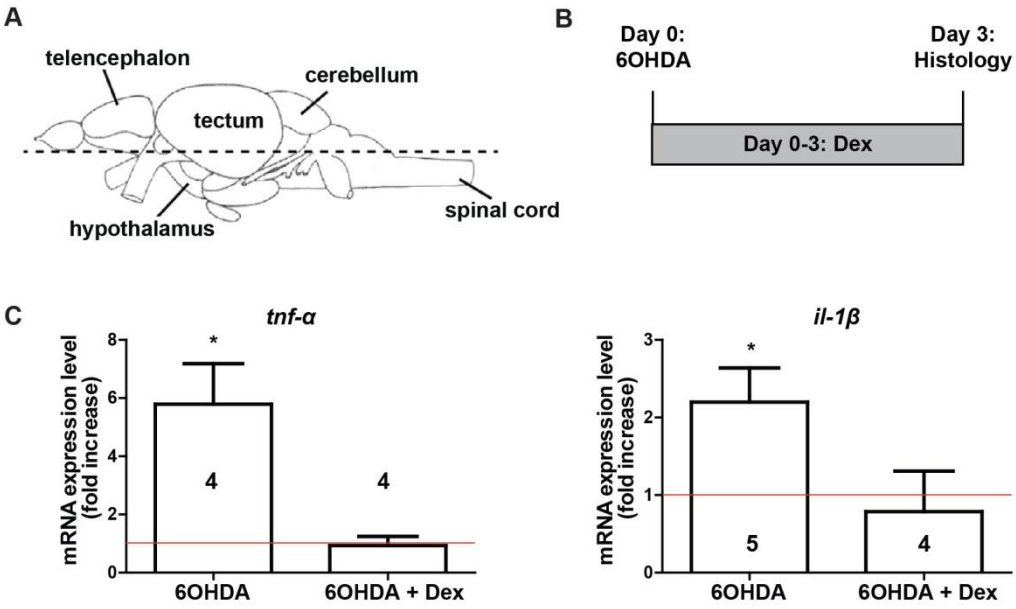

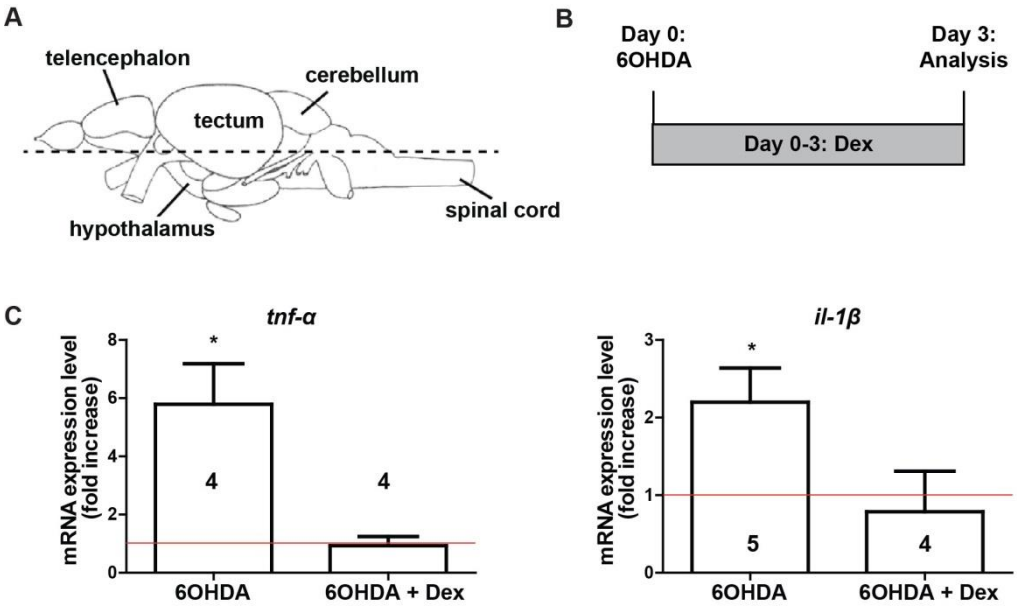

Figure 4. 2 6OHDA increases expression of pro-inflammatory cytokines. A: The level of horizontal section used for analysis is shown. B: The experimental timeline is given. C: Quantitative RT-PCR shows that expression of *il-1β* and *tnf-α* is increased compared to sham injected controls (1, indicated by the red line), but not in fish also treated with dexamethasone. One-tailed one-sample t-tests (*p < 0.05). N numbers on the graphs indicate the number of fish used in each condition. Figure is adapted from (Caldwell & Davies et al. 2018).

4.2.2 6OHDA increases proliferation of ERGs, and an immune response is necessary for this increase in progenitor proliferation

As discussed in the previous chapter, in the adult zebrafish brain Th^+ cells are derived from ERGs lining the diencephalic ventricle (Figure 3. 3), and these cells are a heterogeneous population in terms of expression of *gfap* and *olig2* (Figure 3. 2), with subpopulations of *gfap*:GFP^+/*olig2*:$DsRed^-$ cells, *olig2*:$DsRed^+$/*gfap*:GFP^- cells, and *gfap*:GFP^+/*olig2*:$DsRed^+$ cells. I could therefore investigate the effects of injecting 6OHDA and modulating the immune response on the proliferation of these progenitor cells by counting the number of EdU^+ cells in each of these subpopulations.

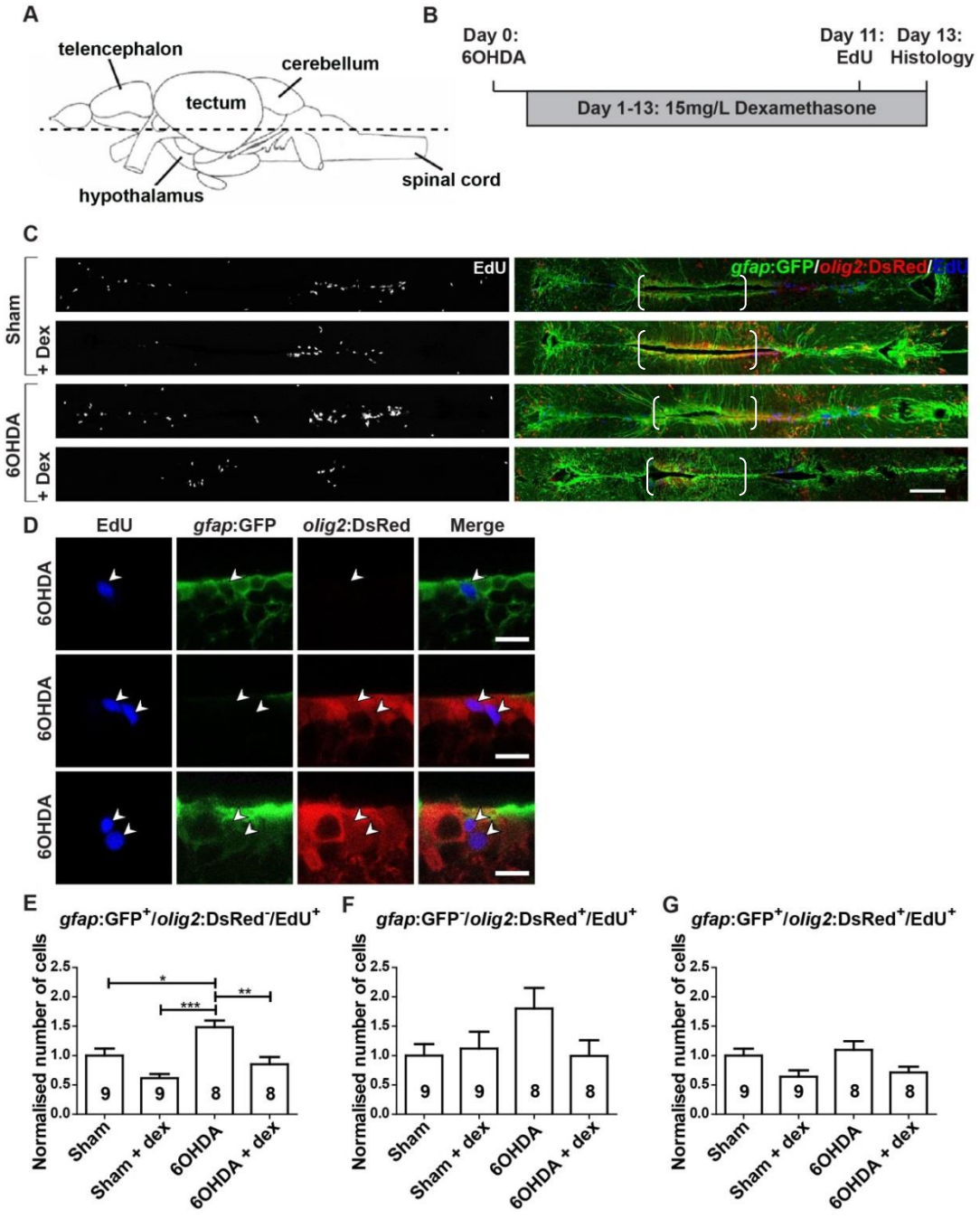

Figure 4. 3 6OHDA injection increases ERG proliferation, which is abolished by dexamethasone treatment. A: The section level of photomicrographs (A, rostral is left). B: The experimental timeline is given. C,D: Overviews (C) of the quantification areas and higher magnifications of ventricular cells (D) are given. EdU-labelled ERGs are *gfap*:GFP$^+$, *olig2*:DsRed$^+$, or both. White brackets indicate the approximate location of Th$^+$ cells in population 5/6. E-G: Quantification of the normalised numbers of EdU$^+$ ERGs in each treatment co-labelled with only *gfap*:GFP (E), only *olig2*:DsRed (F) or both *gfap*:GFP and *olig2*:DsRed (G). One-way ANOVA with Bonferroni post-hoc test, *p < 0.05, **p < 0.01, ***p<0.001. Scale bars in C = 100 µm; in D = 10 µm. Figure is adapted from (Caldwell & Davies et al.2018).

Injection of 6OHDA led to an increase in the number of *gfap*:GFP$^+$/*olig2*:DsRed$^-$EdU$^+$ ERGs (p=0.022). I found 6OHDA had no effect on the numbers of EdU$^+$ cells for

gfap:GFP$^-$/*olig2*:DsRed$^+$ (p=0.079) or*gfap*:GFP$^+$/*olig2*:DsRed$^+$ cells (p=1.000). However, the effect of 6OHDA on *gfap*:GFP$^-$/*olig2*:DsRed$^+$ cells was approaching significance, and so more animals could be used to determine whether there is a significant increase in this population of ERGs or not (Figure 4. 3E-G: EdU$^+$/*gfap*:GFP$^+$/*olig2*:DsRed$^-$ cells: sham: 1.000 ± 0.1190, sham + dex: 0.6147 ± 0.0718, 6OHDA: 1.483 ± 0.1138, 6OHDA + dex: 0.8525 ± 0.1239; EdU$^+$/*gfap*:GFP$^-$/*olig2*:DsRed$^+$ cells: sham: 1.000 ± 0.1958, sham + dex: 1.120 ± 0.2847, 6OHDA: 1.801 ± 0.3491, 6OHDA + dex: 0.9953 ± 0.2654; *gfap*:GFP$^+$/*olig2*:DsRed$^+$ cells: sham: 1.000 ± 0.1170, sham + dex: 0.6397 ± 0.1088, 6OHDA: 1.098 ± 0.1464, 6OHDA + dex: 0.7113 ± 0.1003).

To test whether an immune response affects the number of proliferating progenitor cells I incubated adult zebrafish in the immunosuppressant dexamethasone and counted the number of EdU$^+$ cells expressing markers of ERGs. Immunosuppression did not affect the number of EdU$^+$ progenitor cells after a sham injection; however, the 6OHDA-induced increase in proliferation was abolished by immunosuppression (Figure 4. 3E-G: EdU$^+$/*gfap*:GFP$^+$/*olig2*:DsRed$^-$ cells: sham: 1.000 ± 0.1190, sham + dex: 0.6147 ± 0.0718, 6OHDA: 1.483 ± 0.1138, 6OHDA + dex: 0.8525 ± 0.1239; EdU$^+$/*gfap*:GFP$^-$/*olig2*:DsRed$^+$ cells: sham: 1.000 ± 0.1958, sham + dex: 1.120 ± 0.2847, 6OHDA: 1.801 ± 0.3491, 6OHDA + dex: 0.9953 ± 0.2654; *gfap*:GFP$^+$/*olig2*:DsRed$^+$ cells: sham: 1.000 ± 0.1170, sham + dex: 0.6397 ± 0.1088, 6OHDA: 1.098 ± 0.1464, 6OHDA + dex: 0.7113 ± 0.1003). Hence, the immune response elicited by 6OHDA is necessary to increase the proliferation of ERGs.

4.2.3 An immune response is necessary for efficient regeneration of Th$^+$ neurons

I hypothesised that immunosuppression may also impair regeneration of Th$^+$ cells. Therefore, I compared the numbers of newly generated Th$^+$ neurons in fish treated

with dexamethasone with vehicle-treated fish 42 days after 6OHDA injection. In population 5/6, the number of Th^+ neurons generated after 6OHDA injection (Th^+/EdU^+ cells) was reduced by 58.8% in immunosuppressed fish compared to vehicle-treated controls (Figure 4. 4D, 6OHDA: 8.25 ± 1.708, 6OHDA + dex: 3.4 ± 0.8944). I then tested whether suppressing the immune reaction caused by a 6OHDA injection would also lead to lower numbers of overall Th^+ cells. I found lower numbers of Th^+ neurons in the 5/6 population in fish treated with dexamethasone compared to controls, confirming that dexamethasone treatment impaired the replacement of Th^+ neurons following ablation (Figure 4. 4E, 6OHDA: 270.0 ± 16.94, 6OHDA + dex: 201.4 ± 14.25).

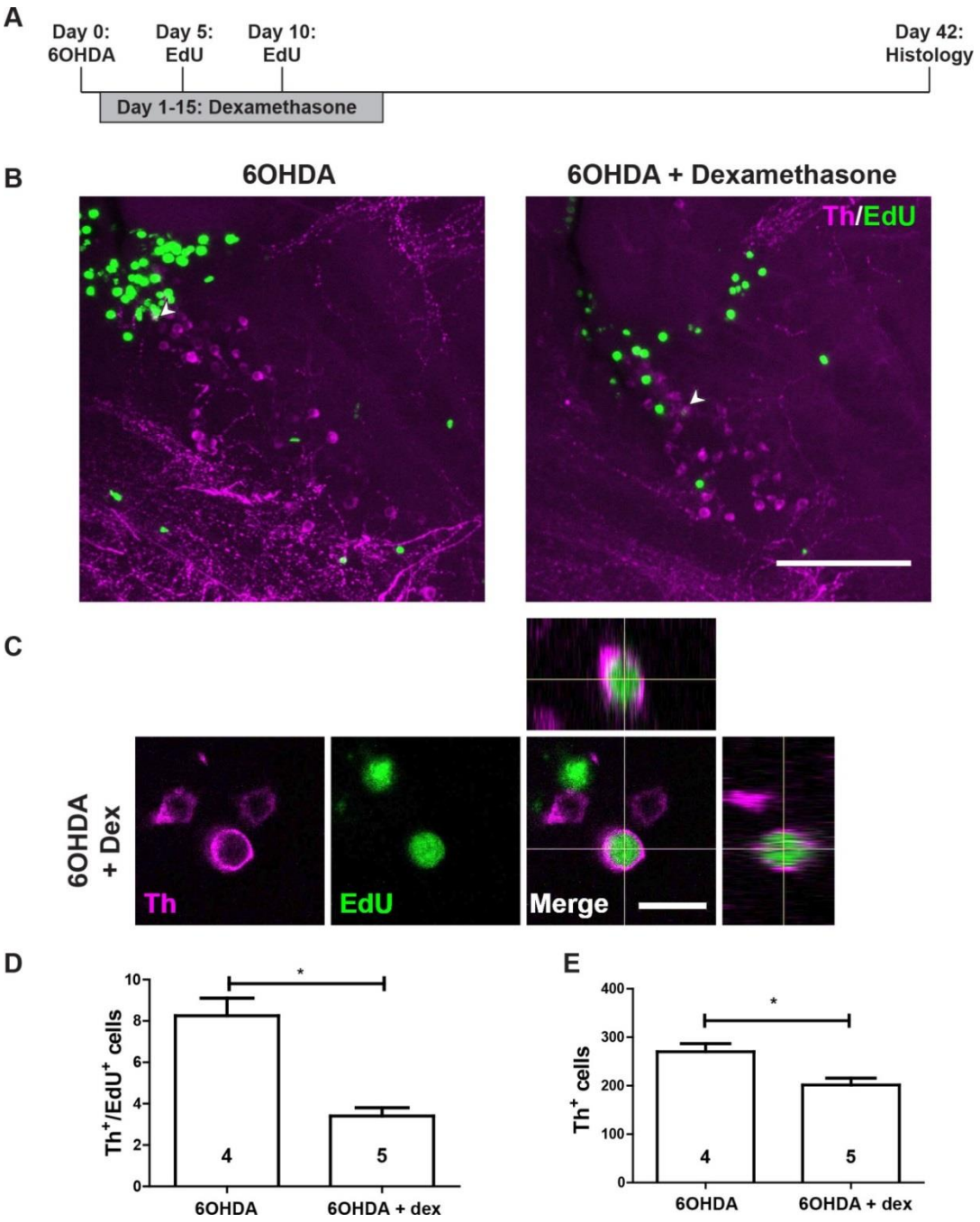

Figure 4. 4 Dexamethasone inhibits regeneration of Th^+ neurons in the 5/6 population. A: The experimental timeline is given. B: In sagittal sections, EdU^+/Th^+ neurons can be observed (arrows) after 6OHDA injection, with or without addition of dexamethasone. C: High magnification and orthogonal views of an EdU^+/Th^+ neuron are shown. D,E: The number of EdU^+/Th^+ (D) and the overall number of Th^+ neurons (E) are reduced by treating 6OHDA-injected animals with dexamethasone (Mann Whitney-U test, $*p < 0.05$ (D), Student's t test, $*p < 0.05$ (E)). Scale bar in B = 100 µm, scale bar in C = 10 µm. Figure is reproduced from (Caldwell & Davies et al. 2018).

4.2.4 Activating an immune response is sufficient to increase progenitor proliferation, but does not significantly enhance 6OHDA-induced ERG proliferation

I hypothesised that a microglial response could be sufficient to increase proliferation of ERGs, leading to more efficient regeneration of Th^+ neurons. Therefore, I decided to stimulate an immune response by injecting zymosan, a component of fungal cells walls used to induce sterile inflammation (Underhill 2003; Kyritsis et al. 2012). Nick Davies, a previous PhD student in our group, showed that injection of zymosan into the brain caused an immune response, demonstrated by the increase in microglia labelled with 4C4 (Caldwell and Davies et al. 2018). I injected zymosan into the brain and extracted RNA from a horizontal section containing population 5/6 and the diencephalic ventricle. Quantitative RT-PCR results for the pro-inflammatory cytokines *tnf-α* and *il-1β* were highly variable, but the average increase in mRNA for both cytokines was more than 40-fold compared to sham injected fish, which combined with the p values suggests that zymosan had an effect on the immune system (Figure 4. 5, fold increase compared to sham, *tnf-α*: 46.89 ± 24.63 compared to sham: 1.00 ± 0.00 (p=0.2035), *il-1β*: 49.06 ± 22.31 compared to sham: 1.00 ± 0.00 (p=0.1641)). As the results of this experiment did not reach statistical significance and the variation of the result was so high, more animals could help determine whether zymosan affected the level of cytokines or not.

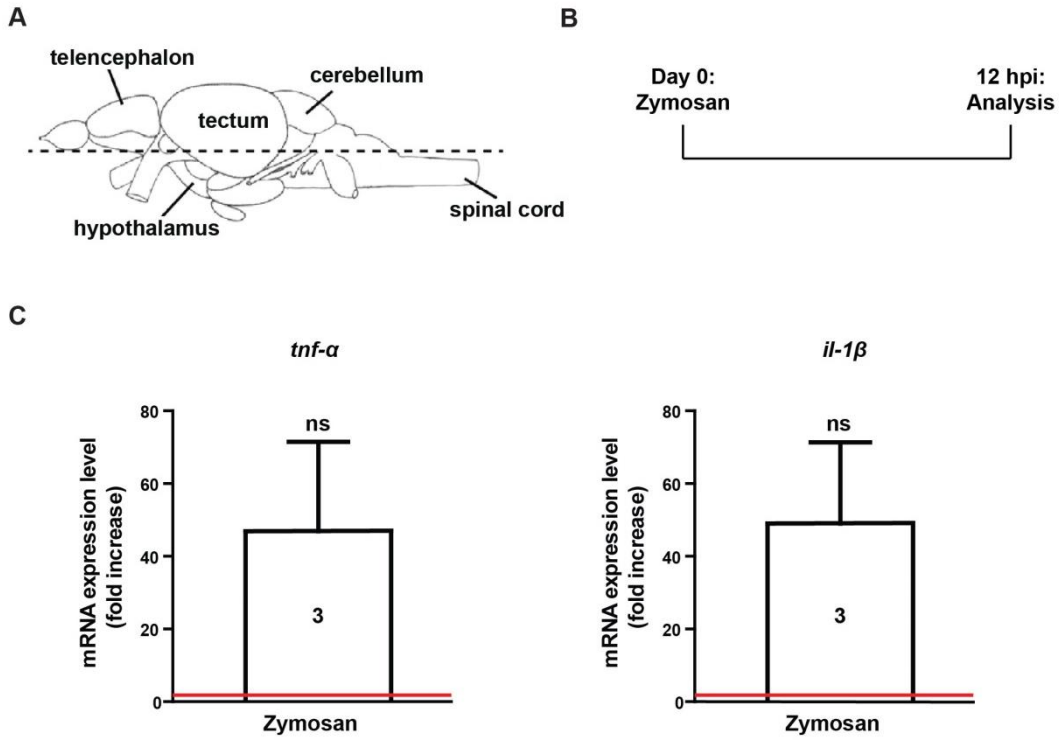

Figure 4. 5 Zymosan increases expression of pro-inflammatory cytokines. A: The level of the horizontal section used for analysis is shown. B: The experimental timeline is given. C: Quantitative RT-PCR shows expression of *il-1β* and *tnf-α* is increased compared to sham injected controls (1, indicated by the red line). One-tailed one-sample t-tests (*p < 0.05). N numbers on the graphs indicate the number of fish used in each condition.

Injections of zymosan alone were sufficient to increase the number of EdU^+ progenitor cells for both *gfap*:GFP^+/*olig2*:$DsRed^-$ (p=0.004) and *gfap*:GFP^-/*olig2*:$DsRed^+$ cells (p=0.20), indicating that inducing a microglial response is able to affect proliferation of ERGs (Figure 4. 6, EdU^+/*gfap*:GFP^+/*olig2*:$DsRed^-$: sham: 1.000 ± 0.04478, sham + zy: 1.583 ± 0.1695, 6OHDA: 1.560 ± 0.1506, 6OHDA + zy: 2.242 ± 0.2369, EdU^+/*gfap*:GFP^-/*olig2*:$DsRed^+$: sham: 1.000 ± 0.05786, sham + zy: 1.609 ± 0.1344, 6OHDA: 2.157 ± 0.2405, 6OHDA + zy: 2.232 ± 0.2402, EdU^+/*gfap*:GFP^+/*olig2*:$DsRed^+$: sham: 1.000 ± 0.2655, sham + zy: 1.322 ± 0.3214, 6OHDA: 1.417 ± 0.2741, 6OHDA + zy: 1.692 ± 0.3422).

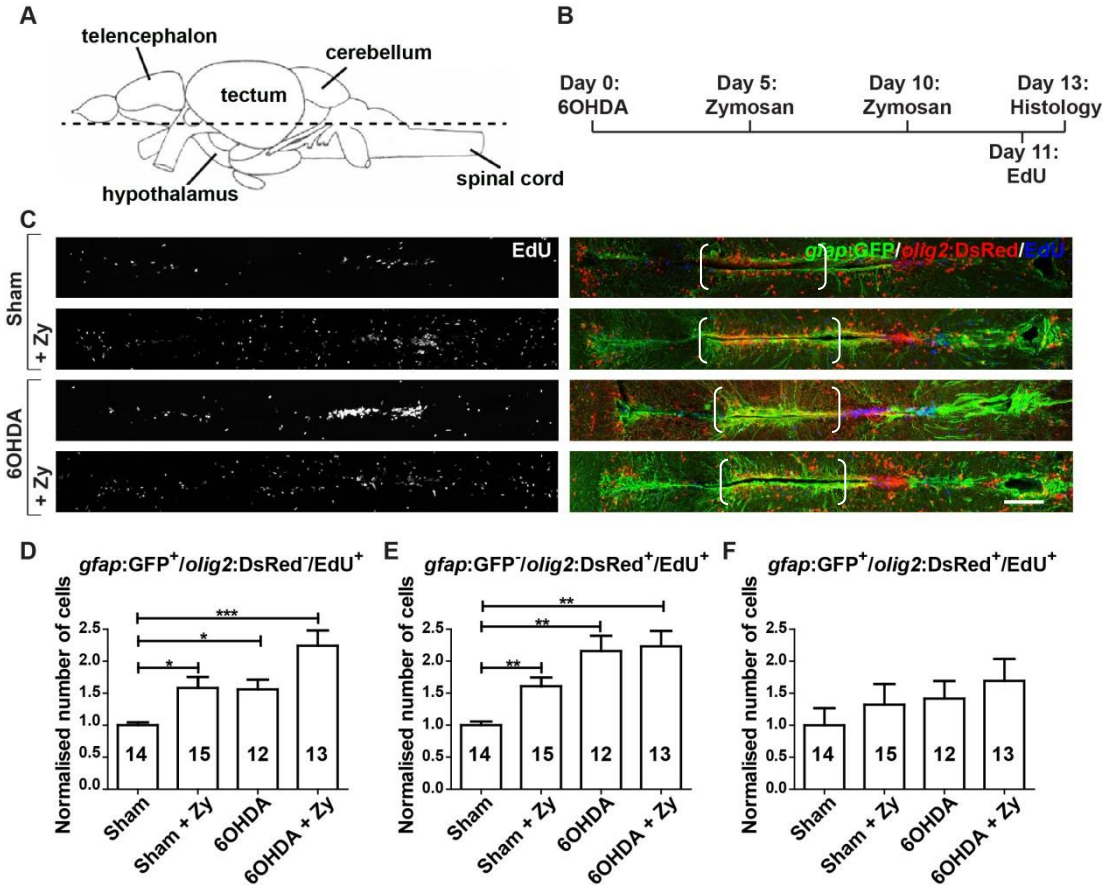

Figure 4. 6 6OHDA and zymosan both increase ERG proliferation. A: The level of the horizontal section used for analysis is shown, marked by the dotted line. B: The experimental timeline is given. C-F: 6OHDA injections and zymosan injections significantly increase proliferation of ventricular cells. White brackets in C indicate the approximate location of Th$^+$ cells in population 5/6. D,-F: One-way ANOVA with Welch's correction and Games-Howell post-hoc test (*p < 0.05, **p < 0.01, ***p < 0.001). Scale bar in C = 100 µm. Figure is adapted from (Caldwell & Davies et al. 2018).

However, zymosan injections did not affect the number of EdU$^+$ ERGs cells after ablation when compared to 6OHDA alone, and this was the case for all of the subtypes of ERGs counted (Figure 4. 6). This suggests that although the proliferation of ERGs may be increased by both drugs alone, there may be a maximal limit to the proliferation capacity of ERGs which cannot be overcome by injecting both zymosan and 6OHDA.

4.2.5 Activating an immune response is not sufficient to increase regeneration of Th^+ neurons

To determine whether enhancing the immune response could increase the regeneration of Th^+ neurons I assessed the number of EdU^+/Th^+ cells after 6OHDA injection with and without zymosan. In line with unchanged ERG proliferation (Figure 4. 6), there was no effect of zymosan on either the number of newly generated Th^+ cells labelled with EdU (Figure 4. 7D, 6OHDA: 7.667 ± 0.8819, 6OHDA + zy: 7.000 ± 1.080), or the overall number of Th^+ cells in population 5/6 (Figure 4. 7E, 6OHDA: 244.4 ± 19.03, 6OHDA + zy: 232.7 ± 21.02). This indicates that inducing a microglial reaction with zymosan is not sufficient to improve the regeneration of Th^+ neurons.

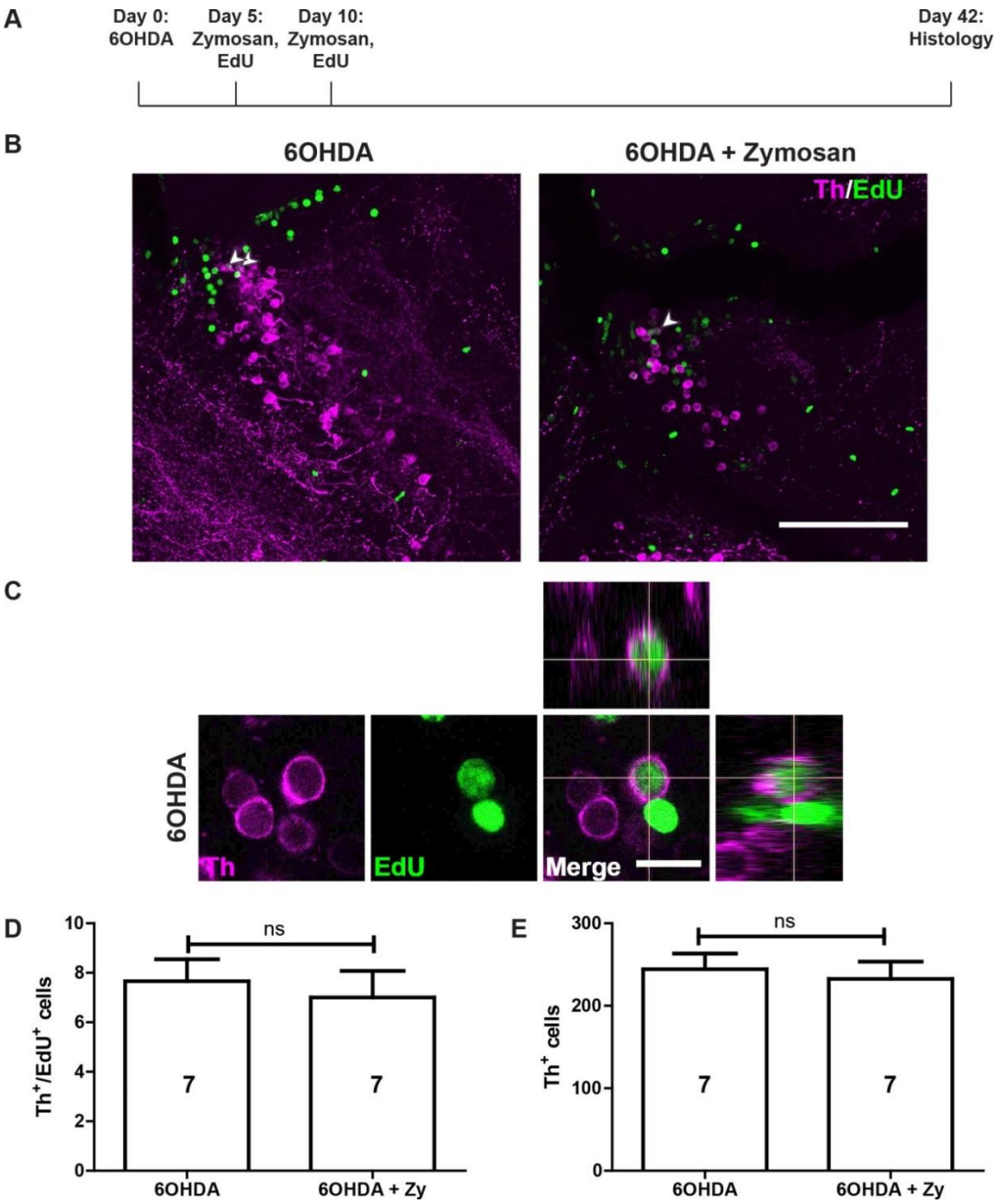

Figure 4. 7 Zymosan treatment does not augment Th^+ neuron replacement in population 5/6. A: The experimental timeline is indicated. B: In sagittal sections, EdU^+/Th^+ neurons can be observed (arrows) after 6OHDA injection, with or without addition of zymosan. C: High magnification and orthogonal views of an EdU^+/Th^+ neuron are shown. D,E: The number of EdU^+/Th^+ (D) and the overall number of Th^+ neurons (E) are not increased by treating 6OHDA-injected animals with zymosan (Student's t-tests, (*$p < 0.05$)). Scale bar in B = 100 µm; in C = 10 µm. Figure is reproduced from (Caldwell & Davies et al. 2018).

4.2.6 Activity of the immune system is neither necessary nor sufficient for constitutive Th$^+$ neurogenesis

A zymosan-induced microglial response was sufficient to increase the number of EdU$^+$ ERGs at the ventricle (Figure 4. 6), from which Th$^+$ neurons are derived (Figure 3. 3). I therefore hypothesised that manipulating the immune response may affect the number of Th$^+$ neurons in the absence of ablation. To test this, I compared the numbers of Th$^+$ cells and newly generated Th$^+$ cells after immunosuppression with dexamethasone and after stimulation of immune cells with zymosan. Sham injected fish were injected with EdU at 5 dpi and 10 dpi, and analysed at 42 dpi. In one group the immune system was activated by injecting zymosan at 5 dpi and 10 dpi, in another the immune system was suppressed by immersing the fish in dexamethasone from 1-15 dpi, and a third group the immune system was unmanipulated (Figure 4. 8A).

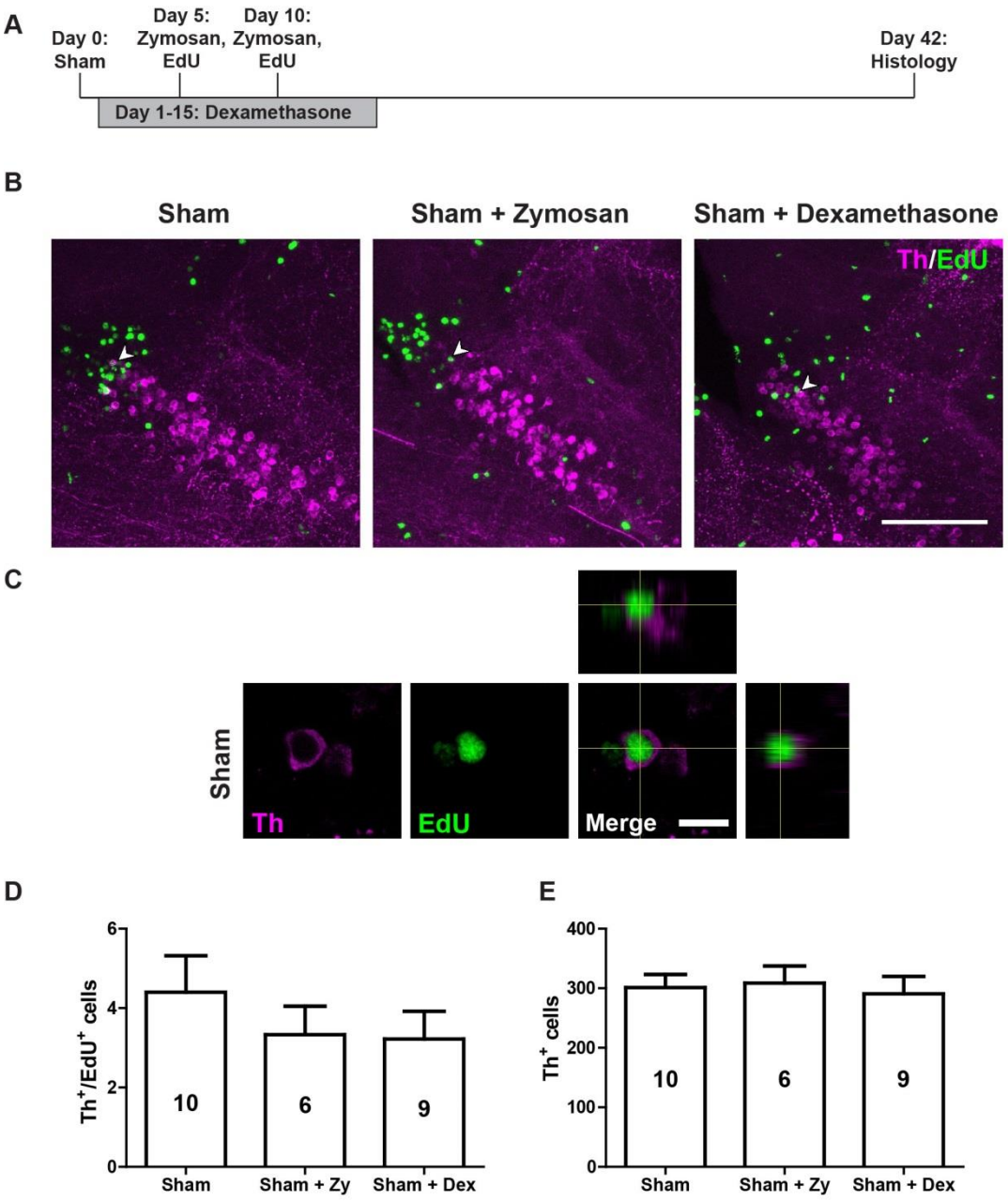

Figure 4. 8 Immune system manipulations in sham animals do not influence addition of new Th^+ cells. A: Timeline of experiments with either zymosan or dexamethasone treatment. B: In sagittal sections, EdU^+/Th^+ neurons (arrowheads) can be observed in all experimental conditions. C: High magnification and orthogonal views of a double-labelled neuron are shown. D,E: No changes were observed in the number of newly generated Th^+ neurons and the overall number of Th^+ neurons after dexamethasone or zymosan treatment (One-way ANOVA with Bonferroni post-hoc test used in D and E, *$p < 0.05$). Scale bar in B = 100 µm, scale bar in C = 10 µm. Figure is reproduced from (Caldwell & Davies et al. 2018).

Both the numbers of newly generated (Th^+/EdU^+) neurons (Figure 4. 8D, sham: 4.400 ± 0.9214, sham + zy: 3.333 ± 0.7149, sham + dex: 3.222 ± 0.7027) and overall Th^+ neuron numbers were found to be the same between all three groups (Figure 4. 8E,

sham: 301.1 ± 21.93, sham + zy: 308.8 ± 28.65, sham + dex: 290.8 ± 29.12). This suggests that activation of the immune system is neither necessary nor sufficient for new Th^+ cells to be generated. Hence, the reduction in the number of new Th^+ cells after dexamethasone treatment is specific to ablation-responsive neurogenesis, and it is not a result of dexamethasone directly inhibiting the constitutive neurogenesis of Th^+ cells.

4.2.7 *Irf8*$^{-/-}$ zebrafish do not have reduced microglia in the adult brain

Dexamethasone is a widely used immunosuppressant; however, the treatment may have unintended effects outside the immune system, confounding the results. I therefore sought to prevent a microglial response using a genetic model to provide more evidence for a requirement of the immune system in regeneration. Together with Karolina Mysiak, I investigated whether *irf8*$^{-/-}$ zebrafish, which have been shown to have fewer microglia in larvae (Shiau et al. 2015), could be used to assess the effects of a reduced immune response on the regeneration of dopaminergic neurons.

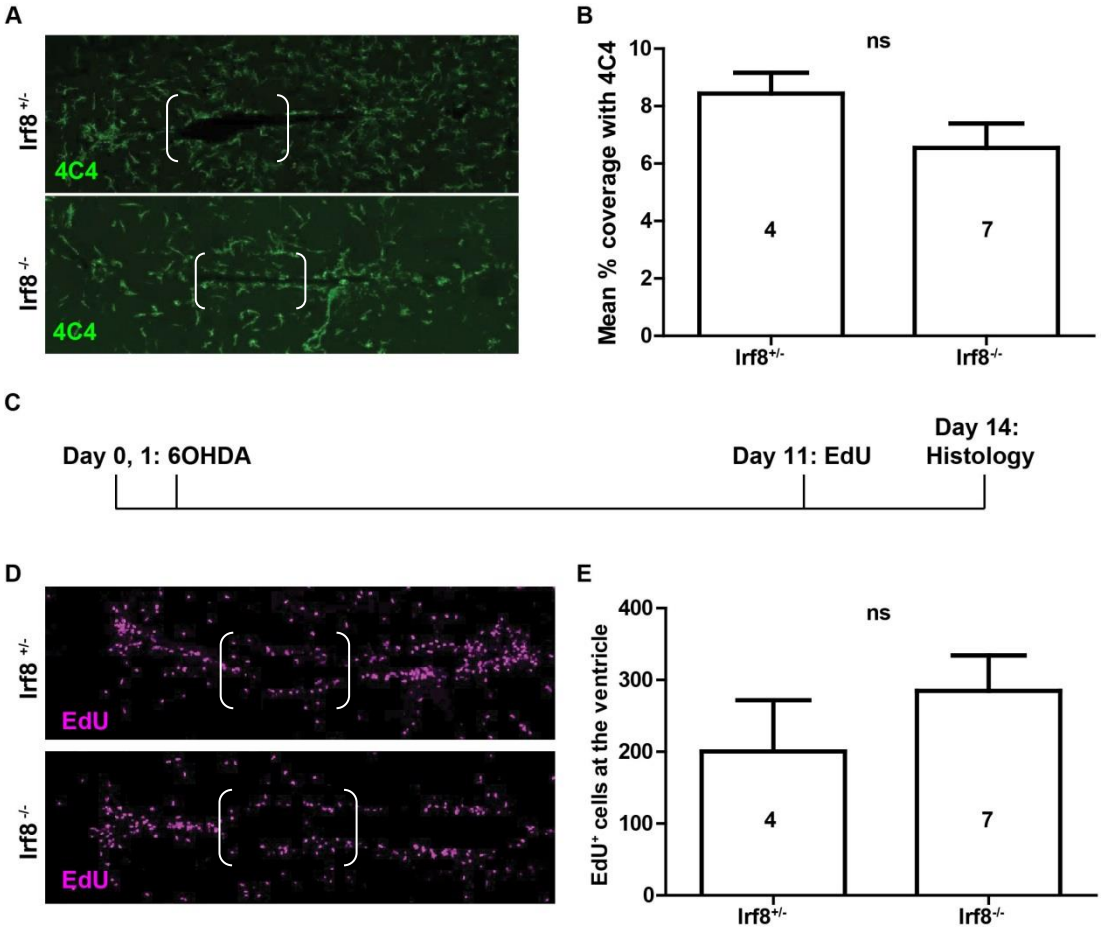

Figure 4. 9 Adult Irf8$^{-/-}$ zebrafish have the same microglia and proliferating cells around the diencephalic ventricle as Irf8$^{+/-}$ fish. A: Horizontal sections around the ventricle show similar 4C4 labelling. White brackets indicate the approximate location of Th^{+} cells in population 5/6. B: Quantification of the percentage of the scanned area covered with 4C4 labelling (Student's t-test, (*p < 0.05)). C: The experimental timeline for D-E is shown. D: Horizontal sections with EdU^{+} cells around the ventricle, white brackets indicate the approximate location of Th^{+} cells in population 5/6. E: Quantification of the numbers of EdU^{+} cells lining the ventricle (Mann Whitney test, (*p < 0.05)). B and C were performed by myself, histology and imaging in D was done by Karolina Mysiak, counting by myself.

First I investigated whether I could detect a difference in the numbers of microglia in the brains of adult *irf8*$^{-/-}$ zebrafish compared to *irf8*$^{+/-}$ zebrafish. Compared to heterozygous fish, *irf8*$^{-/-}$ zebrafish had similar 4C4 labelling (Figure 4. 9A, B), suggesting that the reduced numbers of microglia in these fish during development is not conserved to adulthood (*irf8*$^{+/-}$: 8.438% ± 0.7256%, *irf8*$^{-/-}$: 6.546% ± 0.8479%). Secondly, we investigated whether these fish had a difference in the number of proliferating cells around the diencephalic ventricle in response to 6OHDA ablation. Fish were injected with 6OHDA and with EdU at 11 dpi, and histology was performed

at 14 dpi. We observed no difference in the number of EdU^+ cells lining the ventricle in *irf8*$^{-/-}$ fish compared to *irf8*$^{+/-}$ fish, indicating that there is no difference in the number of proliferating progenitor cells (Figure 4. 9 C-E, *irf8*$^{+/-}$: 200.5 ± 71.49, *irf8*$^{-/-}$: 284.9 ± 49.44). From these results we concluded that *irf8*$^{-/-}$ fish are not a suitable model to investigate the role of the immune system in regeneration of the adult zebrafish brain.

4.2.8 Investigating the molecular signals between microglia and ERGs

Injection of 6OHDA and zymosan both increase the number of proliferating ERGs (Figure 4. 3, Figure 4. 6), and this led us to ask which signals allow ERGs to respond to these manipulations.

4.2.8.1 Leukotriene C4

Both zymosan and 6OHDA elicit an immune response involving an increase in cytokine expression (Figure 4. 2, Figure 4. 5). ERGs in the adult zebrafish brain express receptors for at least some pro-inflammatory cytokines (Kyritsis et al. 2012; Bhattarai et al. 2016). We therefore hypothesised that microglia are influencing progenitor proliferation through the release of a cytokine(s) which signals to ERGs, promoting their proliferation.

Leukotriene C4 (LTC4) has been shown to increase proliferation of ERGs and neurogenesis in the uninjured telencephalon of adult zebrafish (Kyritsis et al. 2012). Together with Karolina Mysiak, I tested whether injecting LTC4 could also increase ERG proliferation and neurogenesis of Th^+ cells.

To address whether injections of LTC4 elicit a microglial response I assessed the level of 4C4 labelling after three consecutive daily injections of LTC4. I observed no significant increase between uninjected and vehicle-injected brains, demonstrating that neither the injection procedure itself nor the vehicle caused a microglial response (Figure 4. 10, uninjected: 1.060 ± 0.06268, vehicle: 1.138 ± 0.03107,

LTC4: 1.621 ± 0.1695). However, LTC4 injected brains had significantly more 4C4 labelling than vehicle-injected brains, indicating that LTC4 induces a microglial response.

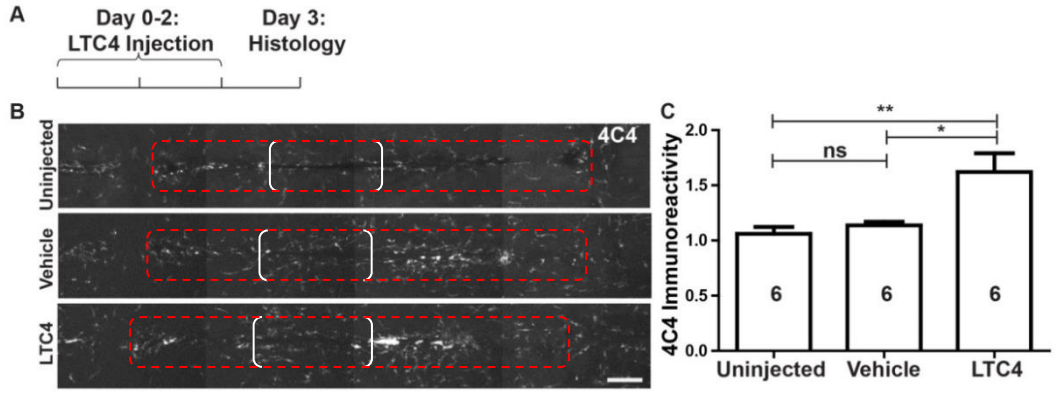

Figure 4. 10 Injection of LTC4 elicits a microglial response. A: The experimental timeline is shown. B: Horizontal sections showing 4C4 labelling around the ventricle (left, rostral). White brackets indicate the approximate location of Th^+ cells in population 5/6. Red dotted lines indicate the area used for quantification of 4C4 immunohistochemistry around the ventricle (see Methods (Section 2.6.2) for details of quantification). C: Quantification of the 4C4 labelling around the ventricle shows LTC4, but not vehicle injection, causes an increase in microglia around the ventricle (One-way ANOVA, *p < 0.05, **p < 0.01). Scale bar in B = 100µm. Figure is adapted from (Caldwell & Davies et al. 2018).

To test whether LTC4 is sufficient to increase proliferation of progenitor cells Karolina Mysiak counted the numbers of ERGs (labelled with *gfap*:GFP, *olig2*:DsRed, or both markers) at the ventricle which were co-labelled with Proliferating Cell Nuclear Antigen (PCNA). We found no difference between animals treated with LTC4 and vehicle treated controls (Figure 4. 11), indicating that LTC4 is sufficient to elicit a microglial response, but it is not sufficient to increase proliferation of ERGs.

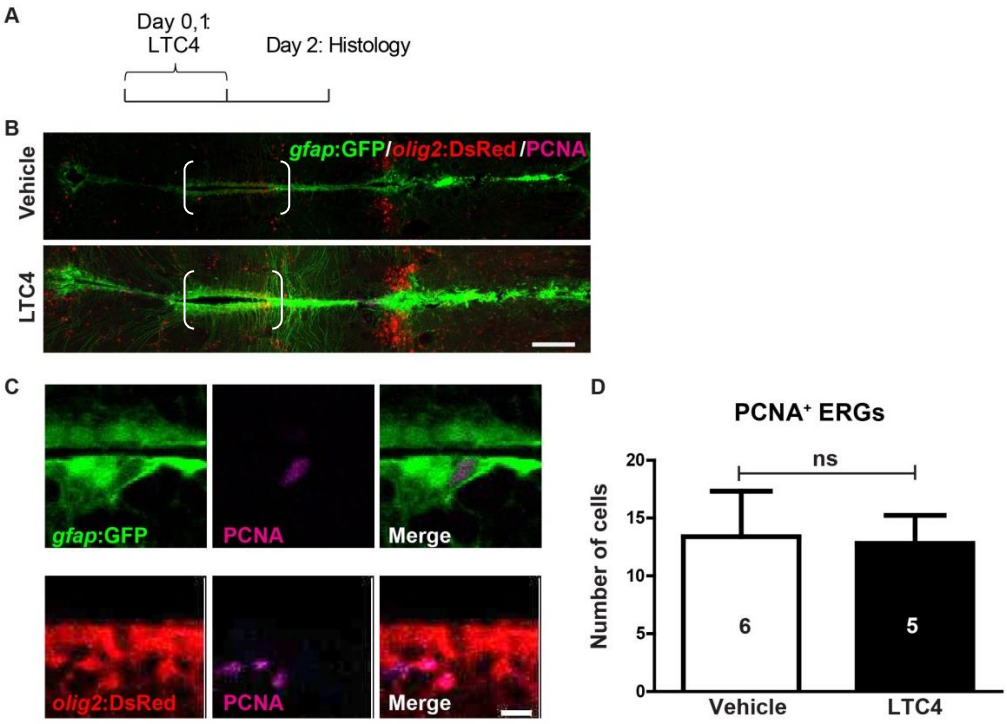

Figure 4. 11 Injection of LTC4 does not affect the number of proliferating ERGs. A: The experimental timeline is shown. B: Horizontal sections showing PCNA$^+$ ERGs around the ventricle. White brackets indicate the approximate location of Th$^+$ cells in population 5/6 . C: High magnification images of PCNA$^+$/*gfap*:GFP$^+$ ERGs and PCNA$^+$/*olig2*:DsRed$^+$ ERGs. D: Quantificstion showing PCNA labelling in ERGs is not increased by LTC4 (Mann Whitney U test, *p < 0.05). Scale bar in B = 100 µm, scale bar in C = 10 µm. Figure is adapted from (Caldwell & Davies et al. 2018).

4.2.8.2 Pomalidomide

The pro-inflammatory cytokine *tnf-α* is elevated in the brains of 6OHDA-injected fish in comparison to sham-injected fish (Figure 4. 2). We hypothesised that *tnf-α* could be one of the key signals linking the microglial response with increased proliferation of ERGs, and may therefore be required for efficient regeneration of Th$^+$ neurons. To test this I used the *tnf-α* signalling inhibitor pomalidomide and observed its effect on ERG proliferation and Th$^+$ cell regeneration.

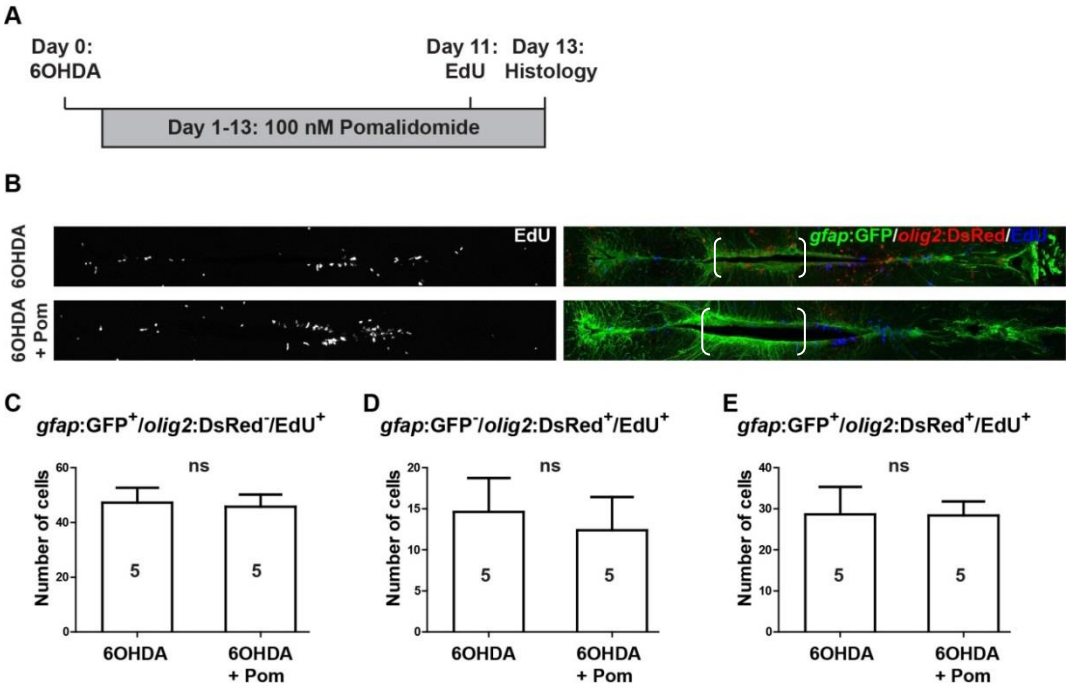

Figure 4. 12 Pomalidomide treatment did not affect proliferation or Th$^+$ neurogenesis. A: The experimental timeline is given. B: Horizontal sections showing EdU$^+$ ERGs around the ventricle. White brackets indicate the approximate location of Th$^+$ cells in the 5/6 population. C-E: Quantification of the number of EdU$^+$ ERGs around the ventricle, Mann Whitney U tests, (*p < 0.05).

Fish were injected with 6OHDA to ablate Th$^+$ neurons and immersed in pomalidomide to inhibit the 6OHDA-induced *tnf-α* signalling. There was no difference in the number of EdU$^+$ ERGs after pomalidomide treatment compared to vehicle-treated controls, suggesting that inhibition of *tnf-α* signalling alone is not sufficient to reduce ERG proliferation (Figure 4. 12, EdU$^+$/*gfap*:GFP$^+$/*olig2*:DsRed$^-$: 6OHDA: 47.20 ± 5.499, 6OHDA + pomalidomide: 45.80 ± 4.363, EdU$^+$/*gfap*:GFP$^-$/*olig2*:DsRed$^+$: 6OHDA: 14.60 ± 4.142, 6OHDA + pomalidomide: 12.40 ± 4.020, EdU$^+$/*gfap*:GFP$^+$/*olig2*:DsRed$^+$: 6OHDA: 28.60 ± 6.742, 6OHDA + pomalidomide: 28.40 ± 3.400). Furthermore, there was no difference in the numbers of new Th$^+$ cells (Figure 4. 13, 6OHDA: 5.500 ± 0.6455, 6OHDA + pomalidomide: 3.500 ± 1.500Figure 4. 12) and in the total numbers of Th$^+$ cells in the 5/6 population (Figure 4. 13, 6OHDA: 226.5 ± 4.500, 6OHDA + pomalidomide: 240.8 ± 25.99).

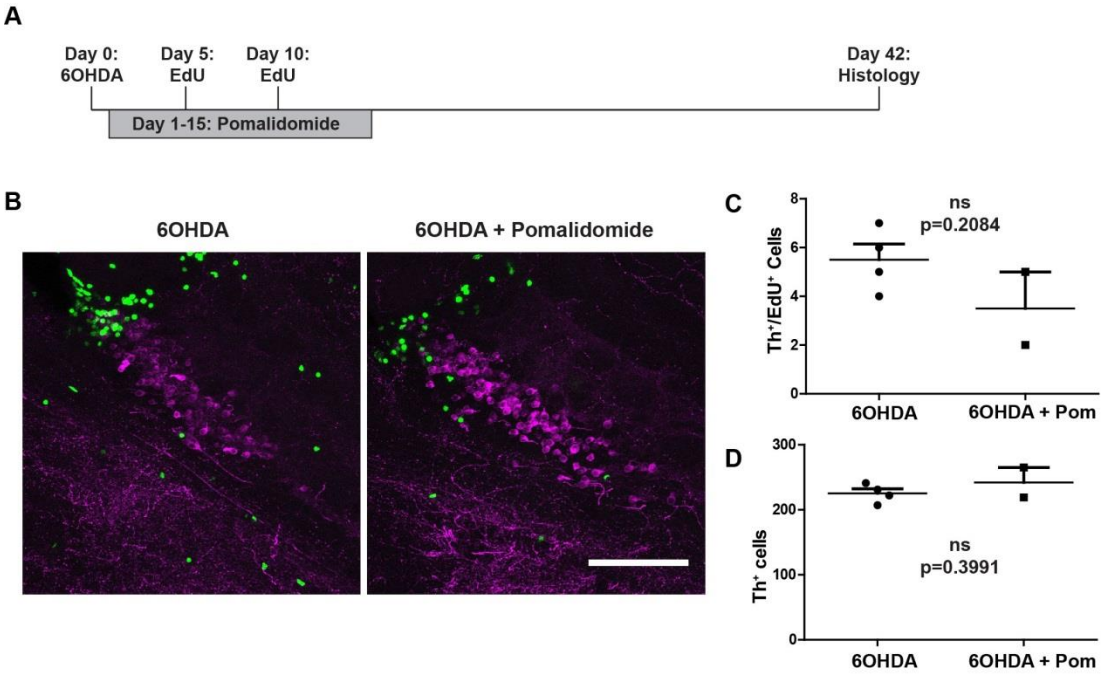

Figure 4. 13 Pomalidomide treatment did not affect the number of new Th$^+$ neurons or the total number of Th$^+$ neurons. A: The experimental timeline is given. B: Sagittal sections of the 5/6 population showing Th$^+$/EdU$^+$ cells. C: Quantification of the number of Th$^+$/EdU$^+$ cells, Student's t-test, (p=0.2084). D: Quantification of the numbers of Th$^+$ cells, Student's t-test, (p=0.3991). Scale bar in B = 100 µm

4.2.8.3 Haloperidol

6OHDA-induced ablation of Th$^+$ neurons reduces the level of dopamine in the brain (Figure 1.2). In the salamander, the number of dopaminergic neurons is regulated by the level of dopamine in the brain (Berg et al. 2011), and so this reduction in dopamine signalling triggers an increase in Th$^+$ neurogenesis. I asked whether dopamine signalling could also affect ERG proliferation and the regeneration of Th$^+$ neurons in the adult zebrafish brain.

To test whether inhibition of dopamine signalling affects the proliferation of ERGs I injected the dopamine receptor antagonist haloperidol and counted the number of EdU$^+$ cells lining the ventricle.

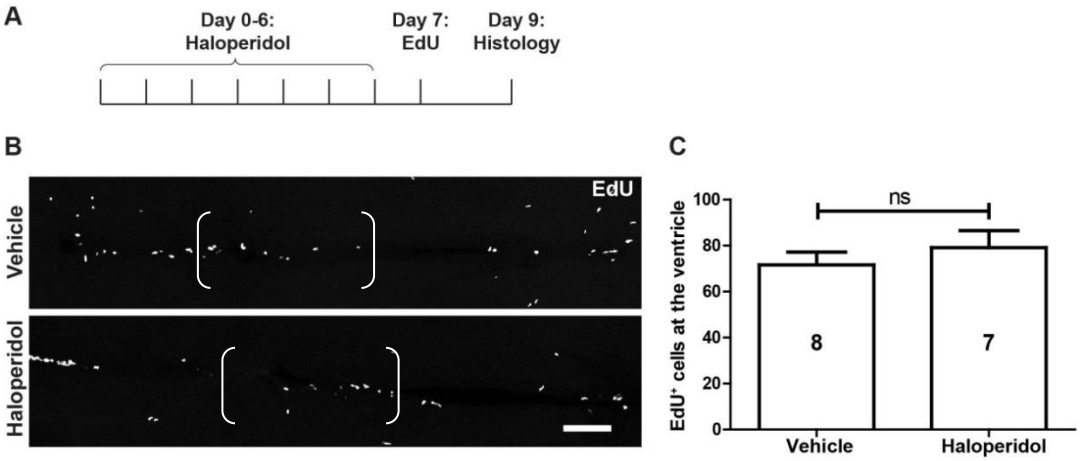

Figure 4. 14 Inhibition of dopamine signalling with the dopamine receptor antagonist haloperidol did not alter the number of EdU⁺ cells lining the ventricle. A: The experimental timeline is shown. B: Horizontal sections of EdU⁺ cells around the ventricle (left, rostral), white brackets indicate the approximate location of Th⁺ cells in the 5/6 population. C: Quantification of the number of EdU⁺ cells lining the ventricle shows no effect of haloperidol (Student's t-test, *p < 0.05). Scale bar in B = 100 µm. Figure is adapted from (Caldwell & Davies et al. 2018).

Compared to vehicle-injected controls, haloperidol did not affect the number of EdU⁺ cells at the ventricle (Figure 4.14, vehicle: 71.63 ± 5.580, haloperidol: 79.14 ± 7.414). This suggests that inhibiting dopamine signalling may not affect the proliferation of ERGs at the diencephalic ventricle in the adult zebrafish brain.

In the absence of ablation zymosan was sufficient to increase ERG proliferation (Figure 4. 6), but this did not lead to increased neurogenesis of Th⁺ cells (Figure 4. 8). We hypothesised that this is because without a lack of Th⁺ cells there is no signal instructing the proliferating ERGs/neuroblasts to become Th⁺ cells. I therefore tested whether a combination of zymosan plus the dopamine receptor antagonist haloperidol could boost the generation of Th⁺ cells in the absence of ablation.

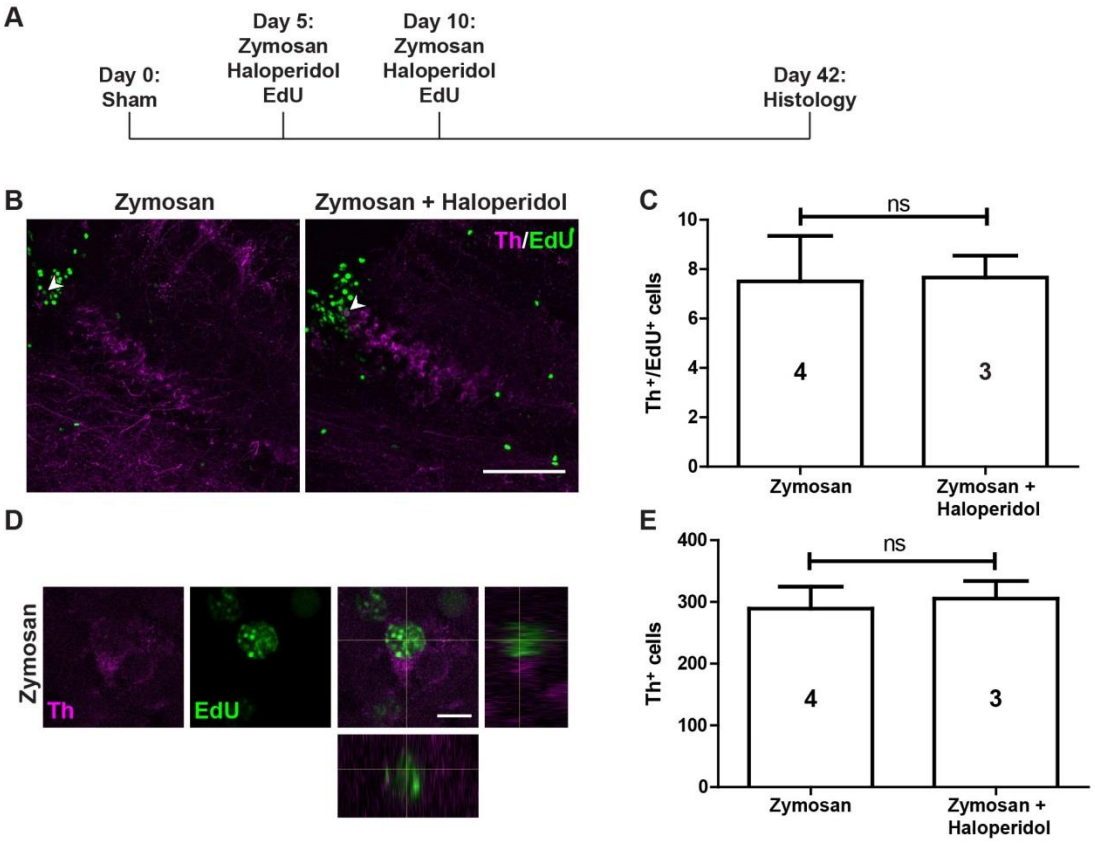

Figure 4. 15 Inhibition of dopamine signalling with the dopamine receptor antagonist haloperidol did not alter the number of EdU$^+$ cells in the ERG layer. A: The experimental timeline is shown. B: Sagittal sections of population 5/6 showing EdU$^+$/Th$^+$ neurons (arrows) after zymosan injection, with or without addition of haloperidol. C: Quantification of the number of EdU$^+$/Th$^+$ cells shows no effect of haloperidol (Student's t-test, *p < 0.05). Scale bar in B = 100 µm, scale bar in D = 5 µm.

Sham-injected fish were injected with zymosan into the brain and intraperitoneal injections of EdU and haloperidol at 5 dpi and 10 dpi, followed by analysis at 42 dpi. To reduce mortality caused by multiple daily injections a long lasting form of haloperidol, haloperidol decanoate, was used. However, the addition of haloperidol did not affect the number of new Th$^+$ neurons (Figure 4. 15, zymosan: 7.500 ± 1.848, zymosan + haloperidol: 7.667 ± 0.8819) and nor was there an effect on the overall number of Th$^+$ neurons in population 5/6 compared to zymosan injection alone (Figure 4. 15, zymosan: 289.0 ± 35.78, zymosan + haloperidol: 305.3 ± 28.54). This indicates that dopamine signalling is not required for Th$^+$ neurogenesis in the adult zebrafish brain.

4.3 Discussion

4.3.1 6OHDA elicits an immune response

Here I demonstrated for the first time that 6OHDA-mediated ablation of Th^+ neurons elicits an immune response in zebrafish (Figure 1, Figure 4. 2). The presence of microglia engulfing $TUNEL^+$ dopaminergic neurons in 6OHDA-injected fish indicates that the immune response is likely an indirect effect of 6OHDA injection, caused by the death of Th^+ neurons. Ablation of Th^+ neurons by injecting 6OHDA has previously been shown to induce an immune response in other in vivo models (Theodore & Maragos 2015). For example, in the salamander 6OHDA-mediated ablation of Th^+ neurons led to an increased number of microglia in the brain at 3 dpi which persists to at least 45 dpi (Kirkham et al. 2011). Furthermore, patients with Parkinson's disease also have immune activation (McGeer et al. 1988; Joshi & Singh 2018), involving increased levels of cytokines including tnf-α and il-1β (Nagatsu et al. 2000). Together this suggests that dopaminergic cell death triggers the response from microglial cells.

4.3.2 6OHDA injection is sufficient to increase proliferation of ERGs

I demonstrated for the first time that 6OHDA injection increases proliferation of ERGs around the diencephalic ventricle in zebrafish (Figure 4. 3, Figure 4. 6), which is in line with the increased Th^+ neurogenesis observed after 6OHDA (Figure 1.4). 6OHDA-induced proliferation of ERGs has previously been reported in the salamander (Berg et al. 2011).

In the previous chapter I showed that the *gfap*:GFP^+ population of ERGs around the diencephalic ventricle contains $her4^+$ ERGs (Figure 3. 2), and that these $her4^+$ ERGs give rise to Th^+ neurons after 6OHDA ablation (Figure 3. 3). In line with these results, here I demonstrate that *gfap*:GFP^+ are among the ERGs which respond to 6OHDA ablation by increasing proliferation (Figure 4. 3, Figure 4. 6).

4.3.3 The immune system is necessary for the regeneration of dopaminergic neurons

Here I demonstrated for the first time that neuroregeneration in the zebrafish brain can be inhibited by preventing an immune response in the absence of a traumatic brain injury (Figure 4. 3, Figure 4. 4).

Dexamethasone treatment abolished the 6OHDA-induced increase in ERG proliferation and Th^+ neurogenesis, impairing the replacement of Th^+ cells in population 5/6. This indicates that an immune response is necessary for the regeneration of Th^+ neurons in population 5/6 of the adult zebrafish brain. In contrast to my results, in the salamander immunosuppression with dexamethasone treatment resulted in an increase in the number of Th^+ neurons, suggesting that immunosuppression enhances regeneration after 6OHDA injection (Kirkham et al. 2011) . The results I have presented here are in agreement with evidence that dexamethasone treatment reduces stab lesion-induced ERG proliferation and neurogenesis in the zebrafish telencephalon (Kyritsis et al. 2012). This suggests that there could be species-specific effects of immunosuppression on the regeneration of neurons in the brain, but that dexamethasone impairs regeneration in various regions of the zebrafish brain.

Dexamethasone has a wide range of effects beyond immunosuppression, including direct effects on the proliferation of stem cells. In the larval zebrafish spinal cord, dexamethasone reduces neurogenesis of motor neurons after spinal cord injury (Ohnmacht et al. 2016), and glucocorticoid signalling was detected in ERGs of lesioned fish, suggesting the impaired regeneration may be due in part to a direct effect on ERGs (Nelson et al. 2018). However, I found no differences in ERG proliferation or Th^+ neurogenesis between sham and sham + dex fish (Figure 4. 3, Figure 4. 8), indicating that dexamethasone does not affect the proliferation of ERGs

or Th^+ neurogenesis in the brains of adult zebrafish at least in a non-regeneration context. This is in keeping with previously published results showing no effect of dexamethasone treatment on constitutive ERG proliferation or neurogenesis in the telencephalon (Kyritsis et al. 2012). Instead, inhibition of the immune system only affected the production of new Th^+ cells after ablation (Figure 4. 3, Figure 4. 4). This is likely because in the sham condition there is not a significant immune response to inhibit.

Dexamethasone treatment has also been shown to protect against dopaminergic cell death in mammalian models (Kurkowska-Jastrzębska et al. 2004). I chose to begin the dexamethasone treatment 24 hours after the injection of 6OHDA, and fish were immersed in dexamethasone for 2 weeks to suppress as much of the immune response as possible during regeneration. From my results presented here (Figure 4. 8), the number of Th^+ cells was unchanged in dexamethasone treated animals, indicating that the drug treatments I used did not significantly affect the survival of mature Th^+ neurons. In the salamander, dexamethasone treatment decreased the number of $TUNEL^+/Th^+$ cells at 4 days post injection of 6OHDA (Kirkham et al. 2011). As this is after the initial period of 6OHDA-induced cell death (1-3 dpi) this was interpreted as an indication that immunosuppression promotes the survival of newly forming Th^+ cells. Here I showed that the number of Th^+/EdU^+ cells was unchanged by dexamethasone treatment (Figure 4. 8), indicating that the survival of newly generated Th^+ neurons in the zebrafish brain is also unaffected by dexamethasone treatment.

I sought to assess the regenerative capacity of dopaminergic neurons in the absence of microglia to corroborate the inhibitory effect of dexamethasone on the regeneration of Th^+ neurons and thus provide more evidence for a requirement of an immune reaction for successful regeneration. To this end, I assessed the numbers of microglia

in Irf8$^{-/-}$ fish, which have been shown to have fewer microglia during development (Shiau et al. 2015). However, the numbers of microglia in the adult zebrafish brain were similar (Figure 4. 9), and so this mutant is not a useful tool for investigating an impaired immune response in this context.

A potential solution would be to use csf1ra/b mutants which have also been shown to have very few microglia in larvae (Tsarouchas et al. 2018). If this phenotype continues into adulthood these fish could be used to assess Th^{+} neuroregeneration in the absence of microglia. This would determine whether 6OHDA-induced proliferation of ERGs is wholly dependent on the immune system or if there are other mechanisms in play which allow ERGs to respond to 6OHDA-induced ablation of Th^{+} neurons which are also affected by dexamethasone treatment.

4.3.4 An immune response is sufficient to increase ERG proliferation but not neurogenesis of Th^{+} cells

Zymosan increased proliferation of ERGs in sham animals, demonstrating that it was able to have an effect (Figure 4. 6). Similarly, injection of zymosan increased ERG proliferation in the adult zebrafish telencephalon and cerebellum (Kyritsis et al. 2012). Furthermore, injection of specific pro-inflammatory cytokines il-4 and LTC4 have been shown to increase ERG proliferation in the zebrafish brain (Kyritsis et al. 2012; Bhattarai et al. 2016), further demonstrating a link between activation of the immune system and ERG proliferation.

Although stimulating the immune response with zymosan in the sham condition is sufficient to increase proliferation of ERGs (Figure 4. 6), the number of newly formed Th^{+} cells is unchanged (Figure 4. 8). In the telencephalon and cerebellum, zymosan injections increased the number of new neurons, colabelled with the pan-neuronal marker HuC^{+}/BrdU^{+} (Kyritsis et al. 2012). Counting the number of HuC^{+}/EdU^{+} cells

around the diencephalic ventricle could determine whether zymosan has an effect on neurogenesis in this brain region, even if the generation of Th^+ cells in particular is not increased.Zymosan may induce proliferation of ERGs, but in the absence of ablation there is no deficit of Th^+ neurons to specifically promote the generation of new Th^+ neurons in population 5/6. Instead, these EdU^+ ERGs may be self-renewing, or generating a range of other neuronal subtypes, or the newly formed cells may be relatively short lived as they are not required. Moreover, it could be speculated that if there is no deficit of Th^+ neurons in the 5/6 population there could be limited trophic support for supernumerary neurons, preventing an increased number of new neurons from being added to population 5/6.

Activation of microglia with zymosan did not enhance ERG proliferation or Th^+ neurogenesis in 6OHDA-injected fish (Figure 4. 6, Figure 4. 7).

Both 6OHDA and zymosan elicited an immune response (Figure 4. 2, Figure 4. 5), and both drugs increased ERG proliferation when used separately. Although the magnitude of the immune response caused by zymosan appeared to be much higher than 6OHDA, the increase in ERG proliferation was comparable (Figure 4. 6). This suggests that although ERGs can proliferate in response to immune activation there is a limit to the number of proliferating cells, and this is already reached at the level of immune activation caused by injection of 6OHDA. Presumably, co-injecting fish with 6OHDA and zymosan elicits an even greater immune response than either drug alone, and this could be confirmed with quantitative RT-PCR. However, if ERGs are already responding maximally to immune activation, this explains why enhancing the immune response even further does not result in increased ERG proliferation.

To assess the increase in cytokine expression after zymosan injection I selected a time point of 12 hpi as this was found to be the peak of expression of *tnf-α* and *il-1β* (Kyritsis et al. 2012). Although the variability of the results obscured the effect (Figure 4. 5), the means, SEMs and p values of the data suggest that if more fish were included then the results may reach significance (fold increase compared to sham injected fish, *tnf-α*: 46.89 ± 24.63 (p=0.2035), *il-1β*: 49.06 ± 22.31 (p=0.1641)). As there is published data showing the expression of these cytokines are increased after zymosan injection (Kyritsis et al. 2012), and that there is an increase in the labelling of L-plastin^{+} cells (Kyritsis et al. 2012) in zymosan injected fish, this suggests that zymosan injections do cause a microglial repsonse.

Zymosan acts through toll-like receptor 2 (TLR2), a transmembrane receptor found on immune cells, including microglia (Underhill 2003), but also expressed by human neural stem cells (Grasselli et al. 2018; Rolls et al. 2007). From the data in this thesis I cannot exclude that there may be a direct action of zymosan on ERGs, and this could influence their proliferation independent of microglial activation. If TLRs are expressed by ERGs at the diencephalic ventricle in zebrafish, treating isolated ERGs with zymosan and measuring the proliferation or changes in gene expression in these cells could determine whether this is a possible mechanism by which zymosan was influencing ERG proliferation. Alternatively, assessing the proliferation of ERGs in csf1ra/b mutants with significantly fewer microglia could also answer this question (Tsarouchas et al. 2018).

4.3.5 Investigations into the molecular signals triggering increased ERG proliferation

These results suggest proliferation of ERGs around the ventricle can be regulated by a signal between microglia and progenitor cells. However, microglial cells release a

myriad of signalling molecules, and any one of these (or a combination) may be the signal between microglia and progenitor cells in our system. In addition, cytokines often attract other immune cells, and so a requirement for any particular cytokine(s) would need to be tested in a system devoid of microglia.

In an effort to elucidate the molecular signals involved in the regeneration of dopaminergic neurons I adopted three pharmacological approaches based on the literature regarding regeneration in the adult zebrafish brain and the regeneration of Th^+ neurons in the adult salamander brain.

4.3.5.1 LTC4

As discussed in the introduction to this chapter, LTC4 was shown to be sufficient for increased neurogenesis in the adult zebrafish telencephalon, and required for lesion-induced neurogenesis (Kyritsis et al. 2012).

LTC4 elicited a response from microglial cells, demonstrated by the increased 4C4 labelling around the diencephalic ventricle compared to vehicle injected fish (Figure 4. 10). This is in contrast to published data which shows that LTC4 does not cause a microglial response in comparison to vehicle injected fish (Kyritsis et al. 2012). However, the vehicle in that case was methanol, which may induce neuronal death and could cause an immune response itself. To prevent a vehicle-mediated microglial reaction, I used LTC4 supplied in 95% ethanol in water. After diluting this with water to the desired concentration of drug, the percentage of ethanol in the injected solution was only 0.45%. I demonstrated that this vehicle did not induce an immune response, as there was no difference in the 4C4 labelling between vehicle-injected and uninjected fish.

The increased 4C4 labelling after injection of LTC4 demonstrates that the treatment was able to exert a biological effect. Despite using a similar injection schedule and

identical concentration of LTC4 to what was shown to increase proliferation of ERGs in the telencephalon (Kyritsis et al. 2012), Karolina and I did not observe an effect of LTC4 on the number of $PCNA^+$ ERGs at the ventricle. This could be a consequence of analysing different areas of the brain, and ERGs in the telencephalon may be more responsive to LTC4.

LTC4 elicited an immune response but we did not observe any change to the number of proliferating ERGs (Figure 4.10, Figure 4. 11). Zymosan also causes in an immune response (Figure 4. 5), however in this case this was accompanied by an increase in proliferating ERGs (Figure 4. 6). This difference could be a result of the different magnitude of microglial activation. Although the data presented here do not allow for a direct comparison, qualitatively the difference in 4C4 labelling between sham injected brains and zymosan injected brains is more pronounced than the comparisons between vehicle and LTC4 injected brains (Figure 4. 5 compared to (Caldwell and Davies et al. 2018)). Quantitative RT-PCR for pro-inflammatory cytokines after LTC4 injection could determine whether this is a valid point.

Another consideration is that the proliferation of ERGs after zymosan and LTC4 was measured in different ways, (EdU labelling and PCNA labelling, respectively), and with different experimental timelines (Figure 4. 5 and Figure 4. 11). Therefore a separate experiment with identical readouts and timelines would be required for a direct comparison between the two compounds in terms of ERG proliferation.

An immune reaction is necessary for the proliferation of ERGs after ablation (Figure 4. 3), and for the full regeneration of Th^+ neurons (Figure 4. 4). It is possible that LTC4 could be the molecule mediating this effect, by promoting a microglial response to 6OHDA injection or directly stimulating ERG proliferation. LTC4 signalling has been

shown to be required for lesion-induced ERG proliferation and neurogenesis after a stab injury to the telencephalon (Kyritsis et al. 2012). Along with *tnf-α* and *il-1β*, LTC4 signalling may be increased after injection of 6OHDA and could be one of the molecular signals involved in eliciting a microglial response. This hypothesis could be tested first by assessing the level of leukotriene C4 signalling through quantitative RT-PCR for CysLT1 to determine whether there is an increase in LTC4 signalling in 6OHDA injected fish compared to sham injected fish. To test whether LTC4 is required for regeneration of Th^+ neurons one could treat 6OHDA-injected fish with the CysLT1 receptor antagonist pranlukast and count the numbers of proliferating ERGs and new Th^+ cells. If pranlukast did inhibit Th^+ regeneration one could then aim to distinguish whether LTC4 signalling is required for microglial activation which then influences ERG proliferation, or to stimulate ERGs directly. This could be tested by assessing the immune response in 6OHDA-injected fish treated with pranlukast compared to 6OHDA alone. If LTC4 signalling is required to elicit an immune response, the level of pro-inflammatory cytokines measured by quantitative RT-PCR and the level of 4C4 labelling would be lower in pranlukast treated fish.

4.3.5.2 Haloperidol

I observed no difference in the number of proliferating cells lining the ventricle after injection of the dopamine receptor antagonist haloperidol (Figure 4. 14). In salamanders, 6OHDA-induced ablation of the dopaminergic innervation to the forebrain results in decreased proliferation of progenitor cells in the striatum (Joven et al. 2018), whereas haloperidol increases proliferation of Th^+ neuron progenitor cells in the midbrain (Berg et al. 2011). This indicates that there may be region-specific effects of dopamine signalling on progenitor cell proliferation. Progenitor cells in areas of the brain where there is no constitutive proliferation, such as the salamander midbrain, may increase proliferation in response to reduced dopamine, while

progenitors in the salamander forebrain and lining the diencephalic ventricle of the zebrafish brain, as described here, may be unresponsive to a reduction in dopamine. However, as there are no dopaminergic neurons in the zebrafish midbrain it is not possible to test whether haloperidol would affect the neurogenesis of dopaminergic neurons in this area of the brain in zebrafish.

As I obtained a negative result it is also possible that this discrepancy is a result of technical issues. In order to deliver a sufficient dose of haloperidol to the brain I followed the method used to significantly affect the regeneration of dopaminergic neurons in the salamander (Berg et al. 2011). I injected fish with haloperidol obtained from the same company with the same catalogue number, and at twice the concentration for 6 days rather than 4 days. This implies that the administration of haloperidol should have been sufficient to deliver at least a similar level of haloperidol to ERGs in the brain.

In situ hybridisation showed that mRNA for *d4a*, the gene encoding one of the D2 dopamine receptors, is upregulated around the central canal in the zebrafish spinal cord after a lesion (Reimer et al. 2013). Moreover, dopamine receptor antagonists, including haloperidol, have been shown to affect neurogenesis in the zebrafish CNS (Reimer et al. 2013). Although these results suggest dopamine receptors are present on ERGs in the zebrafish spinal cord, it is not known whether ERGs in the adult zebrafish brain also have dopamine receptors. It is therefore possible that haloperidol did not affect ERG proliferation in my experiments due to the absence of dopamine receptors on ERGs at the diencephalic ventricle. The presence of these receptors could be determined by in situ hybridisation or immunohistochemistry combined with markers of ERGs.

A limitation of this experiment is that the proliferation was quantified by counting the number of EdU^+ cells lining the ventricle without any marker for ERGs (e.g. gfap, olig2, her4). While the vast majority of cells lining the ventricle are likely ERGs, I have observed other EdU^+ cell types around the ventricle, for example microglia, which may have also been counted and affected the results. If this experiment were to be repeated, Tg(*gfap*:GFP;*olig2*:Dsred) could be used to identify EdU^+ ERGs and exclude any other EdU^+ cell types.

Activation of the immune system with zymosan was sufficient to increase proliferation of ERGs; however, the number of Th^+ neurons was unchanged, as discussed above. On the other hand, manipulating dopamine signalling with haloperidol did not affect the proliferation at the ventricle. I hypothesised that dopamine signalling may be able to promote Th^+ neurogenesis through an alternative method to increased ERG proliferation, for example promoting a Th^+ specification in newly formed neurons.

To test this hypothesis I used zymosan to induce proliferation of ERGs and treated fish with haloperidol to encourage cells to adopt a Th^+ cell fate. However, there was no effect of this treatment on the number of Th^+/EdU^+ cells compared to zymosan treatment alone. This suggests that dopamine signalling may not regulate Th^+ neurogenesis in the adult zebrafish brain as it does in the midbrain of the salamander.

4.3.5.3 Pomalidomide treatment does not affect the proliferation of ERGs or the regeneration of Th^+ neurons

Injection of 6OHDA causes an increase in the level of the pro-inflammatory cytokine *tnf-α* (Figure 4. 2). It has been shown previously that tnf-α is required for injury-induced proliferation of progenitor cells in the adult zebrafish retina (Nelson et al. 2013), and injection of tnf-α into the uninjured retina promotes neurogenesis (Conner et al. 2014). This led us to hypothesise that tnf-α may be required for the efficient regeneration of

Th^+ neurons. However, inhibiting the release of tnf-α with pomalidomide did not affect the number of proliferating ERGs or the number of Th^+/EdU^+ or overall Th^+ cells in population 5/6 (Figure 4. 12, Figure 4. 13).

As with any negative result the first question is whether pomalidomide was exerting an effect on tnf-α signalling in the brain. The concentration of pomalidomide used was determined by considering the IC50 of the drug and reports that around 39% passes through the blood brain barrier (Li et al. 2013). Previous results from our lab and others (Mahony et al. 2013; Tsarouchas et al. 2018) have shown that immersion of zebrafish larvae in pomalidomide is able to have biological effects. However, determining whether pomalidomide is actually reducing *tnf-α* signalling cannot be achieved simply by measuring the levels of *tnf-α* after treatment, because there is conflicting evidence showing the level of *tnf-α* mRNA is reduced, unchanged, or increased by pomalidomide. Instead, a more appropriate readout for the action of pomalidomide would be to examine the levels of downstream molecules of *tnf-α* signalling, for example NF-κB (Schütze et al. 1995).

Even if there was an effect of pomalidomide on the regeneration of Th^+ neurons, this would not be enough evidence to suggest *tnf-a* specifically is required for the regeneration of Th^+ neurons. *tnf-α* is known to attract immune cells (Ming et al. 1987), and as such an inhibitor of *tnf-a* signalling would act as an immunosuppressant, therefore likely having similar effects as dexamethasone, impairing the regeneration of Th^+ neurons. To demonstrate that *tnf-α* could have a direct effect on the ERGs one would first have to show that at least one of the receptors for *tnf-α* is expressed by ERGs at the ventricle, for example by in situ hybridisation combined with markers for ERGs. Secondly, one would need to show that pomalidomide can affect the proliferation of ERGs in the absence of microglia, and this could be done either in vitro

after fluorescent assisted cell sorting (FACS) for ERGs or in csfr1a/b mutants lacking microglia (Tsarouchas et al. 2018).

4.3.5.4 Future investigation into candidate cytokines

Inhibition of tnf-α signalling did not affect proliferation of ERGs or regeneration of Th^+ neurons (Figure 4. 12, Figure 4. 13), however, I also observed a 6OHDA-induced increase in *il-1β* (Figure 4. 2), demonstrating that tnf-α is not the only cytokine affected. In larval zebrafish, *il-1β* signalling has been shown to influence the axonal regeneration and functional recovery after spinal cord transection (Tsarouchas et al. 2018).

Moreover, the cytokine interleukin 4 (*il-4*) has been suggested to increase neurogenesis in the telencephalon, acting through a pathway separate to LTC4 (Bhattarai et al. 2016). This cytokine is upregulated in brains injected with the fast accumulating amyloid beta peptide TR-Aβ42, which is similar to our 6OHDA model in that neuronal cell death is induced without a traumatic brain injury in the adult zebrafish brain. *Il-4* was also shown to be sufficient to increase the number of proliferating ERGs and new neurons formed in unlesioned brains. In TR-Aβ42-injected brains, a morpholino against *il-4* was shown to reduce the number of proliferating ERGs, suggesting that *il-4* may be required for ERG proliferation, although it may also be involved in microglial activation. It would therefore be interesting to assess the effect of il-4 on ERG proliferation in the absence of microglia. This could be achieved using fluorescence-activated cell sorting (FACS) to isolate ERGs, and then assessing their level of proliferation in response to il-4 treatment. Alternatively, the effect of il-4 in vivo could be tested by injecting il-4 into csfr1a/b mutants lacking microglia (Tsarouchas et al. 2018) and counting the numbers of EdU^+ ERGs.

4.4 Conclusions

From the data presented in this chapter, I conclude that injection of 6OHDA causes an immune response involving microglia and leads to increased proliferation of ERGs. This immune response is necessary for the successful regeneration of Th^+ neurons. In the absence of ablation, an immune response is sufficient to increase ERG proliferation but not Th^+ neurogenesis. These conclusions are summarised in a schematic (Figure 4. 16).

The molecular mechanism for how microglial activation impacts ERG proliferation and regeneration of Th^+ neurons is yet to be elucidated. I found no evidence for an effect of haloperidol injections, LTC4 injections, or pomalidomide treatment; however, this does not rule out a contribution of dopamine signalling or cytokine signalling on the regeneration of Th^+ neurons in the adult zebrafish brain.

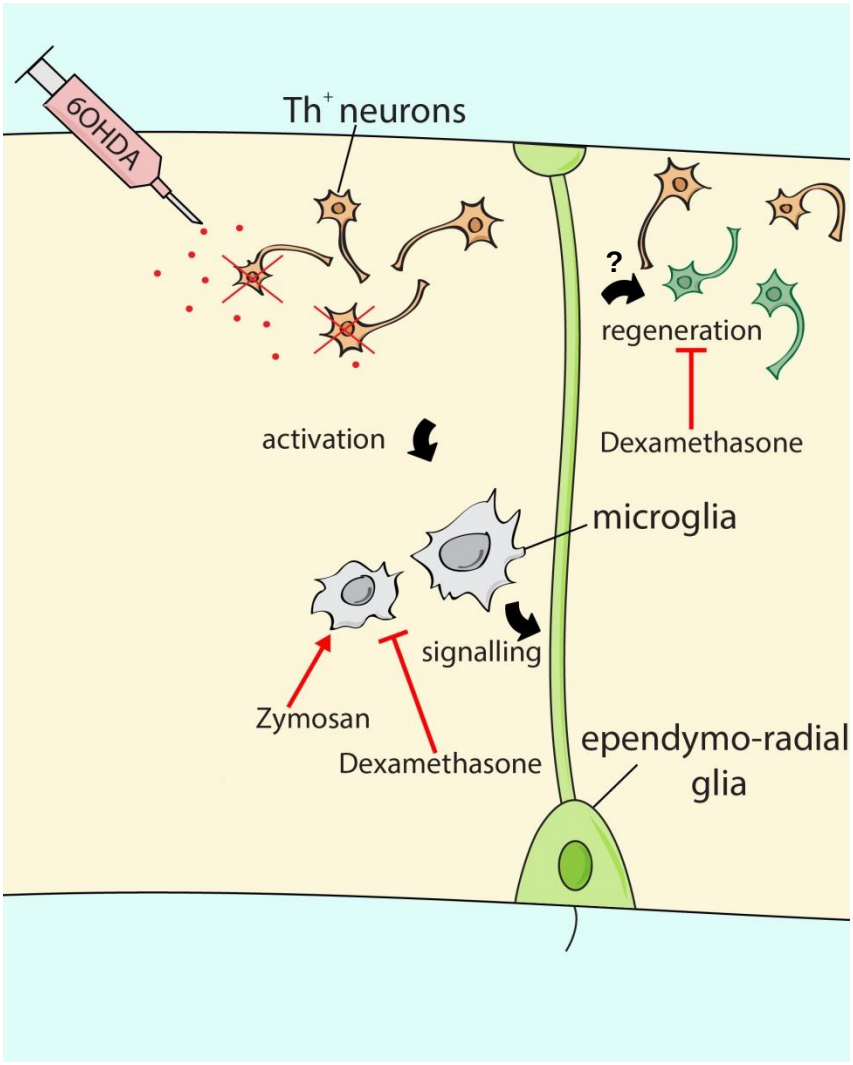

Figure 4. 16 Schematic overview of results, adapted from (Caldwell and Davies et al. 2018)**. Ablation of Th⁺ neurons with 6OHDA elicits a microglia response, which is necessary for regeneration of new dopaminergic neurons from ERGs. Ablation-induced proliferation of ERGs and neurogenesis of Th+ neurons is inhibited by dexamethasone. Zymosan stimulates ERG proliferation, but does not affect the neurogenesis of Th⁺ neurons. The question mark represents the remaining uncertainty in the signal linking proliferating ERGs to increased neurogenesis of Th⁺ neurons.**

Chapter Five: Investigating Alternative Methods of Th^+ Neuron Ablation

5.1. Introduction

The dopamine homologue 6OHDA specifically ablates Th^+ neurons in population 5/6, population 11, population 12, and the locus coeruleus, and these populations have varying capacities to be regenerated (Caldwell and Davies et al. 2018). On the other hand, populations 2, 7, 9, 13, and 15/16 were unaffected by injection of 6OHDA. I reasoned that alternative methods used to ablate dopaminergic neurons may affect Th^+ populations which were unaffected by 6OHDA, and that this would allow me to investigate the regenerative capacity of these populations. Three distinct approaches were adopted: a genetic manipulation, a chemogenetic ablation, and chemical ablation.

5.1.1 Genetic manipulation to reduce the number of dopaminergic neurons: *pink1*

Genetic mutations are responsible for approximately 10% Parkinson's disease cases (Klein & Westenberger 2012). For example, mutations in *PINK1* (PTEN-induced putative kinase 1) are the second most common cause of autosomal recessive Parkinson's (Valente et al. 2004; Li et al. 2005; Mills et al. 2008). *PINK1* encodes a mitochondrial serine/threonine kinase and is widely expressed in the human brain (Gandhi et al. 2006). Parkinson's disease-causing mutations in *PINK1* have been shown to result in a loss of function of PINK1 (Sim et al. 2006), which appears to increase the susceptibility of dopaminergic neurons to oxidative stress (Cookson 2012). Hence a number of *pink1* knockout animal models have been generated in order to investigate he selective degeneration of dopaminergic neurons (Dawson et al. 2010).

Pink1 knockout mice do not exhibit any gross morphological abnormalities. Most notably, no abnormalities were found in the dopaminergic system of *pink1* knockout mice, and the numbers of Th^+ neurons, the levels of striatal dopamine, and the levels of dopamine receptors are comparable to wildtype control mice (Kitada et al. 2007). In contrast, loss of function mutations in *pink1* in drosophila result in dopaminergic cell death, along with a range of other phenotypes, including muscle degeneration, an inability to fly, slower climbing speeds, loss of photoreceptors, male sterility, and increased sensitivity to stressors (Clark et al. 2006; Park et al. 2006; Yang et al. 2006). The observed phenotypes were rescued by the introduction of human *PINK1*, demonstrating that these wide-ranging phenotypes were *pink1*-dependent, and that the gene is functionally conserved between drosophila and humans.

The effect of pink1 depletion in zebrafish has been investigated primarily using morpholinos (Anichtchik et al. 2008; Sallinen et al. 2010; Xi et al. 2010; Ryu et al. 2007). These studies have reported variable effects on dopaminergic neurons, from subtle alterations in Th^+ projections from intact nuclei (Xi et al. 2010) to reduced numbers of Th^+ neurons (Anichtchik et al. 2008). However, it is important to note that some of these studies have reported gross morphological abnormalities and generalised increases in cell death, (Anichtchik et al. 2008; Xi et al. 2010), suggesting toxicity of the morpholino which is not specific to *pink1* deficiency.

Furthermore, morpholinos are most efficient at inhibiting translation during the first 2-3 days of development (Sumanas & Larson 2002), restricting the time available for phenotypic analysis. Therefore a stable transgenic line has been generated in which there is a premature stop codon in the kinase-encoding domain of *pink1* (Flinn et al. 2013). At 5 dpf $pink1^{-/-}$ larvae had 25% fewer Th^+ neurons and 30% fewer dat^+ neurons than wildtype controls. No differences were observed in the expression patterns of neurodevelopmental genes, suggesting a specific effect on dopaminergic neurons.

However, cell numbers of other neuronal populations, for example serotonergic neurons, could have been compared to age-matched wildtype controls to provide a better control for normal neurodevelopment. Adult *pink1*$^{-/-}$ zebrafish were reported to have 50% fewer Th^{+} neurons in the posterior tuberculum. The greater difference in Th^{+} neurons in adults compared to larvae suggested that these fish may have a progressive loss of dopaminergic neurons. In addition, a higher number of apolilоprotein E (ApoE)$^{+}$ cells was observed in *pink1*$^{-/-}$ fish at 3 dpf, which was interpreted as an indicator of microglial activation. However, it is not clear whether the reduced numbers of Th^{+} neurons in *pink1*$^{-/-}$ fish are a result of fewer dopaminergic neurons being produced, or a result of dopaminergic cell death.

5.1.2 Chemogenetic ablation of dopaminergic neurons

While genetic ablation can specifically target a certain population of cells, chemogenetic ablation also allows for temporal control. This means an animal can develop normally without potentially deleterious effects of mutations, and ablation can be induced at a specific time point. Several different approaches have been developed for chemogenetic ablation, but in this chapter I will focus on the nitroreductase system, which has been used extensively in zebrafish (Curado et al. 2008).

Nitroreductase (NTR), an enzyme isolated from Escherichia coli, is expressed under a tissue-specific promoter, often in combination with a fluorescent reporter gene. Upon application of a non-toxic substrate, nitroreductase converts the prodrug into a DNA interstrand cross-linking agent, inducing apoptotic cell death (Lindmark & Müller 1976). A reduction in the number of fluorescent cells can be used as an indicator of successful ablation. The previously used substrate of nitroreductase, CB1954 [5-(aziridin-1-yl)-2,4-dinitrobenzamide], was shown to have bystander effects, killing neighbouring cells due to the cell permeability of the cytotoxic metabolite (Bridgewater

et al. 1997; Helsby et al. 2004). However, the toxic metabolite of metronidazole is confined to the NTR-expressing cell, and thus specifically ablates only cells expressing the nitroreductase enzyme (Pisharath et al. 2007; Curado et al. 2008).

Two independent groups pioneered the use of the nitroreductase system to ablate cells and study their regeneration in zebrafish (Curado et al. 2007; Pisharath et al. 2007). Since then, the nitroreductase system has been used to investigate regeneration of a variety of different tissues in zebrafish, including cardiomyocytes (Curado et al. 2007; Zhang et al. 2013), pancreatic β-cells (Curado et al. 2007; Pisharath et al. 2007; Moss et al. 2009), hepatocytes (Curado et al. 2007; Choi et al. 2015), osteoblasts (Singh et al. 2012), skin cells (Chen et al. 2011), ovaries (White et al. 2011), podocytes (Huang et al. 2013; Zhou & Hildebrandt 2012) and oligodendrocytes (Chung et al. 2013).

Furthermore, metronidazole has been shown to cross the blood brain barrier (Nau et al. 2010), and unlike other methods of chemogenetic ablation, nitroreductase is cell cycle independent. This means that this is a suitable method to ablate even non-dividing cells, such as neurons. In zebrafish, metronidazole treatment has been shown to induce specific ablation of neurons including serotonergic neurons of the dorsal raphe, the habenular, otpa^{+} neurons of the hypothalamus, and motor neurons in the spinal cord (Yokogawa et al. 2012; Agetsuma et al. 2010; Lambert et al. 2012; van Ham et al. 2012; Ohnmacht et al. 2016).

Importantly, the NTR system is appropriate for regeneration studies, as withdrawal of metronidazole removes the cytotoxic agent, and the affected tissue can recover. The extent of regeneration can then be assessed both by a recovery in the numbers of fluorescent cells, and by labelling newly generated cells (Curado et al. 2007; Godoy et al. 2015; Pisharath et al. 2007; Choi et al. 2015; Moss et al. 2009; Singh et al. 2012;

Ohnmacht et al. 2016; Huang et al. 2013). Previous regeneration studies in zebrafish using this system have demonstrated that tissue regeneration following exposure to metronidazole results in functional recovery, indicating that there are no deleterious after effects of metronidazole treatment.

In this chapter I use fish expressing nitroreductase and a fluorescent reporter under the control of the promoter for a gene encoding the homeodomain transcription factor orthopedia b (otpb) (Lambert et al. 2012). This promoter drives expression in diencephalic Th^+ neurons in larvae (primarily DC4 and DC6, based on the nomenclature (Rink & Wullimann 2002)), as well as non-dopaminergic Th^- neurons in the rostral diencephalon (Fujimoto et al. 2011), essentially recapitulating the expression pattern of the endogenous *otpb* gene in zebrafish (Ryu et al. 2007; Kastenhuber et al. 2009; Tay et al. 2011b). Successful ablation has been achieved by immersing larval zebrafish in metronidazole, demonstrated by an 88% decrease in the number of Th^+/GFP^+ cells and the presence of $TUNEL^+/GFP^+$ cells in metronidazole treated larvae (Lambert et al. 2012).

5.1.3 Chemical ablation of dopaminergic neurons: MPTP and MPP^+

In addition to 6OHDA there are a number of other chemicals which have been shown to selectively kill dopaminergic neurons *in vivo* (Betarbet et al. 2002). One of the most commonly used toxins is 1-methyl-1,2,3,6-tetrahydropyridine (MPTP). The ability of MPTP to kill dopaminergic neurons was first discovered in patients presenting with Parkinson's disease like symptoms after injecting mis-synthesised heroin (Langston et al. 1983). It was subsequently found that MPTP could selectively ablate dopaminergic neurons to model Parkinson's disease in animals, including primates (Fox & Brotchie 2010), cats (Schneider & Markham 1986), rodents (Heikkila et al. 1984), salamanders (Barbeau et al. 1985), fish (Weinreb & Youdim 2007; Bretaud et al. 2004), and C. Elegans (Braungart et al. 2004).

MPTP is able to cross the blood brain barrier, after which it is converted to its toxic metabolite *N*-methyl-4-phenylpyridine (MPP^+) by monoamine oxidase (MAO) in glial cells (Langston et al. 1984; Chiba et al. 1984). MPP^+ enters dopaminergic neurons through the dopamine transporter ((Miller et al. 1999), where it inhibits complex 1 of the mitochondrial respiratory chain (Nicklas et al. 1985), leading to cell death.

In zebrafish larvae, the effects of MPTP and MPP^+ have had conflicting effects on the dopaminergic system, with some studies reporting gross morphological abnormalities with concentrations others used to demonstrate a reduced number of Th^+ neurons post treatment (Bretaud et al. 2004; McKinley et al. 2005; Lam et al. 2005; Sallinen et al. 2009; Thirumalai & Cline 2008; Xi et al. 2011; Dukes et al. 2016). As none of these studies found evidence for dopaminergic cell death, it is possible that MPTP and MPP^+ treated larvae have been reported to have fewer dopaminergic neurons due to impaired neurodevelopment rather than selective ablation of Th^+ cells.

MPTP has been shown to reduce the number of Th^+ neurons in the adult goldfish brain (Poli et al. 1990; Goping et al. 1995). The amounts of dopamine and noradrenaline in the brain were also reduced by MPTP injection (Poli et al. 1990; Youdim et al. 1992), but recover within 10-13 days post treatment (Pollard et al. 1992). This was accompanied by profound bradykinesia which also recovered, suggesting functional regeneration of Th^+ neurons. Although the behavioural deficits have also been reported in adult zebrafish injected with MPTP, there is not currently any evidence of a reduction in the number of Th^+ neurons (Anichtchik et al. 2003; Bretaud et al. 2004).

5.2 Results

5.2.1 Genetic manipulation to reduce the number of dopaminergic neurons: *pink1*

5.2.1.1 Th^+ cell numbers in the diencephalon were comparable in *pink1*$^{+/+}$ and *pink1*$^{-/-}$ fish

Pink1$^{-/-}$ zebrafish were found to have fewer Th^+ cells at 5 dpf compared to wildtype larvae (Flinn et al. 2013). We wanted to investigate whether this might be a result of delayed development of Th^+ neurons or a loss of Th^+ cells. To this end, we obtained *pink1*$^{-/-}$ fish and *pink1*$^{+/+}$ fish from the authors of this paper, and confirmed their genotypes by sequencing DNA extracted from a fin clip sample (Figure 5. 1A). Together with Adelina Haller, a masters student under my supervision, I compared the numbers of Th^+ cells were between wildtype (*pink1*$^{+/+}$) and homozygous mutant (*pink1*$^{-/-}$) zebrafish at 2, 3, 4, and 5 dpf. We found no significant difference in the numbers of Th^+ neurons at any of the time points analysed (Figure 5. 1, 2 dpf *pink1*$^{+/+}$: 56.12 ± 2.497, 2 dpf *pink1*$^{-/-}$: 55.13 ± 2.641, 3 dpf *pink1*$^{+/+}$: 92.86 ± 4.234, 3 dpf *pink1*$^{-/-}$: 82.71 ± 3.435, 4 dpf *pink1*$^{+/+}$: 96.33 ± 4.910, 4 dpf *pink1*$^{-/-}$: 83.86 ± 5.235, 5 dpf *pink1*$^{+/+}$: 87.80 ± 2.611, 5 dpf *pink1*$^{-/-}$: 93.25 ± 7.409), suggesting that *pink1* does not affect the number of Th^+ neurons in larval zebrafish.

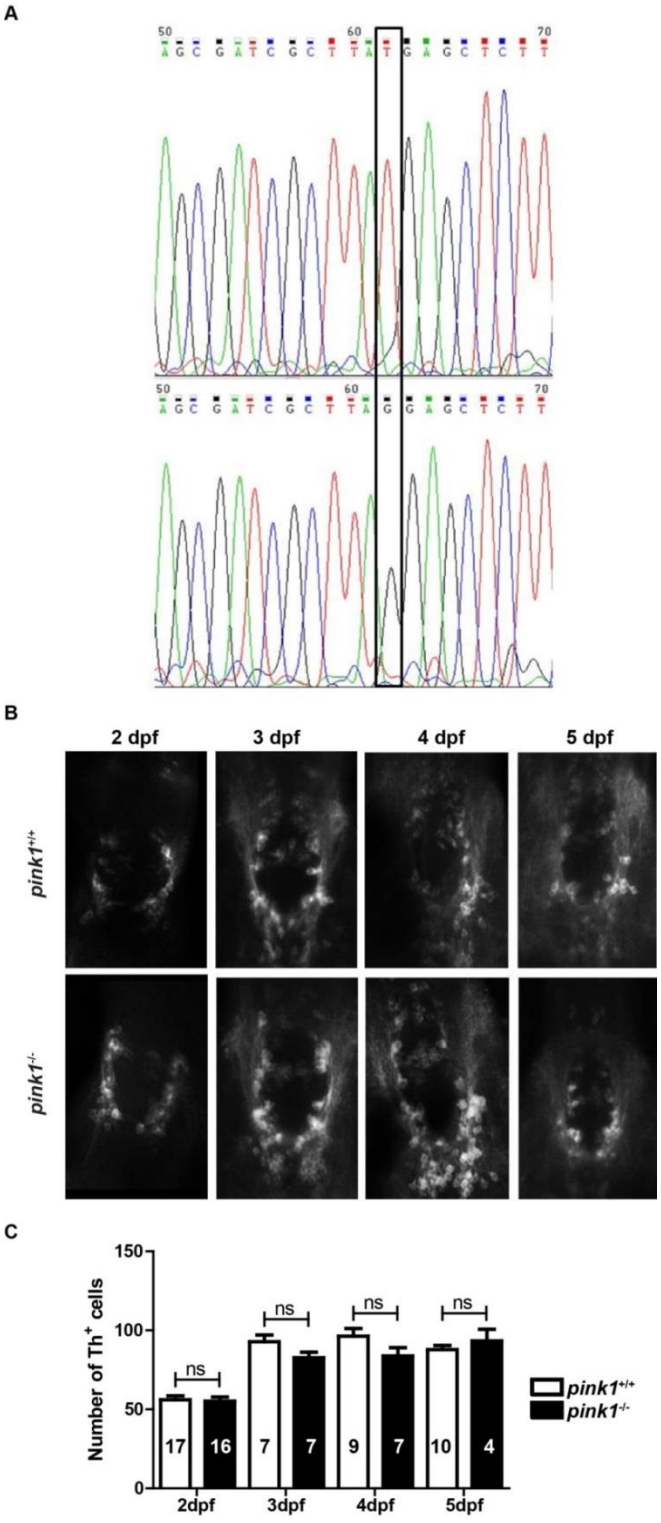

Figure 5. 1 No difference was found in the number of Th$^+$ neurons in the diencephalon of larval zebrafish in pink1$^{+/+}$ and pink1$^{-/-}$ neurons. A: Chromatograms of *pink1*$^{+/+}$ (upper panel) and *pink1*$^{-/-}$ (lower panel) sequences, showing the T>G change, highlighted. B: Maximum projections of Th$^+$ cells in the diencephalon from a dorsal view (rostral is up). C: Quantification of the numbers of Th$^+$ cells at 2, 3, 4, and 5 days post-fertilisation (dpf). Student's t test and Mann Whitney U tests were used for pairwise comparisons, *p < 0.05.

5.2.1.2 Microglia numbers were higher in *pink1*$^{-/-}$ larvae compared to *pink1*$^{+/+}$

It has been shown previously that *pink1*$^{-/-}$ larvae have more ApoE^{+} cells compared to *pink1*$^{+/+}$ larvae, which suggests activation of the immune system (Flinn et al. 2013). To investigate this phenotype further I compared the numbers of microglia in *pink1*$^{-/-}$ larvae and wildtype larvae by counting the number of 4C4^{+} cells in confocal z-stacks containing the entire diencephalon. I found that the number of 4C4^{+} cells in the diencephalon was 63.4% higher in *pink1*$^{-/-}$ larvae at 4 dpf compared to *pink1*$^{+/+}$ larvae (Figure 5. 2, *pink1*$^{+/+}$: 100.5 ± 4.291, *pink1*$^{-/-}$: 164.2 ± 13.00), indicating that there is an immune response.

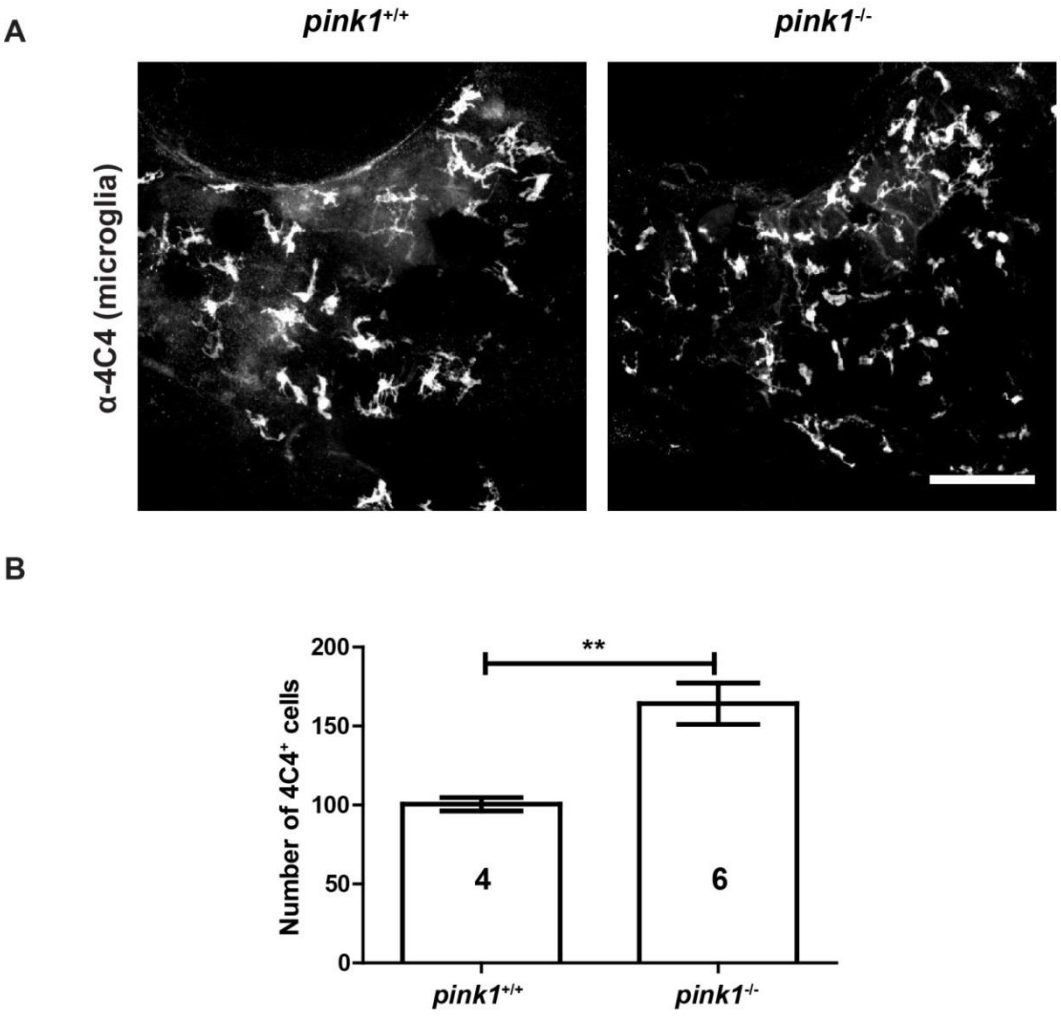

Figure 5. 2 *pink1*$^{-/-}$ fish have more microglia than wildtype larvae. A: *pink1*$^{-/-}$ larvae have more 4C4^{+} microglia in the diencephalon compared to age-matched controls at 4 dpf (dorsal view, rostral is

left). B: Quantification of the number of 4C4$^+$ cells. Mann Whitney U test, **p < 0.01. Scale bar = 100 µm.

5.2.2 Chemogenetic ablation of dopaminergic neurons

5.2.2.1 *Tg(otpb:NTR-GFP)* zebrafish have GFP$^+$ in the adult brain, and these overlap with Th$^+$ populations in some cases

Tg(*otpb*:NTR-GFP) fish have been used to ablate Th$^+$ neurons in the diencephalon of zebrafish larvae (Lambert et al. 2012). To investigate the feasibility of using these fish to ablate Th$^+$ neurons in adult zebrafish I first compared the localisation of GFP$^+$ cells with Th$^+$ populations in sagittal sections of the adult zebrafish brain and found that the populations were different but overlapping (Figure 5. 3).

Double-positive Th$^+$/GFP$^+$ cells were present in population 12, population 13, and the locus coeruleus, although not all Th$^+$ cells in these populations were GFP$^+$ (population 12: 97.5% population 13: 34.9%, locus coeruleus: 28.6% Th$^+$ cells were also GFP$^+$). In contrast, no GFP$^+$ cells were found in other Th$^+$ populations. For example, GFP$^+$ cells were seen in proximity to population 3/4, but no Th$^{+/}$GFP$^+$ cells were observed in this area of the brain (Figure 5. 3).

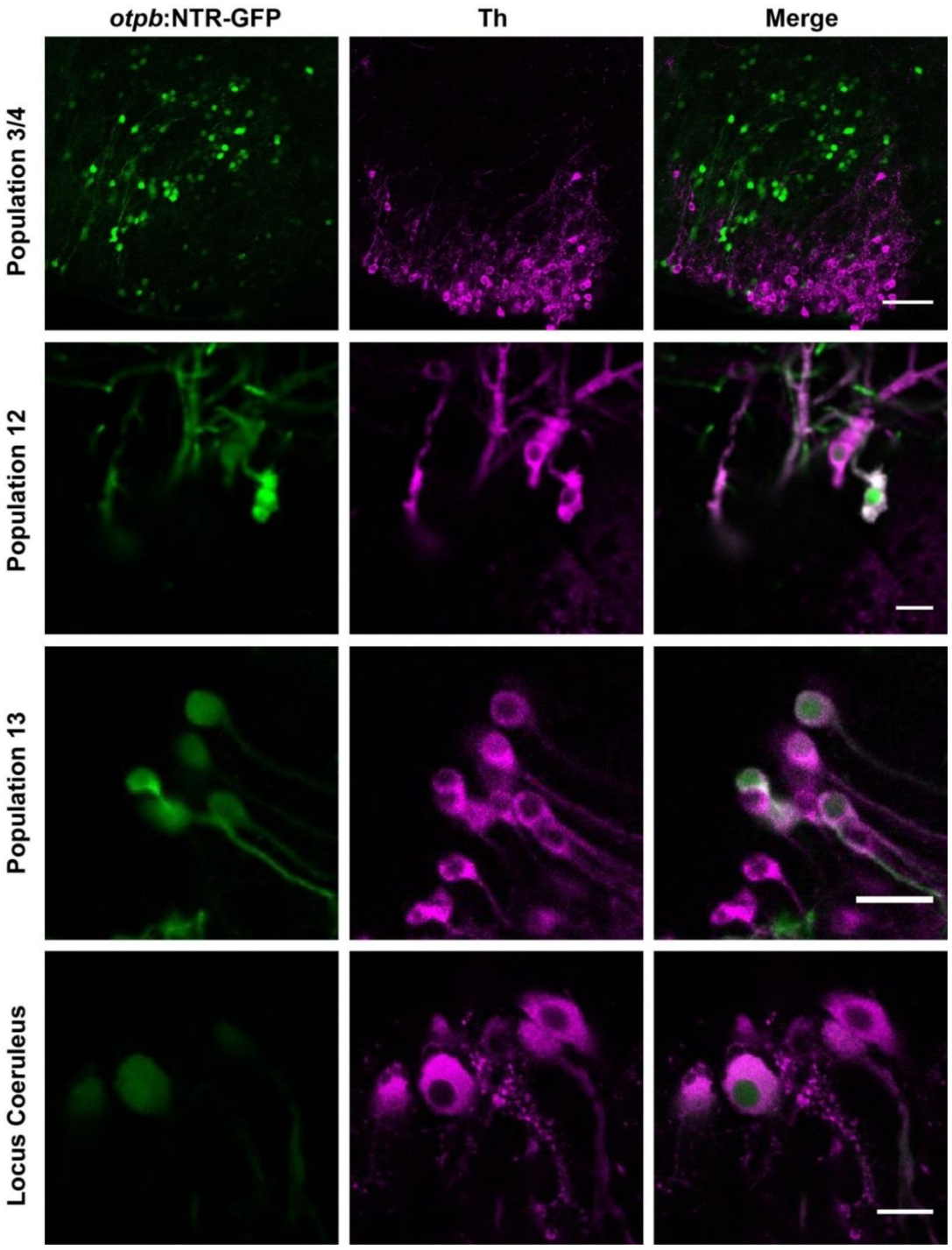

Figure 5. 3 There are different but overlapping populations of Th^+ and GFP^+ cells in the brains of adult *otpb*:NTR-GFP zebrafish. GFP^+ cells are seen in proximity to population 3/4. Population 12, population13, and the locus coeruleus all contain Th^+/GFP^+ cells. Scale bar for top row = 50 µm, scale bar in bottom three rows = 20 µm.

5.2.2.2 Immersion of adult zebrafish in metronidazole did not affect GFP$^+$ axons in the spinal cord

Immersion of otpb:NTR-GFP larvae in metronidazole induced dopaminergic cell death (Lambert et al. 2012). Metronidazole immersion has also been used to ablate NTR$^+$ cells in the CNS of adult zebrafish (Agetsuma et al. 2010; Soares Godoy 2015). I therefore sought to ablate cells in otpb:NTR-GFP adults by immersing the fish in metronidazole. In larvae, otpb:NTR-GFP$^+$ cells comprise the dopaminergic diencephalospinal tract (Lambert et al. 2012), and the presence of GFP$^+$ cells and axons in population 12 and the locus coeruleus demonstrates Th$^+$/GFP$^+$ axons also project to targets in the spinal cord in adulthood (Figure 5. 3). The absence of these axonal projections in the spinal cord can be used to determine the success of 6OHDA-induced ablation of Th$^+$ cells in the adult zebrafish brain. Hence, I assessed the success of metronidazole-induced ablation by comparing GFP$^+$ axons in the spinal cord. However, by qualitative observation, I detected no difference in the abundance of GFP$^+$ axons in fish immersed in metronidazole compared to vehicle treated controls (Figure 5. 4).

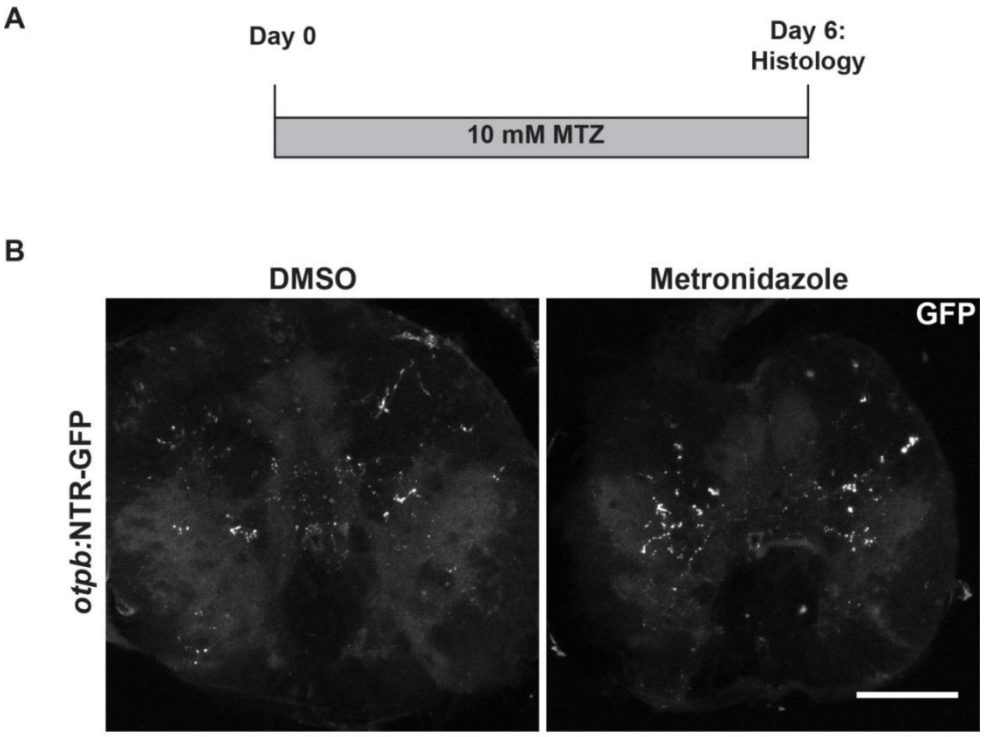

Figure 5. 4 No difference was observed between GFP$^+$ axons in the spinal cord of adult zebrafish immersed in metronidazole and vehicle treated controls. A: The experimental timeline is given. B: Maximum projections of GFP$^+$ axons in coronal sections of the adult spinal cord (dorsal is up). Scale bar = 100 µm.

5.2.2.3 Injection of metronidazole into adult zebrafish did not affect GFP$^+$ axons in the spinal cord

The Th$^+$ cells in population 12 and the locus coeruleus are located deep within the brain, and so we hypothesised that the lack of ablation could be due to insufficient levels of metronidazole reaching these cells. To avoid this potential issue I administered metronidazole by intraperitoneal injection. However, I still observed no qualitative difference in GFP$^+$ axons in the spinal cord between metronidazole and vehicle treated fish (Figure 5. 5).

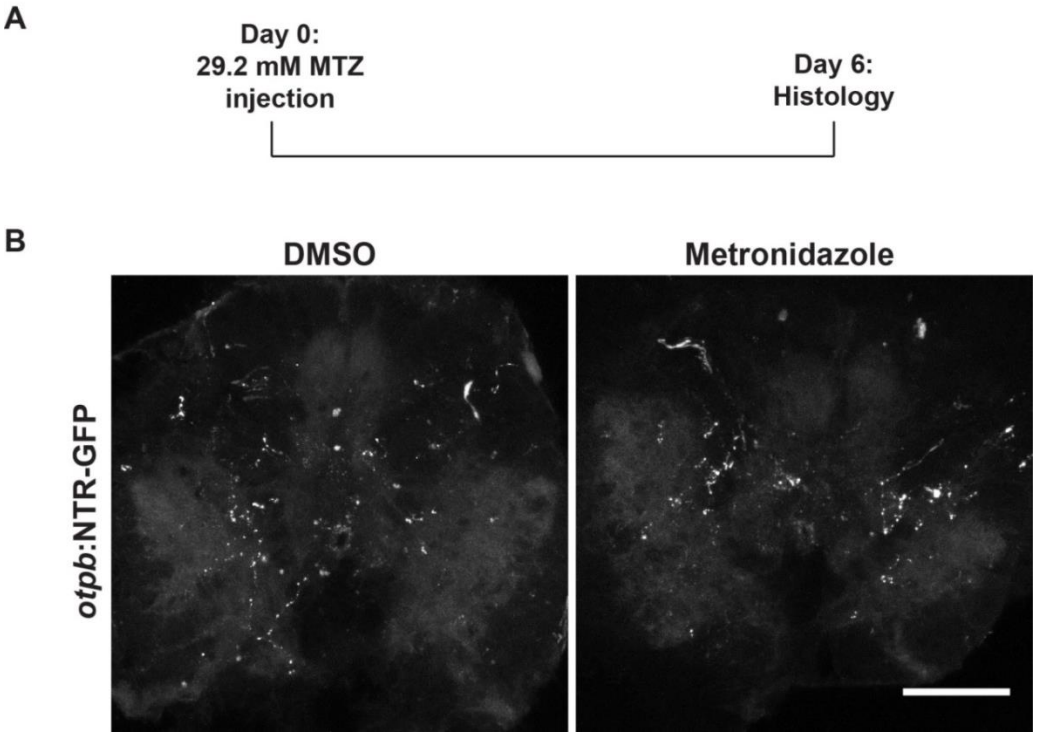

Figure 5. 5 No apparent difference was observed between GFP$^+$ axons in the spinal cord of adult zebrafish injected with metronidazole and vehicle treated controls, assessed by qualitative observation. A: The experimental timeline is given. B: Maximum projections of GFP$^+$ axons in coronal sections of the adult spinal cord (dorsal is up). Scale bar = 100 µm.

5.2.3 Chemical ablation of dopaminergic neurons: MPTP and MPP$^+$

Together with Leonardo Cavone, a postdoctoral researcher in our group, I attempted to ablate Th$^+$ neurons using MPTP and MPP$^+$. MPP$^+$ was injected directly into the ventricle in the brain, as it does not cross the blood brain barrier, whereas MPTP was administered by intraperitoneal injection. However, we observed no difference between Th$^+$ axons in MPTP and MPP$^+$ injected fish compared to vehicle injected controls, whereas 6OHDA-induced ablation of Th$^+$ cells (used as a positive control) caused a dramatic reduction in Th$^+$ axons present in the spinal cord (Figure 5. 6).

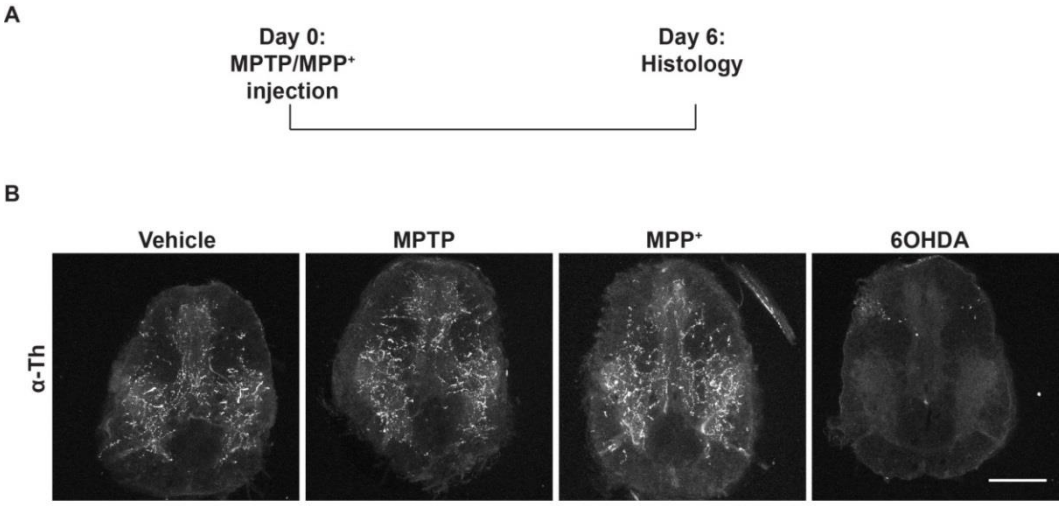

Figure 5. 6 No difference was observed in Th^+ axons the spinal cords of MPTP and MPP^+ injected fish compared to vehicle injected fish. A: The experimental timeline is given. B: Maximum projections of Th^+ axons in coronal sections of the adult spinal cord (dorsal is up). 6OHDA was used as a positive control, demonstrating the absence of Th^+ axons seen when ablation of population 12 is successful. Scale bar = 100 µm.

As Th^+ axons in the spinal cord all project from population 12, I also looked at the brains of MPTP and MPP^+ injected fish to determine whether other Th^+ populations may be more susceptible to the toxins. However, there were no obvious differences in the densities of Th^+ cells in population 12, population 13, and the locus coeruleus between MPTP and MPP^+ injected fish and controls. In the goldfish brain, MPTP causes a significant reduction in the level of noradrenaline, and a clear loss of Th^+ cells in the medulla (Poli et al. 1990), suggesting significant ablation of the locus coeruleus. Furthermore, the locus coeruleus has been shown to contain remarkably high levels of MAO, the enzyme responsible for the conversion of MPTP into MPP^+. I therefore reasoned that this population would be most susceptible to MPTP and MPP^+ toxicity. However, no differences in the Th^+ cells in the locus coeruleus was observed between MPTP and MPP^+ injected fish and controls (Figure 5. 7).

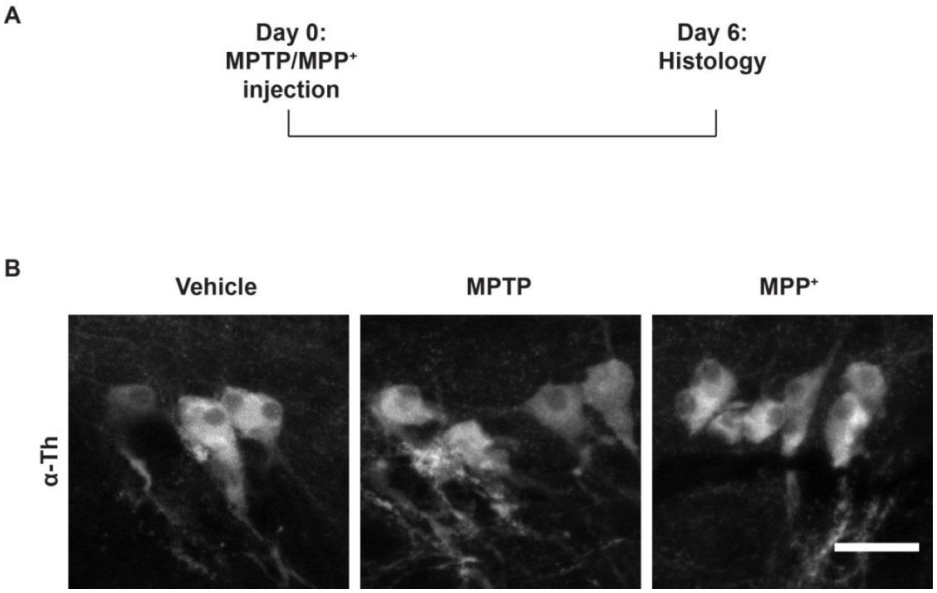

Figure 5. 7 No difference was observed in Th^+ neurons in the locus coeruleus of MPTP and MPP^+ injected fish compared to vehicle injected fish. A: The experimental timeline is given. B: Maximum projections of Th^+ neurons in sagittal sections of the adult brain (rostral is left). Scale bar = 50 µm.

We used a range of different concentrations of both MPTP and MPP^+ in our attempts to ablate Th^+ cells (

Table 5. 1). Higher concentrations of MPP^+ resulted in death of the animals, and so ablation of Th^+ cells could not be determined, but we could be confident that the compound was having some biological effect. Lower concentrations of MPP^+ and MPTP showed no signs of Th^+ neuron ablation.

Compound	Concentration (mM)	Mortality	Ablation of Th^+ axons in the spinal cord	Ablation of Locus Coeruleus
MPTP	11.5	No	No	No
	17.3	No	No	No
MPP^+	1	No	No	No

	3	No	No	No
	5	No	No	No
	7.5	Yes	-	-
	10	Yes	-	-

Table 5. 1Summary of attempts to ablate Th^+ neurons with MPTP and MPP^+. Only MPTP is able to permeate the blood brain barrier, and so MPP^+ was injected directly into the brain.

5.3 Discussion

5.3.1 Genetic manipulation to reduce the number of dopaminergic neurons: pink1

5.3.1.1 We found no differences in the numbers of Th^+ neurons in *pink1*$^{-/-}$ larvae compared to wildtype controls

In this chapter I showed that the number of Th^+ cells in *pink1*$^{-/-}$ larvae were similar to wildtype at 2, 3, 4, and 5 dpf (Figure 5. 1). This is in contrast to published results showing 25% fewer Th^+ cells at 5 dpf compared to wildtype controls (Flinn et al. 2013). All of the parent fish we used to breed embryos for this experiment were genotyped and confirmed to be *pink1*$^{-/-}$ (Figure 5. 1A). As there are several different strains of "wildtype" zebrafish (Guryev et al. 2006), and there may be variation between these strains, we used fish from the TL strain, the same background which was used to create the *pink1*$^{-/-}$ fish, as *pink1*$^{+/+}$ controls.

It is possible that the difference between our results and the previously published data could be due to the method used to detect Th^+ cells. We detected Th^+ cells using immunohistochemistry against the protein, whereas the published results used *in situ*

hybridisation with a probe against *Th* mRNA (Flinn et al. 2013). Therefore it is possible that a lower number of Th^+ cells detected by *in situ* hybridisation could be a result of decreased transcription of *Th* in dopaminergic neurons of *pink1*$^{-/-}$ larvae.

An even greater reduction in the number of Th^+ cells in population 12 was reported in adult *pink1*$^{-/-}$ fish (Flinn et al. 2013), compared to the difference seen at 5 dpf. However, a previous PhD student from our group performed detailed cell counts on each of the Th^+ populations in adult fish and did not find this reduction (Davies 2016). In both cases Th^+ cells were counted using Th immunohistochemistry.

It is possible that the environment the fish were raised in impacted the number of Th^+ neurons. In many cases, it is thought that a selective loss of dopaminergic neurons in patients and in animal models of Parkinson's disease is a result of genetic factors predisposing individuals to environmental toxins (Cannon & Greenamyre 2013). For example, zebrafish injected with *pink1* morpholino have fewer Th^+ neurons in the pretectal area than wildtype fish only when both groups were treated with MPTP, demonstrating an increased susceptibility to environmental stressors (Sallinen et al. 2010). It is possible that fish in the published study (Flinn et al. 2013) were exposed to an unidentified environmental factor which was not present in our zebrafish facility.

There are a number of other Parkinson's disease-associated genes which when manipulated in animals result in fewer dopaminergic neurons (Dawson et al. 2010). However, the lack of a reduction in Th^+ neurons I described here is consistent with other zebrafish models in which genes related to Parkinson's disease do not affect the numbers of dopaminergic neurons. For example, disruption of the Leucine-Rich Repeat Kinase 2 (LRRK2) encoding gene does not have a specific effect on the number of dopaminergic neurons in zebrafish. Morpholino-mediated knockdown LRRK2 had either no effect on the number of dopaminergic neurons (Ren et al. 2011)

or a decrease in Th^+ cells which was accompanied by a general increase in apoptotic cells throughout the whole fish (Sheng et al. 2010). $LRRK2^{-/-}$ zebrafish have reduced neurogenesis during development and after a stab lesion to the telencephalon, however no defects specific to dopaminergic neurons was found (Suzzi et al. 2017). Similarly, knockdown of *parkin* and *DJ-1* also had comparable numbers of dopaminergic neurons to controls (Fett et al. 2010; Bretaud et al. 2006). Even mutations which cause early-onset Parkinson's disease do not cause patients to develop symptoms for a number of decades (Kilarski et al. 2012), and so it could be expected that no loss of dopaminergic neurons is seen in these fish, particularly during the first few days of development.

Furthermore, counting the number of dopaminergic neurons does not distinguish between increased death of Th^+ neurons and reduced Th^+ neurogenesis. In the future this could be addressed by combining Th immunohistochemistry with markers for cell death, for example TUNEL, and with EdU to assess neurogenesis. The decreased generation of Th^+ neurons and generalised increased cell death seen in other zebrafish genetic models of Parkinson's disease demonstrate the relevance of this point (Sheng et al. 2010; Suzzi et al. 2017). Future experiments with these models should take these measures to examine the turnover of Th^+ neurons.

5.3.1.2 *pink1*$^{-/-}$ larvae have more 4C4$^+$ cells than wildtype controls

The results presented here show *pink1*$^{-/-}$ fish had approximately 50% more microglia in the diencephalon at 4 dpf compared to wildtype larvae (Figure 5. 2). This is in agreement with the 50% increase in $ApoE^+$ cells previously reported in these mutant fish (Flinn et al. 2013).

The microglial phenotype previously reported in *pink1*$^{-/-}$ fish was present at 3 dpf, before the fewer dopaminergic cells at 5 dpf (Flinn et al. 2013). To test whether the microglial activation may be causing the lower numbers of dopaminergic neurons in

pink1$^{-/-}$ fish, the authors used morpholino-mediated knockdown of the transcription factor *pu.1* to prevent microglial development. This morpholino had no effect on the number of dopaminergic neurons in *pink1*$^{-/-}$ fish compared to uninjected *pink1*$^{-/-}$ fish. This failure to rescue the lower numbers of Th^{+} neurons in *pink1*$^{-/-}$ larvae suggested that the microglial phenotype is a result of dying Th^{+} neurons, rather than an upstream mechanism which leads to reduced numbers of Th^{+} neurons. However, sufficient evidence that the morpholino affected the numbers of microglial cells in these fish is not provided.

Interestingly, *pink1*$^{-/-}$ mice have similar numbers of Th^{+} neurons to wildtype control mice, but they too exhibit a microglial phenotype, which precedes dopaminergic deficits. Levels of *il-1β*, *il-12*, and *il-10* were increased in the striatum of *pink1*$^{-/-}$ mice injected with the immunostimulant lipopolysaccharide (LPS) compared to wildtype mice also injected with LPS (Akundi et al. 2011). Furthermore, the only post-mortem report from a patient with two mutations in *pink1* mentions a moderate microgliosis (Samaranch et al. 2010). As this is relatively common among patients with neurodegenerative diseases it is often assumed that this is a result of neuronal cell death. However, as *pink1* is ubiquitously expressed it is possible that *pink1* mutations result in a microglial phenotype which is not caused by dopaminergic cell death. This could help to explain why I observed a microglial phenotype in *pink1*$^{-/-}$ fish but no difference in the number of Th^{+} neurons.

5.3.2 Chemogenetic ablation of dopaminergic neurons

The results presented here show overlapping but different patterns of GFP^{+} cells and Th^{+} cells in the brains of *otpb*:NTR-GFP adult zebrafish (Figure 5. 3). This corresponds to previous results in larvae (Lambert et al. 2012). For example, GFP^{+} cells are found in population 12 and the locus coeruleus, the Th^{+} neurons whose axons project to the spinal cord both in larvae and adults.

Metronidazole treatment did not lead to a reduction in GFP^+ cells in adult zebrafish (Figure 5. 4, Figure 5. 5). I immersed fish in 10 mM metronidazole, a concentration which has been shown to be sufficient to ablate cells in the CNS of adult zebrafish (Agetsuma et al. 2010; Soares Godoy 2015), although different lines are known to require different concentrations of metronidazole to induce cell death (Curado et al. 2008). Immersion of adult fish in concentrations higher than 10 mM metronidazole has been reported to increase mortality (Soares Godoy 2015), and for this reason I did not test higher concentrations. In an attempt to increase the availability of metronidazole to neurons in the fish I injected metronidazole intraperitoneally, however, this was also unsuccessful in ablating GFP^+ cells (Figure 5. 5).

I assessed the success of ablation by the presence of GFP fluorescence in the spinal cord in metronidazole treated and vehicle treated fish. It has previously been shown that cells which contribute to the dopaminergic diencephalic tract (DDT) are *otpb*$^+$ (Tay et al. 2011a; Ryu et al. 2007; Lambert et al. 2012). Therefore, successful ablation of *otpb*:NTR-GFP cells in the brain would dramatically reduce the amount of GFP^+ axons in the spinal cord.

It is possible that the lack of ablation is due to a reduction in the copy number of the transgene over several generations of breeding. Although the copy number may be high enough to detect fluorescence in which the transgene is expressed (Godoy et al. 2015), expression levels may not by high enough to metabolise metronidazole and cause cell death.

There are other zebrafish lines which express NTR in dopaminergic neurons. For example, a line has been created in which CFP-NTR is expressed in cells expressing the dopamine transporter (dat) (Godoy et al. 2015; Soares Godoy 2015). Double positive Th^+/CFP^+ cells were reportedly found in the olfactory bulb, ventral

telencephalon, PPa/PPp, PVO, PPr, and diencephalon. However, while metronidazole treatment did reduce the level of CFP in the brain by up to 80%, there was no difference in the level of Th, measured by western blotting with whole brain homogenate. This suggests that the majority of Th^+ neurons in the adult zebrafish were not successfully ablated in these fish. Nonetheless, cell counts showed metronidazole treated fish had fewer Th^+ neurons in the olfactory bulb. Furthermore, the numbers of CFP^+ cells, Th^+ cells, and Th^+/CFP^+ cells were recovered to vehicle treated levels by 45 days post metronidazole treatment. This was accompanied by an increased number of $BrdU^+/CFP^+$ cells in one region of the olfactory bulb 45 days post treatment. Together these results indicate that Th^+ cells of the olfactory bulb can be regenerated in the adult zebrafish brain, but that these fish may not be suitable to assess the regenerative capacity of other populations of Th^+ neurons due to unsuccessful ablation.

Another line expresses NTR under the control of the Th promoter (Fernandes et al. 2012). Metronidazole treatment of Tg(*BAC th:Gal4VP16*)^{m1233}; Tg(*UAS-E1b:NfsB-mCherry*)^{c294} larvae has been reported to ablate dopaminergic neurons in diencephalic groups 2 and 4 at 7 dpf, although the quantification of Th^+ cells indicated variable efficiency of the ablation. However, this driver line does not drive expression in all cells labelled by Th immunohistochemistry, and several areas of ectopic expression have been observed (Haehnel-Taguchi et al. 2018). In the NTR line the pattern of mCherry expression was not shown, so it is not possible to determine which other Th^+ populations expressed the NTR transcript. In the future, the overlap of $mCherry^+$ cells in the adult brain of these fish could be compared to Th^+ cells detected by immunohistochemistry to determine which populations express NTR. Treating these fish with metronidazole and assessing the level of ablation could then establish

whether these fish would be a useful tool for the ablation of Th^+ neurons in the adult zebrafish brain.

5.3.3 Chemical ablation of dopaminergic neurons: MPTP and MPP^+

The results I have presented here show we were unable to ablate Th^+ neurons in the adult zebrafish brain using MPTP and MPP^+ (Figure 5. 6, Figure 5. 7, Table 5. 1). This is in accordance with published results showing MPTP injections into adult zebrafish do not affect the numbers of Th^+ cells in the brain (Anichtchik et al. 2003; Bretaud et al. 2004). Although this is in contrast to the selective degeneration of Th^+ neurons reported in other species, there is known variation in the toxicity of MPTP between species (Speciale 2002; Langston 2017).

A key factor for MPTP-mediated ablation of dopaminergic neurons is the availability of monoamine oxidases (MAOs), the enzymes responsible for the conversion of MPTP into the toxic metabolite MPP^+. One explanation that has been suggested for this variability between species is the different levels of expression of MAO at the blood brain barrier. Rats, which are remarkably resistant to MPTP neurotoxicity, have very high levels of MAO at the blood brain barrier, and so systemically administered MPTP is converted into MPP^+ at the blood brain barrier. As MPP^+ is not lipophilic it cannot permeate the blood brain barrier, preventing the toxic compound from reaching the brain (Riachi et al. 1988; Riachi et al. 1989). In comparison, MAO is expressed to a lesser degree at the blood brain barrier in mice, and mice are moderately affected by MPTP, because some MPTP reaches the brain unconverted (Heikkila et al. 1984). Humans are most susceptible to MPTP, and, in line with this theory, human microvessels were the poorest in converting MPTP to MPP^+ (Riachi et al. 1988; Langston 2017). Although the level of MAO at the blood brain barrier in the adult zebrafish is not known, quantitative RT-PCR showed that MAO is expressed in adult zebrafish at relatively high levels outside the CNS, including the intestines and

liver (Anichtchik et al. 2006). This could explain why MPTP has been shown to cause peripheral effects in adult zebrafish such as quickened opercular movements and darkened skin pigmentation (Bretaud et al. 2004). Furthermore, *in situ* hybridisation was used to compare the expression of MAO in different areas of the adult zebrafish brain, and surprisingly low levels of expression were found around dopaminergic populations (Anichtchik et al. 2006). In contrast, noradrenergic neurons of the locus coeruleus contained relatively high levels of MAO (Anichtchik et al. 2006). Taken together, these findings suggest that the location of MAO may protect dopaminergic neurons in the adult zebrafish brain from MPTP-induced cell death.

To circumvent the problems associated with the conversion of MPTP into MPP^+, we injected MPP^+ directly into the brain, but this was also unsuccessful in ablating Th^+ neurons (Figure 5. 6, Figure 5. 7). Injection of MPP^+ has been shown to cause peripheral effects in zebrafish, including altered opercular movements (Bretaud et al. 2004). Therefore it is possible that the concentration needed to kill dopaminergic neurons in the adult zebrafish brain is higher than the concentration at which peripheral effects of MPP^+ become lethal.

I assessed whether successful ablation of Th^+ neurons was achieved by assessing the Th^+ immunoreactivity in the spinal cord and the number of Th^+ cell in the locus coeruleus (Figure 5. 6, Figure 5. 7). However, it is possible that other Th^+ populations were affected by MPTP/MPP^+ while these populations were unaffected. Detailed cell counts of each individual population would determine whether this is the case.

The four most commonly used chemicals to induce dopaminergic cell death in animal models are 6OHDA, MPTP, rotenone, and paraquat (Bové et al. 2005). Rotenone and paraquat are pesticides implicated in the pathogenesis of Parkinson's disease (Le Couteur et al. 1999), but neither compound had an effect on Th^+ neurons in the adult

zebrafish brain after 4 weeks of treatment (Bretaud et al. 2004). Hence 6OHDA is currently the only chemical which has been shown to reproducibly ablate Th^+ neurons in the adult zebrafish brain (Caldwell and Davies et al. 2018; Vijayanathan et al. 2017; Matsui et al. 2017).

5.4 Conclusions

In this chapter I attempted to find an alternative method to 6OHDA to ablate Th^+ neurons in the zebrafish brain. *pink1*$^{-/-}$ larvae had no difference in the numbers of Th^+ cells during development, although I did observe an increase in the numbers of $4C4^+$ cells. Tg*(otpb:NTR-GFP)* zebrafish had double positive Th^+/GFP^+ cells in populations of Th^+ neurons which are vulnerable to 6OHDA, however, I observed no ablation with metronidazole treatment. Thirdly, I tried injecting fish with MPTP and MPP^+, but I did not observe any indication of successful ablation.

Chapter Six: Investigating the Regeneration of Interneurons in the Spinal Cord

6.1 Introduction

6.1.1 Neuronal diversity in the zebrafish spinal cord

The neuronal circuitry of the spinal cord contains a number of different types of neurons. Anatomical observations of the zebrafish spinal cord have led to the classification of neurons based on their cellular morphology, axonal projections, and location (Figure 6. 1, (Bernhardt et al. 1992; Hale et al. 2001)). Neurons can also be grouped according to their neurotransmitter phenotype, as this often correlates with its functional role in the spinal cord circuitry, e.g. acetylcholine can be used to identify motor neurons. The majority of excitatory interneurons in the spinal cord are glutamatergic, while GABAergic neurons represent some of the main inhibitory neurons.

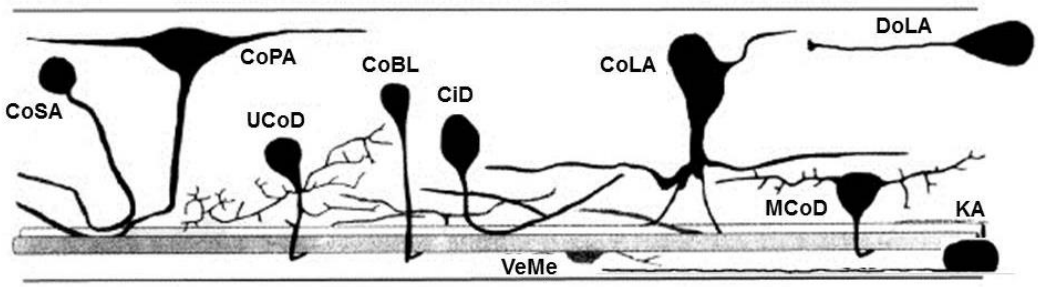

Figure 6. 1 A summary of the diversity of interneurons in the zebrafish spinal cord at 4-5 dpf, adapted from (Lewis & Eisen 2003)**. CoSA: Commissural Secondary Ascending neurons, CoPA: Commissural Primary Ascending neurons, UCoD: Unipolar Commissural Descending neurons, CoBL: Commissural Bifurcating Longitudinal neurons, CiD: Circumferential Descending neurons, VeMe: Ventral Medial neurons, CoLA: Commissural Longitudinal Ascending, MCoD: Multipolar Commissural Descending neurons, DoLA: Dorsal Longitudinal Ascending neurons, KA: Kolmer-Agduhr neurons.**

6.1.1.1. GABAergic neurons in the zebrafish spinal cord

GABAergic neurons can be detected by the presence of glutamate decarboxylase (gad), an essential enzyme in the synthesis of γ-aminobutyric acid (GABA) (Martin et

al. 1998). A combination of *in situ* hybridisation for *gad1* and immunohistochemistry for GABA has been used to identify GABAergic neurons in the zebrafish spinal cord. Both markers have been shown to have near identical distribution, indicating that gad1 is a suitable marker for GABAergic neurons in zebrafish (Higashijima, Mandel, et al. 2004). Of the several different types of interneurons which have been described in the developing spinal cord (Hale et al. 2001), four have been shown to be GABAergic in embryos, namely Dorsal Longitudinal Ascending (DoLA) neurons, Commissural Secondary Ascending (CoSA) neurons, Ventral Longitudinal Descending (VeLD) neurons, and Kolmer-Agduhr (KA) neurons ((Bernhardt et al. 1992), Figure 6. 1). In the larval zebrafish, the distribution of *gad1* expression correlates with the same cell types (Higashijima, Mandel, et al. 2004), and both DoLA and KA neurons have been confirmed to be GABAergic at 4-5 dpf by α-GABA immunolabelling (Higashijima, Schaefer, et al. 2004). While suspected technical difficulties in backfilling these neurons has prevented the identification of the exact cell types of GABAergic neurons in the dorsal and medial *gad1* expression domains (Higashijima, Schaefer, et al. 2004), extrapolating from GABAergic neurons found in embryos it is likely these cells are VeLDs and/or CoSAs.

6.1.1.2. Glutamatergic neurons in the zebrafish spinal cord

Glutamatergic neurons can be identified by the presence of vesicular glutamate transporters, which utilise the proton gradient to load glutamate into synaptic vesicles (Fremeau et al. 2004; Takamori et al. 2000). Previous studies indicate that the majority of glutamatergic neurons express *vglut2* (Fremeau et al. 2004; Herzog et al. 2004). Based on location and cellular morphology, six different types of vglut2a^{+} interneurons have been identified in the larval zebrafish spinal cord, including Circumferential Descending (CiD) interneurons, Multipolar Commissural Descending (MCoD) interneurons, Unipolar Commissural Descending (UCoDs) neurons, Ventral

Medial (VeMe) interneurons, Commissural Primary Ascending (CoPA) interneurons, and glutamatergic Commissural Secondary Ascending (CoSA) interneurons (Figure 6. 1), in addition to sensory Rohon Beard neurons (Hale et al. 2001; Higashijima, Schaefer, et al. 2004; Higashijima, Mandel, et al. 2004).

The creation of fluorescent reporter lines in which RFP or GFP is driven by neurotransmitter-specific promoters has provided further insights into the relative distributions of GABAergic and glutamatergic neurons in the zebrafish spinal cord (Satou et al. 2013). Consistent with previous *in situ* hybridisation and immunostaining (Higashijima, Schaefer, et al. 2004; Higashijima, Mandel, et al. 2004), these lines showed that *vglut2a*$^{+}$ and *gad1b*$^{+}$ neurons are distinct populations in the larval zebrafish spinal cord (Satou et al. 2013). These lines represent useful tools for investigating the distribution of GABAergic and glutamatergic neurons in the adult zebrafish spinal cord.

6.1.2. Neurogenesis in zebrafish spinal cord regeneration

6.1.2.1. Adult zebrafish spinal cord regeneration

Following complete transection of the spinal cord adult zebrafish are able to recover function and regain normal swimming capacity by six weeks post lesion (Becker et al. 2004; Reimer et al. 2008).

A spinal cord lesion induces neuronal cell death, and successful regeneration involves the replacement of these neurons. New neurons are generated from ependymo-radial glial cells (ERGs), which have a soma contacting the ventricle and long processes extending to the pial edge (Becker & Becker 2015). In the unlesioned adult spinal cord ERGs are essentially quiescent, demonstrated by very low numbers of PCNA^{+} and BrdU^{+} cells (Reimer et al. 2008). However, a lesion stimulates ERGs proximal to the

lesion site to proliferate and generate new neurons to replace those which have been lost, shown by an increase in PCNA$^+$ and BrdU$^+$ cells at the ventricle from 3 -14 dpl (Reimer et al. 2008).

At least some of these new neurons are motor neurons, demonstrated by the presence of BrdU$^+$ cells at 2 wpl which are also HB9:GFP$^+$ and/or islet-1:GFP$^+$ (Reimer et al. 2008), markers of differentiating motor neurons (Flanagan-Steet et al. 2005; Higashijima et al. 2000). However, fewer than 8% of BrdU labelled cells at 2 wpl also express markers for motor neurons (Reimer et al. 2008), indicating that other neuronal subtypes may also be produced in the lesioned adult spinal cord. Moreover, lesion-induced proliferation is not restricted to ERGs in the motor neuron progenitor domain, as PCNA$^+$ cells are seen surrounding the entire central canal (Reimer et al. 2008). Previous studies have discovered that a range of neuronal subtypes are regenerated in zebrafish after a spinal cord lesion (Kuscha, Frazer, et al. 2012; Kuscha, Barreiro-Iglesias, et al. 2012). The various neuronal subtypes which have been shown to be newly generated after a spinal cord lesion in adult zebrafish are summarised in Figure 6. 2. However, it is still unclear whether GABAergic and glutamatergic neurons are replaced after a spinal cord lesion.

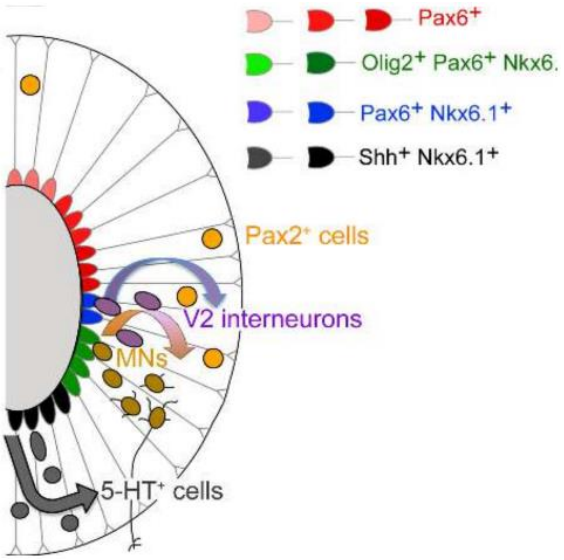

Figure 6. 2 Summary of different neuronal subtypes previously shown to be newly generated in the lesioned spinal cord of adult zebrafish, illustrated on a schematic cross-section. 5-HT$^+$ (serotonergic) neurons (Kuscha, Barreiro-Iglesias, et al. 2012)**, motor neurons** (Reimer et al. 2008; Reimer et al. 2009)**, V2 cells** (Kuscha, Frazer, et al. 2012)**, and Pax2$^+$ interneurons** (Kuscha, Frazer, et al. 2012) **have been demonstrated to be newly generated after a spinal cord lesion. Taken from** (Kuscha, Frazer, et al. 2012)**.**

6.1.2.2 Larval zebrafish spinal cord regeneration

Similarly, larval zebrafish lesioned at 3 days post-fertilisation (dpf) can regenerate their spinal cord and recover normal swimming behaviour by 2 days post-lesion (dpl) (Ohnmacht et al. 2016). At this stage of development, ERGs around the central canal are still proliferative, but the majority of neurogenesis is completed by 3 dpf (Park et al. 2007). The number of newly generated motor neurons (HB9:GFP$^+$/EdU$^+$ cells) is increased two days after a lesion compared to unlesioned age-matched controls (Ohnmacht et al. 2016), demonstrating that there is a lesion-induced increase in neurogenesis in order to replace neurons which have been lost. However, the extent to which different neuronal subtypes are replaced after a spinal cord lesion in larval zebrafish has not been fully elucidated.

In this chapter I aim to investigate the localisation of glutamatergic and GABAergic neurons in the adult zebrafish spinal cord, and assess the capacity to regenerate these neuronal subtypes following a spinal cord lesion in both larvae and adults.

6.2 Results

6.2.1 *gad1b*$^+$ neurons are regenerated after a lesion

6.2.1.1 The number of newly generated *gad1b*:RFP$^+$ neurons is increased in lesioned larvae

I assessed the formation of new GABAergic neurons in the spinal cord of larval zebrafish at 5 dpf with and without a lesion using a transgenic line in which *gab1b*$^+$ neurons are labelled with RFP (Satou et al. 2013). Larvae were lesioned at 3 dpf and immersed in EdU until histology at 5dpf (Figure 6. 3A). The number of new GABAergic

neurons (EdU$^+$/RFP$^+$ cells) was significantly higher in lesioned animals compared to unlesioned fish (unlesioned: 0.7778 ± 0.2222, lesioned: 2.444 ± 0.2422, Figure 6. 3), indicating that GABAergic neurons can be regenerated after a spinal cord injury.

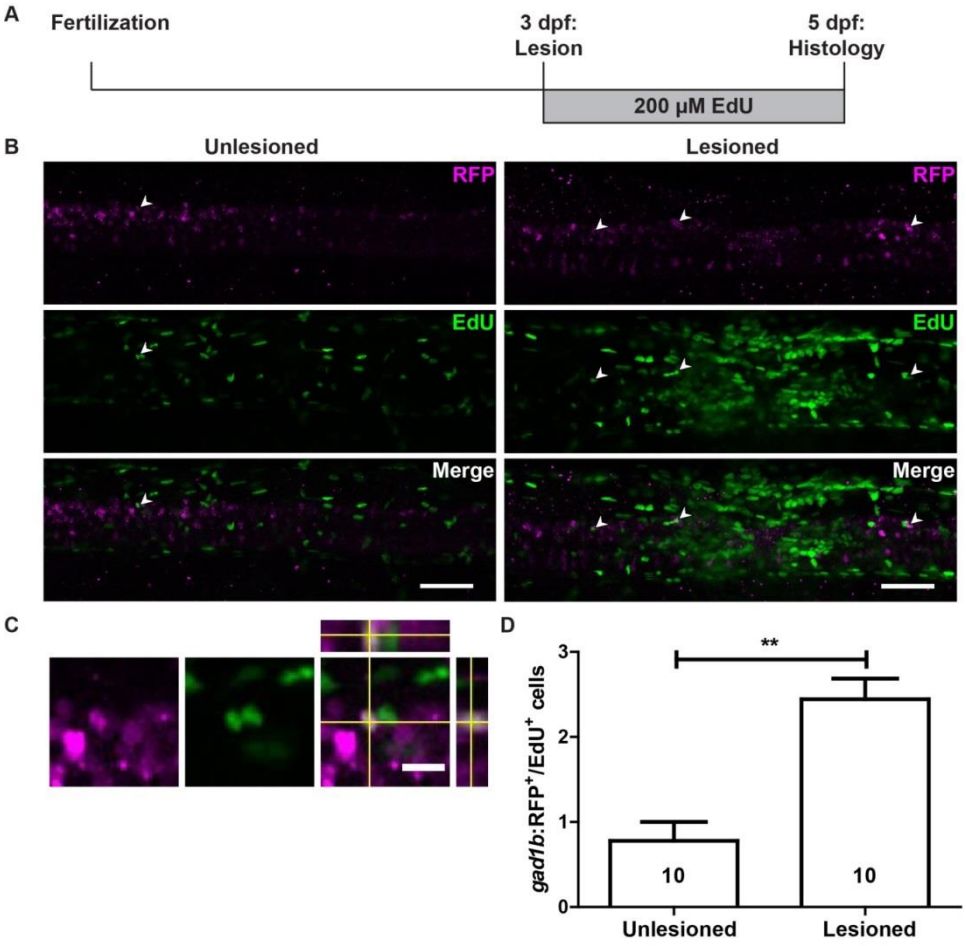

Figure 6. 3 *gad1b*:RFP$^+$ neurons are regenerated following a spinal cord lesion in the larval zebrafish. A: The experimental timeline is shown. B: Single optical sections showing EdU$^+$ and RFP$^+$ cells in the spinal cord around the lesion site, with double labelled cells indicated by the arrows (lateral view, rostral left). C: Zoomed in images showing an EdU$^+$/RFP$^+$ cell. D: Quantification showing the numbers of EdU$^+$/RFP$^+$ cells. Mann Whitney U test, ** p < 0.01. Scale bar in B = 50 µm, scale bar in C = 10 µm.

6.2.1.2 Lesion-induced *gad1b*:RFP$^+$ neurogenesis in the adult spinal cord

To determine whether *gad1b*$^+$ neurons could also be regenerated in the adult spinal cord, I injected fish with EdU at 3 and 6 days post-lesion (dpl) and counted the numbers of EdU$^+$/RFP$^+$ cells at 14 dpl. Double labelled cells were never observed in unlesioned controls, only in lesioned spinal cords (Figure 6. 4, unlesioned: 0 ± 0, 2

wpl: 35.83 ± 5.388). This demonstrates that there is lesion-induced neurogenesis of GABAergic neurons following a spinal cord lesion in adult zebrafish.

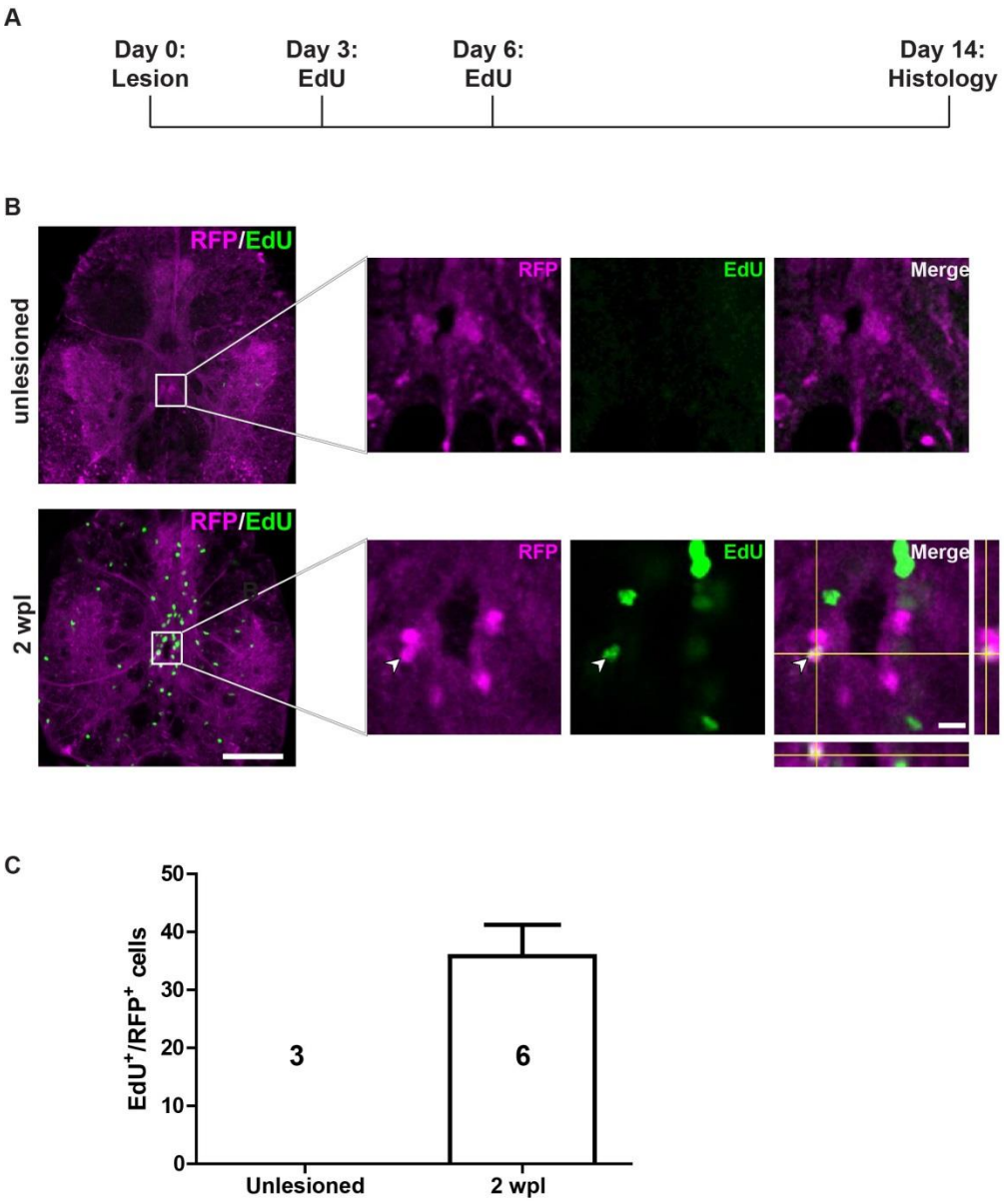

Figure 6. 4 *gad1b*:RFP$^+$ neurons are regenerated after an injury to the adult zebrafish spinal cord. A: The experimental timeline is given. B: Maximal projections showing EdU$^+$ cells and RFP$^+$ cells in coronal sections of the adult zebrafish spinal cord, with zoomed in images of single sections around central canal. The arrow indicates a EdU$^+$/RFP$^+$ cell close to the central canal. D: Quantification showing the numbers of EdU$^+$/RFP$^+$ cells. Scale bars = 100 µm, 10 µm

6.2.2 *Vglut2a*:GFP$^+$ neurons are regenerated after a lesion

6.2.2.1 The number of newly generated *vglut2a*:GFP$^+$ neurons is increased in lesioned larvae

I assessed the formation of new glutamatergic neurons in the spinal cord of larval zebrafish at 5 dpf with and without a lesion using a transgenic line in which *vglut2a*$^+$ neurons are labelled with GFP (Satou et al. 2013). Larvae were lesioned at 3 dpf and immersed in EdU until histology at 5 dpf (Figure 6. 5A). Double labelled GFP$^+$/EdU$^+$ cells were rarely observed in control animals, suggesting the majority of glutamatergic neurogenesis is completed by 3 dpf. The number of new *vglut2a*:GFP$^+$ neurons (EdU$^+$/GFP$^+$) neurons was significantly higher in lesioned animals compared to unlesioned fish (unlesioned: 0.2500 ± 0.1637, lesioned: 3.444 ± 0.3768, Figure 6. 5), indicating that glutamatergic neurons can be regenerated after a spinal cord injury.

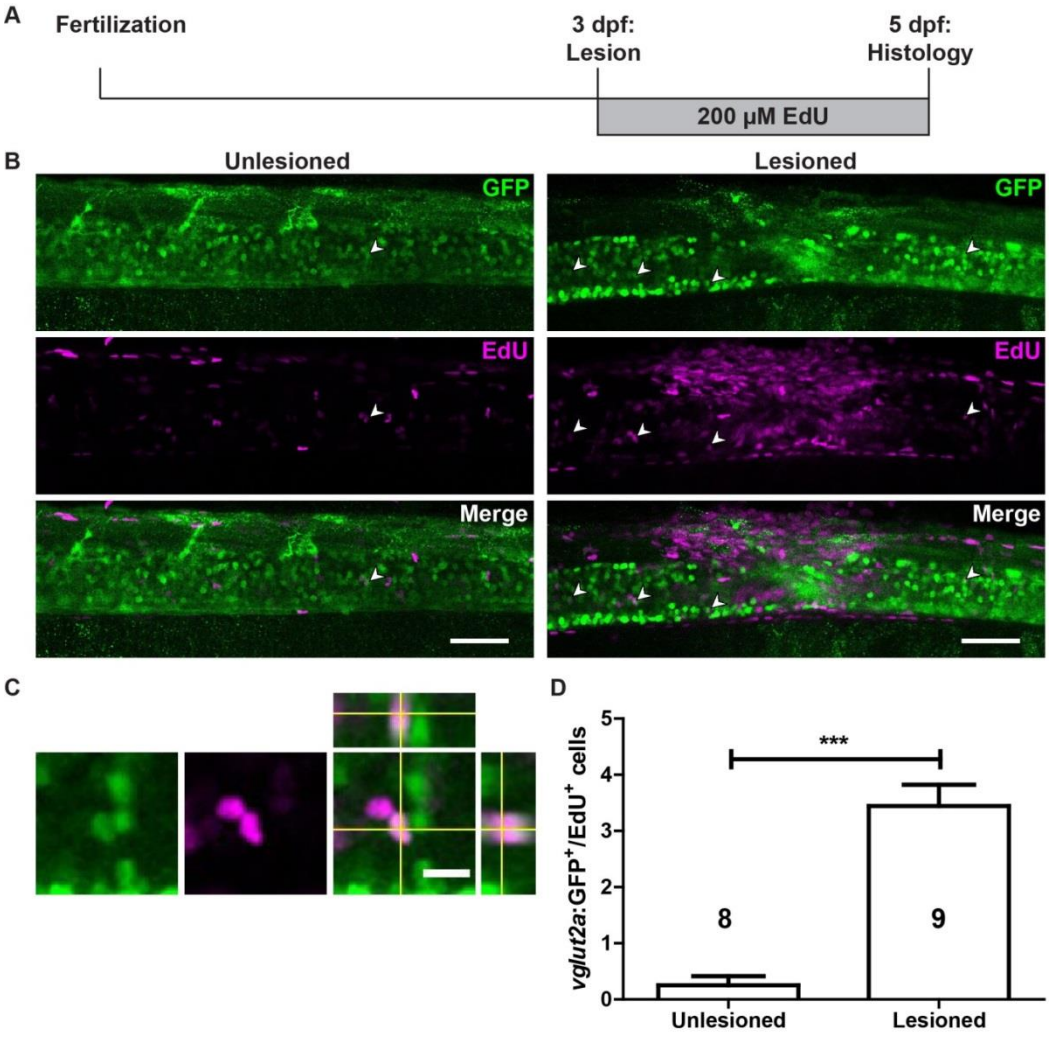

Figure 6. 5 *Vglut2a*:GFP$^+$ neurons are regenerated following a spinal cord lesion in the larval zebrafish. A: The experimental timeline is shown. B: Maximum projections showing EdU$^+$ and GFP$^+$ cells in the spinal cord around the lesion site, with double labelled cells indicated by the arrows (lateral view, rostral left). C: Zoomed in images showing an EdU$^+$/GFP$^+$ cell. D: Quantification showing the numbers of EdU$^+$/GFP$^+$ cells. Mann Whitney U test, *** p < 0.001. Scale bar in B = 50 µm, scale bar in C = 10 µm.

6.2.2.2 No newly generated *vglut2a*:GFP$^+$ neurons were found in the adult zebrafish spinal cord

To determine whether *vglut2a*$^+$ neurons could also be regenerated in the adult spinal cord, I injected fish with EdU at 3 and 6 dpl and counted the numbers of EdU$^+$/RFP$^+$ cells at 14 dpl (Figure 6. 6A). In the dorsal area of the spinal cord GFP$^+$ cells were observed in both conditions, but were not present in every section. These were accompanied by what appeared to be GFP$^+$ axons projecting in a rostral caudal

direction. Large cell bodies were also found close to the central canal, with long axons extending diagonally outwards. No double labelled GFP^+/EdU^+ cells were observed in the unlesioned (n=4) or the lesioned spinal cord (n=3).

To better understand the pattern of GFP labelling in adult zebrafish I collaborated with Cristina Gonzalez Martinez to obtain images of the intact spinal cord without sectioning the tissue. The cleared tissue allowed us to view up to just over one hemisection of the spinal cord (Figure 6. 6C). Using Imaris software we were able to rotate the 3D reconstruction, and this verified that the dorsal spinal cord contained GFP^+ axons projecting in a rostral-caudal direction. Cells were visible along these axons, however they were relatively heterogeneously distributed, with up to 100 µm with no cells. In the ventral spinal cord, we observed thick axons running in a rostral-caudal direction in the ventral lateral corner of the spinal cord, with axons extending diagonally to cells in the medial region of the spinal cord.

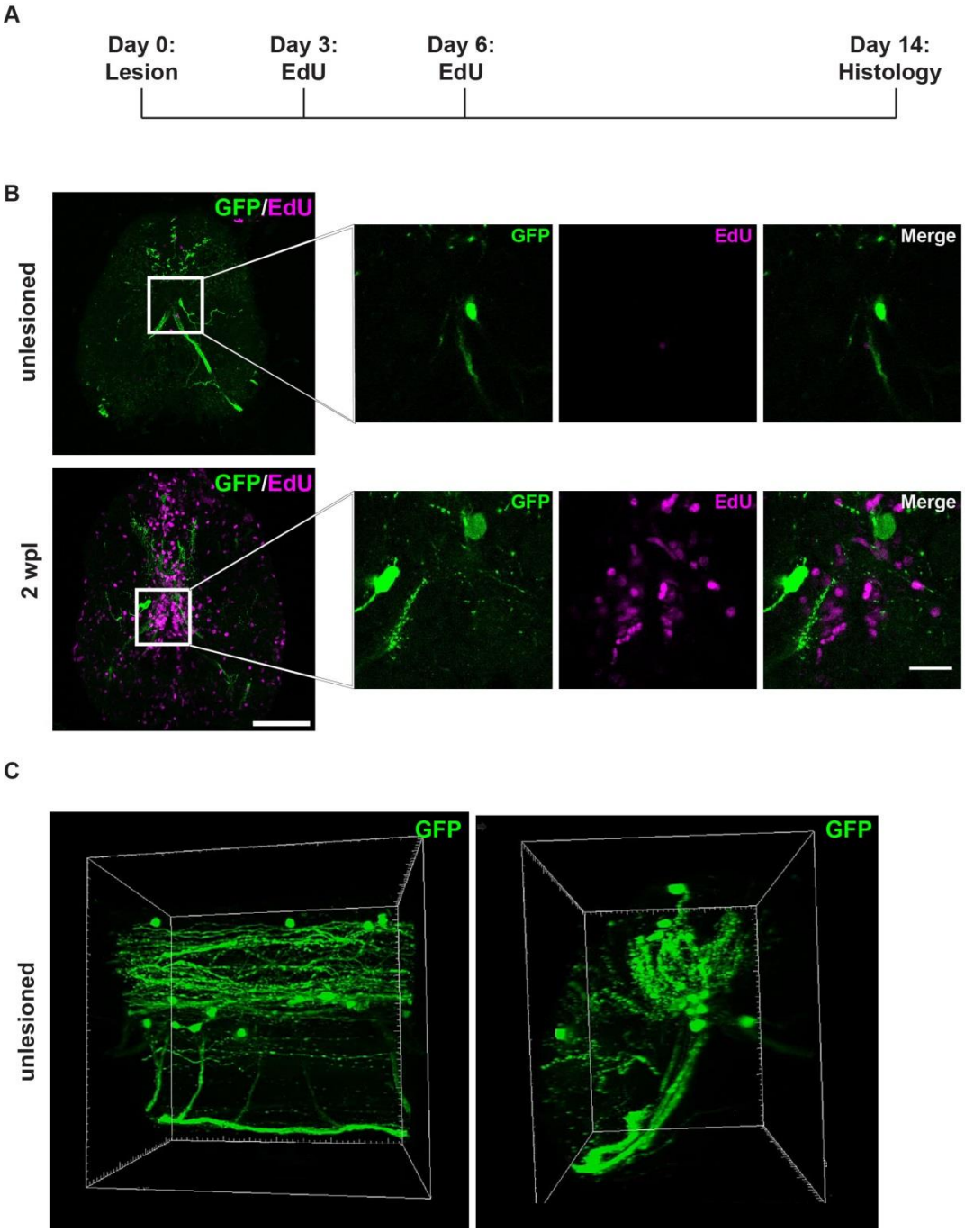

Figure 6. 6 *vglut2a*:GFP^{+} neurons in the adult zebrafish spinal cord. A: The experimental timeline for B is shown. B: Maximum projections showing EdU^{+} and GFP^{+} cells in coronal sections of the adult spinal cord, with zoomed in images of single sections around the central canal. No double labelled GFP^{+}/EdU^{+} cells were observed in either condition. C: Images of the adult spinal cord showing the distribution of *vglut2a*:GFP^{+} axons and cells from a lateral view (left rostral) and coronal cross section. Scale bars in B = 100 µm, 25 µm

6.3 Discussion

6.3.1 *gad1b*:RFP$^+$ neurons are present around the central canal in the adult zebrafish spinal cord, and are newly generated after a spinal cord lesion

gad1b:RFP$^+$ cells were observed close to the central canal in the adult zebrafish spinal cord (Figure 6. 4). Based on their position in the spinal cord these appear to be Kolmer-Agduhr (KA) neurons, which have been described previously in the developing zebrafish spinal cord (Bernhardt et al. 1992; Martin et al. 1998; Higashijima, Schaefer, et al. 2004).

In this chapter I have demonstrated that a spinal cord lesion induces neurogenesis of *gad1b*:RFP$^+$ neurons in the adult zebrafish spinal cord (Figure 6. 4). This indicates that GABAergic neurons are regenerated in addition to the other neuronal subtypes already shown to be regenerated in the adult zebrafish spinal cord (Figure 6. 2, (Reimer et al. 2008; Kuscha, Frazer, et al. 2012; Kuscha, Barreiro-Iglesias, et al. 2012)). A previous PhD student (Veronika Kuscha) reported a trend for increased GABAergic interneurons after a lesion ((unlesioned: 576.15 ± 47.20, n = 3; 2 wpl: 621.46 ± 7.18, n = 2)(Kuscha 2011)) , however, this did not reach statistical significance, and no BrdU$^+$/GABA$^+$ cells were observed in either unlesioned or lesioned spinal cords at 2 wpl. Future experiments could use the *gad1b*:RFP$^+$ reporter line in combination with immunohistochemistry for GABA to determine whether the two labels completely overlap in the adult spinal cord, as has been demonstrated in the developing spinal cord (Higashijima, Mandel, et al. 2004).

In the adult zebrafish brain, GABAergic neurons have been shown to be newly generated following excitotoxic injury (Skaggs et al. 2014). Genetic lineage tracing demonstrated these GABAergic neurons can be produced from *her4*$^+$ ERGs. Future

experiments could use a similar approach to establish whether newly generated GABAergic neurons are also derived from *her4*$^+$ progenitor cells in the spinal cord.

Immunohistochemistry for the postsynaptic protein SV2 has confirmed that regenerated motor neurons make synaptic contacts, demonstrating that they can integrate into the existing neuronal circuitry (Reimer et al. 2008). Applying the same method and looking for overlap between SV2 labelling and GABAergic neurons would determine whether these neurons also establish synaptic connections.

6.3.2 *vglut2a*:GFP$^+$ neurons are present in the adult zebrafish spinal cord

The GFP labelling in the spinal cord of *vglut2a*:GFP$^+$ fish showed that there are *vglut2a*$^+$ neurons and axons in the adult zebrafish spinal cord. However, no GFP$^+$/EdU$^+$ cells were observed in either the unlesioned or lesioned spinal cords, suggesting that *vglut2a*$^+$ neurons are not newly generated in the adult zebrafish spinal cord, even after a spinal cord lesion. However, it is possible that *vglut2a*$^+$ neurogenesis does occur, but at a lower level than other neuronal subtypes, thus making it less likely to observe *vglut2a*$^+$:GFP$^+$/EdU$^+$ cells. The low density of GFP$^+$ cells meant there were several sections with no GFP$^+$ cells at all, and this combined with the limited bioavailability of EdU means the probability of observing a double labelled cell may be very low, even if they do exist. Future experiments could look to repeat this experiment with more fish, and use the tissue clearing to view a larger area of the whole spinal cord rather than individual 50 µm sections. In addition, increasing the number of EdU injections would label more proliferating ERGs, and therefore give a higher chance of detecting any newly generated *vglut2a*$^+$ neurons.

In the developing zebrafish spinal cord, *vglut2a*$^+$ neurons have been shown to be derived from dorsal progenitor domains, including pd1, pd3, and pd4/5 (Satou et al. 2013). A previous member of our research group found that markers of dorsal

progenitor domains, for example *pax3* and *pax7*, are not expressed after a lesion (Dr. Veronika Kuscha, unpublished). In contrast, genes expressed in the ventral progenitor domains during development, for example *olig2*, *nkx6.1*, and *pax6*, showed increased expression following a lesion in adult zebrafish spinal cord (Reimer et al. 2009). All of the neurons which have been shown to be regenerated after a spinal cord lesion in adult zebrafish are derived from ventral progenitor domains (Figure 6.2, (Reimer et al. 2008; Kuscha, Barreiro-Iglesias, et al. 2012; Kuscha, Frazer, et al. 2012). This suggests that the different capacity to regenerate neurons after a spinal cord lesion may be a reflection of the dorso-ventral location of the progenitor domains from which neurons are derived during development.

Future experiments could investigate whether the *vglut2a*:GFP$^+$ axonal projections are regenerated following a spinal cord lesion. The majority of GFP$^+$ axons I observed in the adult spinal cord ran in a rostral-caudal direction (Figure 6.6), and so must be disrupted by a complete transection of the spinal cord. The regeneration of axons is essential for the re-establishment of neuronal circuity and functional recovery (Becker et al. 1997). Tissue clearing could be used to obtain a lateral view of the tissue bridging the lesion site to determine whether *vglut2a*:GFP$^+$ axons are able to regrow across the lesion site. This could then be used in combination with immunohistochemistry for synaptic markers, such as SV2, to identify any *vglut2a*:GFP$^+$ axons successfully bridging the lesion site and making synaptic contacts.

6.3.3 Glutamatergic and GABAergic interneurons are newly generated following a spinal cord lesion in larval zebrafish

Here I demonstrate for the first time that there is a lesion-induced increase in newly formed *gad1b*:RFP$^+$ and *vglut2a*:GFP$^+$ interneurons in the larval zebrafish spinal cord (Figure 6. 3, Figure 6. 5). The low numbers of EdU$^+$ neurons observed in both

experiments suggest that neurogenesis of these cell types is largely complete by 3 dpf, consistent with previous observations. The results presented here align with previous publications showing glutamatergic neurons are regenerated after a spinal cord injury in lamprey (Fernández-López et al. 2016), suggesting this capability is not species-specific.

In a similar model of spinal cord injury, in which larval zebrafish were lesioned at 5 dpf and analysed at time points up to 9 dpi, proliferation of ERGs in the p0 progenitor domain was increased in lesioned fish compared to sham controls (Briona & Dorsky 2014b). This domain is defined by expression of *dbx1*, and both glutamatergic neurons and GABAergic neurons are derived from this population of progenitor cells during embryogenesis (Satou et al. 2012). Approximately 75% of newly generated neurons ($BrdU^+/HuC/D^+$ cells) in the proximal zone were also *dbx1a*:GFP^+ (Briona & Dorsky 2014b), indicating that the majority of newly generated neurons produced after a spinal cord lesion are derived from this progenitor domain. However, it is not known whether this domain also generates both glutamatergic and GABAergic neurons after a lesion. Future experiments could employ genetic lineage tracing to learn more about the progenitor cells responsible for the newly generated neurons. Zebrafish lines have been created in which Cre is specifically expressed in cells in particular progenitor domains of the spinal cord, and these have been used in combination with Tg(*gad1b*:loxP-RFP-loxP-GFP) and Tg(*vglut2a*:loxP-GFP-loxP-RFP) lines to successfully determine the origin of interneurons during development (Satou et al. 2013; Kani et al. 2010). Replacing the constitutively active Cre with an inducible form would allow for temporal control. Immersing these larvae in 4OHT at the time of injury could determine which progenitor domains proliferate in response to the lesion and generate new neurons.

As discussed in the introduction to this chapter, there are several different types of glutamatergic and GABAergic neurons in the larval zebrafish spinal cord (Figure 6. 1), and the fluorescent reporter lines I used do not discriminate between these classes of neurons. Neuronal cell bodies were clearly visible in the images I obtained (Figure 6. 3, Figure 6. 5), but the axonal projections of individual cells could not be followed due to relatively weaker fluorescent signal in the axonal projections and the high density of neuronal cell bodies. This prevented the identification of different types of interneurons labelled by each line (Hale et al. 2001). Future experiments could aim to determine which classes of glutamatergic and GABAergic interneurons are regenerated after a spinal cord lesion. Labelling only newly generated neurons, for example using genetic lineage tracing with inducible drivers, would produce a sparser labelling of neurons. This could increase the ability to evaluate the axonal projections of newly generated neurons and determine which types of interneurons are newly generated after a lesion.

6.4 Conclusions

In larvae, a spinal cord lesion induces an increase in the numbers of newly generated GABAergic and glutamatergic neurons. In adult zebrafish, GABAergic neurons are found in the medial spinal cord close to the central canal, and at least some are regenerated following a spinal cord lesion. Glutamatergic neurons are found in the dorsal spinal cord, with the majority of axons projecting in a rostral-caudal direction. I found no evidence of regenerated glutamatergic neurons in adult zebrafish following a spinal cord lesion.

Chapter Seven: General Discussion

In this thesis I investigated which populations of neurons are capable of being regenerated in the zebrafish central nervous system, which cells give rise to regenerated neurons, and the signalling pathways involved in their regeneration. Through genetic lineage tracing I was able to determine the origin of dopaminergic neurons formed after 6OHDA-induced ablation of Th^+ cells. I also investigated the involvement of signalling pathways in the successful regeneration of dopaminergic neurons. I then attempted to find an alternative method to ablate Th^+ neurons in the zebrafish brain. Finally, I investigated the extent to which glutamatergic and GABAergic neurons are regenerated after a spinal cord lesion.

7.1 Investigating the Origin of New Th^+ Neurons in the Adult Zebrafish Brain

In investigating the origin of Th^+ neurons in the adult zebrafish brain I found that cells lining the diencephalic ventricle display the morphology of ERGs, and described the heterogeneity of these cells in terms of their expression of *gfap*, *olig2*, and *her4*. Using genetic lineage tracing I showed that new Th^+ neurons can be generated from *her4*$^+$ ERGs at the diencephalic ventricle.

Neurogenesis in the adult rodent brain is thought to be restricted to the olfactory bulb, the subventricular zone (SVZ) of the lateral ventricles in the telencephalon and the subgranular zone (SGZ) of the dentate gyrus in the hippocampus (Altman & Das 1965; Altman 1969; Bergmann et al. 2015). However, there have been reports of newly generated neurons in other areas, including the area of the brain affected by Parkinson's disease in humans. Investigations into whether new Th^+ neurons can be found in the substantia nigra have delivered conflicting results, and, as a result, whether new Th^+ neurons are added to the mammalian substantia nigra in adulthood is still a matter of debate (He & Nakayama 2009; Lamm et al. 2014; Borta & Höglinger

2007). $BrdU^+/Th^+$ cells have been detected in the substantia nigra of adult mice, although the number of double-labelled cells was very low, which the authors suggest may be one of the reasons they have been overlooked by others (Zhao et al. 2003). The new Th^+ neurons were shown to be derived from cells at the ventricle, which express markers of neural stem cells (Zhao et al. 2003; Shan et al. 2006). This suggests that there may be similarities in the cells from which Th^+ neurons originate in the mammalian brain and in salamanders and zebrafish, species which are capable of successful regeneration of Th^+ neurons. Therefore further investigation into the genes expressed by ERGs giving rise to Th^+ neurons in zebrafish could help to identify a pool of progenitor cells in the adult mammalian brain which could be stimulated to replace Th^+ neurons lost in Parkinson's disease. However, it should be noted that the population of Th^+ neurons investigated here (population 5/6) is not considered to be equivalent to the substantia nigra (Kaslin and Panula 2001; Rink and Wullimann 2001), and that despite the replacement of dopaminergic neurons in this population the functional deficits observed after 6OHDA-induced ablation of Th^+ neurons observed in behavioural studies are not recovered (Caldwell and Davies et al. 2018). This is likely a consequence of the permanent loss of descending axonal projections from the locus coeruleus and population 12, which provide the only catecholaminergic innervation of the spinal cord.

Having established the origin of new Th^+ cells in the brain, future work could investigate the fate of new Th^+ neurons generated after 6OHDA-induced ablation of dopaminergic neurons. For successful neuroregeneration it is necessary for neurons to make synaptic contacts and integrate into the existing neural circuitry. Analysis of a terminal field ventral to population 5/6 found that the axon density in 6OHDA-injected fish was reduced in 6OHDA injected fish compared to uninjected controls (Caldwell and Davies et al. 2018). The axon density was still lower in 6OHDA-injected

fish at 42 dpi and 180 dpi, when cell numbers have recovered. However, the axon density did reach control levels at 540 dpi. This indicates that there is a slow restoration of axonal projections from population 5/6 after neurons are replaced. To investigate whether newly formed neurons successfully integrate into the existing circuitry, one could look for the presence of new Th^+ neurons colabelled with markers of synaptic contacts, for example SV2. Interestingly, both the newly generated Th^+ neurons found in the mouse brain and Th^+ neurons derived from stem cell transplanted into the brains of Parkinson's disease patients have been shown to innervate the correct target structures and form synapses, indicating successful integration into the existing neuronal circuitry (Kriks et al. 2011; Grealish et al. 2014; Kikuchi et al. 2017; Grealish et al. 2015; Zhao et al. 2003).

7.2 Investigating the Signalling Pathways Involved in the Regeneration of Th^+ Neurons

I investigated whether several different signalling pathways are involved in the regeneration of Th^+ neurons in the adult zebrafish brain. The results I presented in chapter 4 demonstrate that ablation of Th^+ neurons elicited an immune response, and also increased the number of proliferating ERGs at the diencephalic ventricle. Following on from this, I showed that this ablation-induced immune response is necessary but not sufficient for successful regeneration of Th^+ neurons.

Subsequently, I investigated the effects of three molecular signals on ERG proliferation and the production of Th^+ neurons. However, I did not observe any effect of LTC4, the dopamine receptor antagonist haloperidol, or the tnf-α signalling inhibitor pomalidomide, on the number of proliferating ERGs at the diencephalic ventricle, or on Th^+ neurogenesis. Future work could focus on elucidating the mechanism through which microglial activation influences ERG proliferation, identifying which molecules released from microglia may bind to receptors on ERGs and affect their proliferation.

Others have also shown that the immune system plays a crucial role in the successful regeneration of the CNS (Kyritsis et al. 2012; Tsarouchas et al. 2018; Bollaerts et al. 2017; Bhattarai et al. 2016). Interestingly, neuroinflammation appears to promote regeneration in a number of different ways. Here I showed that an immune response increases neurogenesis, which is important for the replacement of neurons. However, there is growing evidence that activation of the immune system can also improve axonal regeneration (Bollaerts et al. 2017). Intravitreal injection of zymosan has been shown to promote the retinal ganglion cell axonal regeneration in zebrafish and rodents (Becker et al. 2000; Leon et al. 2000; Lorber et al. 2005). In the zebrafish spinal cord, stimulating an immune response with lipopolysaccharide (LPS) was shown to increase the percentage of fish with axons bridging the lesion site (Tsarouchas et al. 2018). Furthermore, immune activation promotes the integration of new neurons into the existing neuronal circuity. Intrahippocampal injection of LPS resulted in larger clusters of postsynaptic receptors on the dendrites of new neurons in the rat brain, indicating successful integration into the neuronal circuitry (Jakubs et al. 2008).

The pro-regenerative effects of immune stimulation could inspire future treatments for CNS diseases and injuries. Immune activation is known to be involved in a range of neurodegenerative diseases, as well as stroke, traumatic brain injury, and spinal cord injuries (Joshi & Singh 2018; Clayton et al. 2017; Herranz et al. 2016; Lehnardt 2009). Stimulation of the immune system can promote regeneration in all areas of the CNS. Therefore, further investigation into the relationship between immune activation and CNS repair could lead to the development of treatments with the potential to improve neuroregeneration in humans in a wide range of circumstances.

7.3 Investigating Alternative Methods of Th^+ Neuron Ablation

In order to assess the regenerative capacity of Th^+ populations unaffected by 6OHDA I investigated the potential of using other methods of ablation. I found no difference in the numbers of Th^+ neurons in *pink1*$^{-/-}$ larvae compared to *pink1*$^{+/+}$ larvae, and did not achieve successful ablation with either chemogenetic ablation or injections of MPTP or MPP^+. Hence 6OHDA remains the most reproducible method of ablating Th^+ neuron in the adult zebrafish brain (Caldwell and Davies et al. 2018; Vijayanathan et al. 2017; Matsui et al. 2017).

7.4 Investigating the Regeneration of Interneurons in the Spinal Cord

Finally, I investigated the regenerative capacity of glutamatergic and GABAergic neurons in the spinal cord in adult and larval zebrafish after a spinal cord injury. I found that both glutamatergic and GABAergic neurogenesis are increased after a spinal cord lesion in larvae, and GABAergic neurons are regenerated after a spinal cord lesion in the adult spinal cord. Future work could focus on the origin of these newly generated cells, and aim to identify which progenitor domains are responsible for producing these new cells after a lesion. Furthermore, immunohistochemistry for the postsynaptic protein SV2 combined with labelled glutamatergic and GABAergic neurons could determine whether these new neurons also establish synaptic connections and thus integrate into the existing neuronal circuitry.

In the mammalian spinal cord neurogenesis stops during development and is not induced by a spinal cord injury. However, replacing neurons lost after an injury has been shown to promote functional recovery. Neural stem cells derived from embryonic rat spinal cord were expanded in vitro, labelled with BrdU, and transplanted into adult rat spinal cords injured by contusion (Ogawa et al. 2002). After five weeks, these cells had differentiated into a range of cell types, including astrocytes, oligodendrocytes, and neurons. Importantly, these new neurons formed synaptic contacts, indicating

their integration into the existing neuronal circuitry. Furthermore, behavioural testing showed that the transplants improved functional recovery from the injury. This shows that there is potential for cell replacement therapy to restore function and improve outcomes for patients with spinal cord injuries.

Investigations into the successful regeneration of neurons in the zebrafish spinal cord have already identified a number of different signalling pathways which involved in the replacement of neurons and regrowth of axons, leading to functional recovery (Barreiro-Iglesias et al. 2015; Wehner et al. 2017; Reimer et al. 2013). This could inform future experiments in mammals with the aim of improving neuronal replacement after injury either through transplantation of exogenous stem cells or through promoting neurogenesis from endogenous stem cell populations.

7.5 Overall remarks

Overall, the results I have presented in this thesis add to our current understanding of the extent to which zebrafish are capable of replacing neurons of the CNS, and of how this is achieved. Ultimately, a greater understanding of the regeneration of neurons in the CNS could help to inform future strategies to improve neuroregeneration in mammals. This could potentially be useful in developing new treatments for neurodegenerative disease such as Parkinson's, as well as physical injuries to the spinal cord.

References

Adolf, B. et al., 2006. Conserved and acquired features of adult neurogenesis in the zebrafish telencephalon. *Developmental biology*, 295(1), pp.278–93.

Agetsuma, M. et al., 2010. The habenula is crucial for experience-dependent modification of fear responses in zebrafish. *Nature Neuroscience*, 13(11), pp.1354–1356.

Akundi, R.S. et al., 2011. Increased mitochondrial calcium sensitivity and abnormal expression of innate immunity genes precede dopaminergic defects in Pink1-deficient mice. *PloS one*, 6(1), p.e16038.

Altman, J., 1969. Autoradiographic and histological studies of postnatal neurogenesis. IV. Cell proliferation and migration in the anterior forebrain, with special reference to persisting neurogenesis in the olfactory bulb. *The Journal of Comparative Neurology*, 137(4), pp.433–457.

Altman, J. & Das, G.D., 1965. Autoradiographic and histological evidence of postnatal hippocampal neurogenesis in rats. *The Journal of comparative neurology*, 124(3), pp.319–35.

Andersson, E. et al., 2006. Identification of intrinsic determinants of midbrain dopamine neurons. *Cell*, 124(2), pp.393–405.

Anichtchik, O. et al., 2006. Distinct structure and activity of monoamine oxidase in the brain of zebrafish (Danio rerio). *The Journal of comparative neurology*, 498(5), pp.593–610.

Anichtchik, O. et al., 2008. Loss of PINK1 function affects development and results in neurodegeneration in zebrafish. *The Journal of neuroscience : the official journal of the Society for Neuroscience*, 28(33), pp.8199–207.

Anichtchik, O. V. et al., 2003. Neurochemical and behavioural changes in zebrafish Danio rerio after systemic administration of 6-hydroxydopamine and 1-methyl-4-phenyl-1,2,3,6-tetrahydropyridine. *Journal of Neurochemistry*, 88(2), pp.443–453.

Auer, T.O. & Del Bene, F., 2014. CRISPR/Cas9 and TALEN-mediated knock-in approaches in zebrafish. *Methods*, 69(2), pp.142–150.

Baptiste, D.C. & Fehlings, M.G., 2007. Update on the treatment of spinal cord injury. In *Progress in brain research*. pp. 217–233.

Barbeau, A. et al., 1985. New amphibian models for the study of 1-methyl-4-phenyl-1,2,3,6-tetrahydropyridine (MPTP). *Life sciences*, 36(11), pp.1125–34.

Barbosa, J.S. et al., 2015a. Neurodevelopment. Live imaging of adult neural stem cell behavior in the intact and injured zebrafish brain. *Science (New York, N.Y.)*, 348(6236), pp.789–93.

Barbosa, J.S. et al., 2015b. Neurodevelopment. Live imaging of adult neural stem cell behavior in the intact and injured zebrafish brain. *Science (New York, N.Y.)*, 348(6236), pp.789–93.

Barker, R.A., Drouin-Ouellet, J. & Parmar, M., 2015. Cell-based therapies for Parkinson disease—past insights and future potential. *Nature reviews. Neurology*, 11(9), pp.492–503.

Barker, R.A., Götz, M. & Parmar, M., 2018. New approaches for brain repair—from rescue to reprogramming. *Nature*, 557(7705), pp.329–334.

Barreiro-Iglesias, A. et al., 2015. Serotonin Promotes Development and Regeneration of Spinal Motor Neurons in Zebrafish. *Cell reports*, 13(5), pp.924–32.

Becker, C.G. et al., 2004. L1.1 Is Involved in Spinal Cord Regeneration in Adult Zebrafish. *Journal of Neuroscience*, 24(36), pp.7837–7842.

Becker, C.G. & Becker, T., 2008. Adult zebrafish as a model for successful central nervous system regeneration. *Restorative neurology and neuroscience*, 26(2-3), pp.71–80.

Becker, C.G. & Becker, T., 2015. Neuronal Regeneration from Ependymo-Radial Glial Cells: Cook, Little Pot, Cook! *Developmental Cell*, 32(4), pp.516–527.

Becker, C.G., Meyer, R.L. & Becker, T., 2000. Gradients of ephrin-A2 and ephrin-A5b mRNA during retinotopic regeneration of the optic projection in adult zebrafish. *The Journal of comparative neurology*, 427(3), pp.469–83.

Becker, T. et al., 1997. Axonal regrowth after spinal cord transection in adult zebrafish. *The Journal of comparative neurology*, 377(4), pp.577–95.

Becker, T. & Becker, C.G., 2001. Regenerating descending axons preferentially reroute to the gray matter in the presence of a general macrophage/microglial reaction caudal to a spinal transection in adult zebrafish. *The Journal of Comparative Neurology*, 433(1), pp.131–147.

Berg, D.A. et al., 2011. Dopamine controls neurogenesis in the adult salamander midbrain in homeostasis and during regeneration of dopamine neurons. *Cell stem cell*, 8(4), pp.426–33.

Berg, D.A. et al., 2010. Efficient regeneration by activation of neurogenesis in homeostatically quiescent regions of the adult vertebrate brain. *Development (Cambridge, England)*, 137(24), pp.4127–34.

Van den Berge, S.A. et al., 2011. The proliferative capacity of the subventricular zone is maintained in the parkinsonian brain. *Brain*, 134(11), pp.3249–3263.

Bergmann, O., Spalding, K.L. & Frisén, J., 2015. Adult Neurogenesis in Humans. *Cold Spring Harbor Perspectives in Biology*, 7(7), p.a018994.

Bernardos, R.L. & Raymond, P.A., 2006. GFAP transgenic zebrafish. *Gene Expression Patterns*, 6(8), pp.1007–1013.

Bernhardt, R.R. et al., 1992. Axonal trajectories and distribution of GABAergic spinal neurons in wildtype and mutant zebrafish lacking floor plate cells. *The Journal of comparative neurology*, 326(2), pp.263–72.

Betarbet, R., Sherer, T.B. & Greenamyre, J.T., 2002. Animal models of Parkinson's disease. *BioEssays*, 24(4), pp.308–318.

Bhattarai, P. et al., 2016. *IL4/STAT6 Signaling Activates Neural Stem Cell Proliferation and Neurogenesis upon Amyloid-β42 Aggregation in Adult Zebrafish Brain*,

Bhattarai, P. et al., 2017. The effects of aging on Amyloid-β42-induced neurodegeneration and regeneration in adult zebrafish brain. *Neurogenesis*, 4(1), p.e1322666.

Biebl, M. et al., 2000. Analysis of neurogenesis and programmed cell death reveals a self-renewing capacity in the adult rat brain. *Neuroscience letters*, 291(1), pp.17–20.

Bollaerts, I. et al., 2017. Neuroinflammation as Fuel for Axonal Regeneration in the Injured Vertebrate Central Nervous System. *Mediators of inflammation*, 2017, p.9478542.

Boniface, E.J. et al., 2009. FlEx-based transgenic reporter lines for visualization of Cre and Flp activity in live zebrafish. *Genesis (New York, N.Y. : 2000)*, 47(7), pp.484–91.

Borta, A. & Höglinger, G.U., 2007. Dopamine and adult neurogenesis. *Journal of Neurochemistry*, 100(3), pp.587–595.

Bové, J. et al., 2005. Toxin-induced models of Parkinson's disease. *NeuroRx : the journal of the American Society for Experimental NeuroTherapeutics*, 2(3), pp.484–94.

Bové, J. & Perier, C., 2012. Neurotoxin-based models of Parkinson's disease. *Neuroscience*, 211, pp.51–76.

Braungart, E. et al., 2004. Caenorhabditis elegans MPP+ model of Parkinson's disease for high-throughput drug screenings. *Neuro-degenerative diseases*, 1(4-5), pp.175–83.

Bretaud, S. et al., 2006. p53-dependent neuronal cell death in a DJ-1-deficient zebrafish model of Parkinson's disease. *Journal of Neurochemistry*, 0(0), p.070209222715077–???

Bretaud, S., Lee, S. & Guo, S., 2004. Sensitivity of zebrafish to environmental toxins implicated in Parkinson's disease. *Neurotoxicology and Teratology*, 26(6), pp.857–864.

Bridgewater, J.A. et al., 1997. The bystander effect of the nitroreductase/CB1954 enzyme/prodrug system is due to a cell-permeable metabolite. *Human gene therapy*, 8(6), pp.709–17.

Briona, L.K. & Dorsky, R.I., 2014a. Radial glial progenitors repair the zebrafish spinal cord following transection. *Experimental neurology*, 256, pp.81–92.

Briona, L.K. & Dorsky, R.I., 2014b. Radial glial progenitors repair the zebrafish spinal cord following transection. *Experimental neurology*, 256, pp.81–92.

Caldwell, L.J. et al., 2018. Regeneration of dopaminergic neurons in adult zebrafish depends on immune system activation and differs for distinct populations. *bioRxiv*, p.367151.

Cameron, H.A. et al., 1993. Differentiation of newly born neurons and glia in the dentate gyrus of the adult rat. *Neuroscience*, 56(2), pp.337–344.

Cannon, J.R. & Greenamyre, J.T., 2013. Gene-environment interactions in Parkinson's disease: specific evidence in humans and mammalian models. *Neurobiology of disease*, 57, pp.38–46.

Chapouton, P. et al., 2011. Expression of hairy/enhancer of split genes in neural progenitors and neurogenesis domains of the adult zebrafish brain. *The Journal of comparative neurology*, 519(9), pp.1748–69.

Cheesman, S.E. et al., 2004. Zebrafish and fly Nkx6 proteins have similar CNS expression patterns and regulate motoneuron formation. *Development (Cambridge, England)*, 131(21), pp.5221–32.

Chen, C.-F. et al., 2011. Establishment of a Transgenic Zebrafish Line for Superficial Skin Ablation and Functional Validation of Apoptosis Modulators In Vivo F. Mueller, ed. *PLoS ONE*, 6(5), p.e20654.

Chen, S. et al., 2013. Correlation of Nr4a2 Expression with the Neuron Progenitors in Adult Zebrafish Brain. *Journal of Molecular Neuroscience*, 51(3), pp.719–723.

Chen, Y.-C., Priyadarshini, M. & Panula, P., 2009. Complementary developmental expression of the two tyrosine hydroxylase transcripts in zebrafish. *Histochemistry and cell biology*, 132(4), pp.375–81.

Cheng, H.-C., Ulane, C.M. & Burke, R.E., 2010. Clinical progression in Parkinson disease and the neurobiology of axons. *Annals of neurology*, 67(6), pp.715–25.

Chiba, K., Trevor, A. & Castagnoli, N., 1984. Metabolism of the neurotoxic tertiary amine, MPTP, by brain monoamine oxidase. *Biochemical and biophysical research communications*, 120(2), pp.574–8.

Choi, T.-Y. et al., 2015. Hepatocyte-specific Ablation in Zebrafish to Study Biliary-driven Liver Regeneration. *Journal of Visualized Experiments*, (99), pp.e52785–e52785.

Chung, A.-Y. et al., 2013. Generation of demyelination models by targeted ablation of oligodendrocytes in the zebrafish CNS. *Molecules and cells*, 36(1), pp.82–7.

Clark, I.E. et al., 2006. Drosophila pink1 is required for mitochondrial function and interacts genetically with parkin. *Nature*, 441(7097), pp.1162–6.

Clayton, K.A., Van Enoo, A.A. & Ikezu, T., 2017. Alzheimer's Disease: The Role of Microglia in Brain Homeostasis and Proteopathy. *Frontiers in neuroscience*, 11, p.680.

Cohen, G., 1984. Oxy-radical toxicity in catecholamine neurons. *Neurotoxicology*, 5(1), pp.77–82.

Conner, C. et al., 2014. Repressing notch signaling and expressing TNFα are sufficient to mimic retinal regeneration by inducing Müller glial proliferation to generate committed progenitor cells. *The Journal of neuroscience : the official journal of the Society for Neuroscience*, 34(43), pp.14403–19.

Connolly, B.S. & Lang, A.E., 2014. Pharmacological treatment of Parkinson disease: a review. *JAMA : the journal of the American Medical Association*, 311(16), pp.1670–83.

Cookson, M.R., 2012. Parkinsonism due to mutations in PINK1, parkin, and DJ-1 and oxidative stress and mitochondrial pathways. *Cold Spring Harbor perspectives in medicine*, 2(9), p.a009415.

Le Couteur, D.G. et al., 1999. Pesticides and Parkinson's disease. *Biomedicine & Pharmacotherapy*, 53(3), pp.122–130.

Curado, S. et al., 2007. Conditional targeted cell ablation in zebrafish: A new tool for regeneration studies. *Developmental Dynamics*, 236(4), pp.1025–1035.

Curado, S., Stainier, D.Y.R. & Anderson, R.M., 2008. Nitroreductase-mediated cell/tissue ablation in zebrafish: a spatially and temporally controlled ablation method with applications in developmental and regeneration studies. *Nature protocols*, 3(6), pp.948–54.

Davies, N.O., 2016. Function, regeneration and neuroprotection of dopaminergic neurons in the zebrafish.

Dawson, T.M., Ko, H.S. & Dawson, V.L., 2010. Genetic animal models of Parkinson's disease. *Neuron*, 66(5), pp.646–61.

Deumens, R., Blokland, A. & Prickaerts, J., 2002. Modeling Parkinson's Disease in Rats: An Evaluation of 6-OHDA Lesions of the Nigrostriatal Pathway. *Experimental Neurology*, 175(2), pp.303–317.

Dirian, L. et al., 2014. Spatial Regionalization and Heterochrony in the Formation of Adult Pallial Neural Stem Cells. *Developmental Cell*, 30(2), pp.123–136.

DiSabato, D.J., Quan, N. & Godbout, J.P., 2016. Neuroinflammation: the devil is in the details. *Journal of neurochemistry*, 139 Suppl (Suppl 2), pp.136–153.

Dray, N. et al., 2015. Large-scale live imaging of adult neural stem cells in their endogenous niche. *Development (Cambridge, England)*, 142(20), pp.3592–600.

Dukes, A.A. et al., 2016. Live imaging of mitochondrial dynamics in CNS dopaminergic neurons in vivo demonstrates early reversal of mitochondrial transport following MPP(+) exposure. *Neurobiology of disease*, 95, pp.238–49.

Eriksson, P.S. et al., 1998. Neurogenesis in the adult human hippocampus. *Nature Medicine*, 4(11), pp.1313–1317.

Eslamboli, A., 2005. Marmoset monkey models of Parkinson's disease: Which model, when and why? *Brain Research Bulletin*, 68(3), pp.140–149.

Faul, F. et al., 2007. G*Power 3: A flexible statistical power analysis program for the social, behavioral, and biomedical sciences. *Behavior Research Methods*, 39(2), pp.175–191.

Fearnley, J.M. & Lees, A.J., 1991. Ageing and Parkinson's disease: substantia nigra regional selectivity. *Brain : a journal of neurology*, 114 (Pt 5), pp.2283–301.

Feierstein, C.E., Portugues, R. & Orger, M.B., 2015. Seeing the whole picture: A comprehensive imaging approach to functional mapping of circuits in behaving zebrafish. *Neuroscience*, 296, pp.26–38.

Feil, R. et al., 1997. Regulation of Cre Recombinase Activity by Mutated Estrogen Receptor Ligand-Binding Domains. *Biochemical and Biophysical Research Communications*, 237(3), pp.752–757.

Fernandes, A.M. et al., 2012. Deep brain photoreceptors control light-seeking behavior in zebrafish larvae. *Current biology : CB*, 22(21), pp.2042–7.

Fernández-López, B., Barreiro-Iglesias, A. & Rodicio, M.C., 2016. Anatomical recovery of the spinal glutamatergic system following a complete spinal cord injury in lampreys. *Scientific Reports*, 6(1), p.37786.

Fett, M.E. et al., 2010. Parkin Is Protective against Proteotoxic Stress in a Transgenic Zebrafish Model M. R. Cookson, ed. *PLoS ONE*, 5(7), p.e11783.

Filippi, A. et al., 2007. Expression and function of nr4a2, lmx1b, and pitx3 in zebrafish dopaminergic and noradrenergic neuronal development. *BMC developmental biology*, 7, p.135.

Flanagan-Steet, H. et al., 2005. Neuromuscular synapses can form in vivo by incorporation of initially aneural postsynaptic specializations. *Development (Cambridge, England)*, 132(20), pp.4471–81.

Flinn, L.J. et al., 2013. TigarB causes mitochondrial dysfunction and neuronal loss in PINK1 deficiency. *Annals of neurology*, 74(6), pp.837–47.

Fox, S.H. & Brotchie, J.M., 2010. The MPTP-lesioned non-human primate models of Parkinson's disease. Past, present, and future. In *Progress in brain research*. pp. 133–157.

Fremeau, R.T. et al., 2004. VGLUTs define subsets of excitatory neurons and suggest novel roles for glutamate. *Trends in neurosciences*, 27(2), pp.98–103.

Fujimoto, E. et al., 2011. Identification of a dopaminergic enhancer indicates complexity in vertebrate dopamine neuron phenotype specification. *Developmental biology*, 352(2), pp.393–404.

Gage, F.H. & Temple, S., 2013. Neural Stem Cells: Generating and Regenerating the Brain. *Neuron*, 80(3), pp.588–601.

Gandhi, S. et al., 2006. PINK1 protein in normal human brain and Parkinson's disease. *Brain*, 129(7), pp.1720–1731.

Ganz, J. et al., 2010. Heterogeneity and Fgf dependence of adult neural progenitors in the zebrafish telencephalon. *Glia*, 58(11), p.n/a–n/a.

Gemberling, M. et al., 2013. The zebrafish as a model for complex tissue regeneration. *Trends in genetics : TIG*, 29(11), pp.611–20.

Ghosh, S. & Hui, S.P., 2016. Regeneration of Zebrafish CNS: Adult Neurogenesis. *Neural plasticity*, 2016, p.5815439.

Godoy, R. et al., 2015. Chemogenetic ablation of dopaminergic neurons leads to transient locomotor impairments in zebrafish larvae. *Journal of neurochemistry*, 135(2), pp.249–60.

Goldman, D., 2014. Müller glial cell reprogramming and retina regeneration. *Nature reviews. Neuroscience*, 15(7), pp.431–42.

Goldshmit, Y. et al., 2012. Fgf-dependent glial cell bridges facilitate spinal cord regeneration in zebrafish. *The Journal of neuroscience : the official journal of the Society for Neuroscience*, 32(22), pp.7477–92.

Goping, G. et al., 1995. Effect of MPTP on dopaminergic neurons in the goldfish brain: a light and electron microscope study. *Brain Research*, 687(1-2), pp.35–52.

Grandel, H. et al., 2006. Neural stem cells and neurogenesis in the adult zebrafish brain: origin, proliferation dynamics, migration and cell fate. *Developmental biology*, 295(1), pp.263–77.

Grandel, H. & Brand, M., 2013. Comparative aspects of adult neural stem cell activity in vertebrates. *Development genes and evolution*, 223(1-2), pp.131–47.

Grasselli, C. et al., 2018. Toll-like receptor 4 modulation influences human neural stem cell proliferation and differentiation. *Cell Death & Disease*, 9(3), p.280.

Grealish, S. et al., 2014. Human ESC-derived dopamine neurons show similar preclinical efficacy and potency to fetal neurons when grafted in a rat model of Parkinson's disease. *Cell stem cell*, 15(5), pp.653–65.

Grealish, S. et al., 2015. Monosynaptic Tracing using Modified Rabies Virus Reveals Early and Extensive Circuit Integration of Human Embryonic Stem Cell-Derived Neurons. *Stem cell reports*, 4(6), pp.975–83.

Griffin, A. et al., 2017. Clemizole and modulators of serotonin signalling suppress seizures in Dravet syndrome. *Brain*, 140(3), p.aww342.

Guryev, V. et al., 2006. Genetic variation in the zebrafish. *Genome research*, 16(4), pp.491–7.

Haehnel-Taguchi, M. et al., 2018. Projections of the Diencephalospinal Dopaminergic System to Peripheral Sense Organs in Larval Zebrafish (Danio rerio). *Frontiers in neuroanatomy*, 12, p.20.

Hale, M.E., Ritter, D.A. & Fetcho, J.R., 2001. A confocal study of spinal interneurons in living larval zebrafish. *The Journal of Comparative Neurology*, 437(1), pp.1–16.

Halpern, M.E. et al., 2008. Gal4/UAS Transgenic Tools and Their Application to Zebrafish. *Zebrafish*, 5(2), pp.97–110.

Van Ham, T.J., Kokel, D. & Peterson, R.T., 2012. Apoptotic cells are cleared by directional migration and elmo1- dependent macrophage engulfment. *Current biology : CB*, 22(9), pp.830–6.

Hans, S. et al., 2009. Temporally-controlled site-specific recombination in zebrafish. *PloS one*, 4(2), p.e4640.

Hao, J. et al., 2010. Large Scale Zebrafish-Based In vivo Small Molecule Screen. *Journal of Visualized Experiments*, (46).

Hauser, R.A. et al., 1999. Long-term evaluation of bilateral fetal nigral transplantation in Parkinson disease. *Archives of neurology*, 56(2), pp.179–87.

He, X.J. & Nakayama, H., 2009. Neurogenesis in Neurotoxin-induced Animal Models for Parkinson's Disease-A Review of the Current Status. *Journal of toxicologic pathology*, 22(2), pp.101–8.

Heikkila, R.E. et al., 1984. Effects of 1-methyl-4-phenyl-1,2,5,6-tetrahydropyridine on neostriatal dopamine in mice. *Neuropharmacology*, 23(6), pp.711–3.

Helsby, N.A. et al., 2004. 2-Amino metabolites are key mediators of CB 1954 and SN 23862 bystander effects in nitroreductase GDEPT. *British journal of cancer*, 90(5), pp.1084–92.

Herranz, E. et al., 2016. Neuroinflammatory component of gray matter pathology in multiple sclerosis. *Annals of neurology*, 80(5), pp.776–790.

Herzog, E. et al., 2004. Expression of vesicular glutamate transporters, VGLUT1 and VGLUT2, in cholinergic spinal motoneurons. *The European journal of neuroscience*, 20(7), pp.1752–60.

Higashijima, S. et al., 2003. Imaging Neuronal Activity During Zebrafish Behavior With a Genetically Encoded Calcium Indicator. *Journal of Neurophysiology*, 90(6), pp.3986–3997.

Higashijima, S., Hotta, Y. & Okamoto, H., 2000. Visualization of cranial motor neurons in live transgenic zebrafish expressing green fluorescent protein under the control of the islet-1 promoter/enhancer. *The Journal of neuroscience : the official journal of the Society for Neuroscience*, 20(1), pp.206–18.

Higashijima, S.-I., Mandel, G. & Fetcho, J.R., 2004. Distribution of prospective glutamatergic, glycinergic, and GABAergic neurons in embryonic and larval zebrafish. *The Journal of comparative neurology*, 480(1), pp.1–18.

Higashijima, S.-I., Schaefer, M. & Fetcho, J.R., 2004. Neurotransmitter properties of spinal interneurons in embryonic and larval zebrafish. *The Journal of Comparative Neurology*, 480(1), pp.19–37.

Hofstetter, C.P. et al., 2005. Allodynia limits the usefulness of intraspinal neural stem cell grafts; directed differentiation improves outcome. *Nature neuroscience*, 8(3), pp.346–53.

Hökfelt, T. et al., 1976. Immunohistochemical studies on the localization and distribution of monoamine neuron systems in the rat brain. I. Tyrosine hydroxylase in the mes- and diencephalon. *Medical biology*, 54(6), pp.427–53.

Hong, C.C., 2009. Large-Scale Small-Molecule Screen Using Zebrafish Embryos. In *Methods in molecular biology (Clifton, N.J.)*. pp. 43–55.

Huang, J. et al., 2013. A zebrafish model of conditional targeted podocyte ablation and regeneration. *Kidney international*, 83(6), pp.1193–200.

Hui, S.P., Dutta, A. & Ghosh, S., 2010. Cellular response after crush injury in adult zebrafish spinal cord. *Developmental Dynamics*, 239(11), pp.2962–2979.

Indra, A.K. et al., 1999. Temporally-controlled site-specific mutagenesis in the basal layer of the epidermis: comparison of the recombinase activity of the tamoxifen-inducible Cre-ERT and Cre-ERT2 recombinases. *Nucleic Acids Research*, 27(22), pp.4324–4327.

Jackson-Lewis, V., Blesa, J. & Przedborski, S., 2012. Animal models of Parkinson's disease. *Parkinsonism & Related Disorders*, 18, pp.S183–S185.

Jakubs, K. et al., 2008. Inflammation Regulates Functional Integration of Neurons Born in Adult Brain. *Journal of Neuroscience*, 28(47), pp.12477–12488.

Joshi, N. & Singh, S., 2018. Updates on immunity and inflammation in Parkinson disease pathology. *Journal of Neuroscience Research*, 96(3), pp.379–390.

Joven, A. et al., 2018. Cellular basis of brain maturation and acquisition of complex behaviors in salamanders. *Development (Cambridge, England)*, 145(1), p.dev160051

Jung, S.-H. et al., 2012. Her4-positive population in the tectum opticum is proliferating neural precursors in the adult zebrafish brain. *Molecules and cells*, 33(6), pp.627–32.

Kalia, L. V & Lang, A.E., 2015. Parkinson's disease. *Lancet (London, England)*, 386(9996), pp.896–912.

Van Kampen, J.M., McGeer, E.G. & Stoessl, A.J., 2000. Dopamine transporter function assessed by antisense knockdown in the rat: protection from dopamine neurotoxicity. *Synapse (New York, N.Y.)*, 37(3), pp.171–8.

Kani, S. et al., 2010. Proneural gene-linked neurogenesis in zebrafish cerebellum. *Developmental biology*, 343(1-2), pp.1–17.

Kaslin, J., Ganz, J. & Brand, M., 2008. Proliferation, neurogenesis and regeneration in the non-mammalian vertebrate brain. *Philosophical transactions of the Royal Society of London. Series B, Biological sciences*, 363(1489), pp.101–22.

Kastenhuber, E. et al., 2009. Netrin-DCC, Robo-Slit, and heparan sulfate proteoglycans coordinate lateral positioning of longitudinal dopaminergic diencephalospinal axons. *The Journal of neuroscience : the official journal of the Society for Neuroscience*, 29(28), pp.8914–26.

Kefalopoulou, Z. et al., 2014. Long-term Clinical Outcome of Fetal Cell Transplantation for Parkinson Disease. *JAMA Neurology*, 71(1), p.83.

Kikuchi, T. et al., 2017. Human iPS cell-derived dopaminergic neurons function in a primate Parkinson's disease model. *Nature*, 548(7669), pp.592–596.

Kilarski, L.L. et al., 2012. Systematic Review and UK-Based Study of *PARK2 (parkin), PINK1, PARK7 (DJ-1)* and *LRRK2* in early-onset Parkinson's disease. *Movement Disorders*, 27(12), pp.1522–1529.

Kirkham, M., Berg, D.A. & Simon, A., 2011. Microglia activation during neuroregeneration in the adult vertebrate brain. *Neuroscience letters*, 497(1), pp.11–6.

Kitada, T. et al., 2007. Impaired dopamine release and synaptic plasticity in the striatum of PINK1-deficient mice. *Proceedings of the National Academy of Sciences of the United States of America*, 104(27), pp.11441–6.

Kizil, C. et al., 2012. Regenerative neurogenesis from neural progenitor cells requires injury-induced expression of Gata3. *Developmental cell*, 23(6), pp.1230–7.

Klein, C. & Westenberger, A., 2012. Genetics of Parkinson's disease. *Cold Spring Harbor perspectives in medicine*, 2(1), p.a008888.

Knopf, F. et al., 2010. Dually inducible TetON systems for tissue-specific conditional gene expression in zebrafish. *Proceedings of the National Academy of Sciences*, 107(46), pp.19933–19938.

Kriks, S. et al., 2011. Dopamine neurons derived from human ES cells efficiently engraft in animal models of Parkinson's disease. *Nature*, 480(7378), pp.547–551.

Kroehne, V. et al., 2011. Regeneration of the adult zebrafish brain from neurogenic radial glia-type progenitors. *Development (Cambridge, England)*, 138(22), pp.4831–41.

Kucenas, S. et al., 2008. CNS-derived glia ensheath peripheral nerves and mediate motor root development. *Nature neuroscience*, 11(2), pp.143–51.

Kurkowska-Jastrzębska, I. et al., 2004. Dexamethasone protects against dopaminergic neurons damage in a mouse model of Parkinson's disease. *International Immunopharmacology*, 4(10-11), pp.1307–1318.

Kuscha, V., 2011. Cellular and axonal plasticity in the lesioned spinal cord of adult zebrafish.

Kuscha, V., Frazer, S.L., et al., 2012. Lesion-induced generation of interneuron cell types in specific dorsoventral domains in the spinal cord of adult zebrafish. *The Journal of comparative neurology*, 520(16), pp.3604–16.

Kuscha, V., Barreiro-Iglesias, A., et al., 2012. Plasticity of tyrosine hydroxylase and serotonergic systems in the regenerating spinal cord of adult zebrafish. *The Journal of comparative neurology*, 520(5), pp.933–51.

Kwan, K.M. et al., 2007. The Tol2kit: a multisite gateway-based construction kit for Tol2 transposon transgenesis constructs. *Developmental dynamics : an official publication of the American Association of Anatomists*, 236(11), pp.3088–99.

Kyritsis, N. et al., 2012. Acute inflammation initiates the regenerative response in the adult zebrafish brain. *Science (New York, N.Y.)*, 338(6112), pp.1353–6.

Lam, C.S., Korzh, V. & Strahle, U., 2005. Zebrafish embryos are susceptible to the dopaminergic neurotoxin MPTP. *European Journal of Neuroscience*, 21(6), pp.1758–1762.

Lambert, A.M., Bonkowsky, J.L. & Masino, M.A., 2012. The conserved dopaminergic diencephalospinal tract mediates vertebrate locomotor development in zebrafish larvae. *The Journal of neuroscience : the official journal of the Society for Neuroscience*, 32(39), pp.13488–500.

Lamm, O. et al., 2014. Harnessing neurogenesis for the possible treatment of Parkinson's disease. *Journal of Comparative Neurology*, 522(12), pp.2817–2830.

Langston, J.W. et al., 1984. 1-Methyl-4-phenylpyridinium ion (MPP+): identification of a metabolite of MPTP, a toxin selective to the substantia nigra. *Neuroscience letters*, 48(1), pp.87–92.

Langston, J.W. et al., 1983. Chronic Parkinsonism in humans due to a product of meperidine-analog synthesis. *Science (New York, N.Y.)*, 219(4587), pp.979–80.

Langston, J.W., 2017. The MPTP Story. *Journal of Parkinson's disease*, 7(s1), pp.S11–S22.

De Lau, L.M.L. & Breteler, M.M.B., 2006. Epidemiology of Parkinson's disease. *The Lancet. Neurology*, 5(6), pp.525–35.

Lehnardt, S., 2009. Innate immunity and neuroinflammation in the CNS: The role of microglia in Toll-like receptor-mediated neuronal injury. *Glia*, 58(3), p.NA–NA.

Leon, S. et al., 2000. Lens Injury Stimulates Axon Regeneration in the Mature Rat Optic Nerve. *Journal of Neuroscience*, 20(12).

Lewis, K.E. & Eisen, J.S., 2003. From cells to circuits: development of the zebrafish spinal cord. *Progress in Neurobiology*, 69(6), pp.419–449.

Li, W. et al., 2016. Extensive graft-derived dopaminergic innervation is maintained 24 years after transplantation in the degenerating parkinsonian brain. *Proceedings of the National Academy of Sciences of the United States of America*, 113(23), pp.6544–9.

Li, Y. et al., 2005. Clinicogenetic study of PINK1 mutations in autosomal recessive early-onset parkinsonism. *Neurology*, 64(11), pp.1955–7.

Li, Z. et al., 2013. Pomalidomide shows significant therapeutic activity against CNS lymphoma with a major impact on the tumor microenvironment in murine models. *PloS one*, 8(8), p.e71754.

Lieschke, G.J. & Currie, P.D., 2007. Animal models of human disease: zebrafish swim into view. *Nature Reviews Genetics*, 8(5), pp.353–367.

Lindmark, D.G. & Müller, M., 1976. Antitrichomonad action, mutagenicity, and reduction of metronidazole and other nitroimidazoles. *Antimicrobial agents and chemotherapy*, 10(3), pp.476–82.

Lorber, B., Berry, M. & Logan, A., 2005. Lens injury stimulates adult mouse retinal ganglion cell axon regeneration via both macrophage- and lens-derived factors. *European Journal of Neuroscience*, 21(7), pp.2029–2034.

Mahler, J., Filippi, A. & Driever, W., 2010. DeltaA/DeltaD regulate multiple and temporally distinct phases of notch signaling during dopaminergic neurogenesis in zebrafish. *The Journal of neuroscience : the official journal of the Society for Neuroscience*, 30(49), pp.16621–35.

Mahony, C. et al., 2013. Pomalidomide is nonteratogenic in chicken and zebrafish embryos and nonneurotoxic in vitro. *Proceedings of the National Academy of Sciences of the United States of America*, 110(31), pp.12703–8.

Marro, S. et al., 2011. Direct Lineage Conversion of Terminally Differentiated Hepatocytes to Functional Neurons. *Cell Stem Cell*, 9(4), pp.374–382.

Martin, S.C., Heinrich, G. & Sandell, J.H., 1998. Sequence and expression of glutamic acid decarboxylase isoforms in the developing zebrafish. *The Journal of comparative neurology*, 396(2), pp.253–66.

Matsui, H. et al., 2017. An optimized method for counting dopaminergic neurons in zebrafish J. Kanungo, ed. *PLOS ONE*, 12(9), p.e0184363.

McKinley, E.T. et al., 2005. Neuroprotection of MPTP-induced toxicity in zebrafish dopaminergic neurons. *Molecular Brain Research*, 141(2), pp.128–137.

Meletis, K. et al., 2008. Spinal Cord Injury Reveals Multilineage Differentiation of Ependymal Cells A. Abeliovich, ed. *PLoS Biology*, 6(7), p.e182.

Merkle, F.T., Mirzadeh, Z. & Alvarez-Buylla, A., 2007. Mosaic Organization of Neural Stem Cells in the Adult Brain. *Science*, 317(5836), pp.381–384.

Miller, G.W. et al., 1999. Dopamine transporters and neuronal injury. *Trends in Pharmacological Sciences*, 20(10), pp.424–429.

Mills, R.D. et al., 2008. Biochemical aspects of the neuroprotective mechanism of PTEN-induced kinase-1 (PINK1). *Journal of Neurochemistry*, 105(1), pp.18–33.

Ming, G. & Song, H., 2011. Adult Neurogenesis in the Mammalian Brain: Significant Answers and Significant Questions. *Neuron*, 70(4), pp.687–702.

Ming, W.J., Bersani, L. & Mantovani, A., 1987. Tumor necrosis factor is chemotactic for monocytes and polymorphonuclear leukocytes. *Journal of immunology (Baltimore, Md. : 1950)*, 138(5), pp.1469–74.

Moss, J.B. et al., 2009. Regeneration of the pancreas in adult zebrafish. *Diabetes*, 58(8), pp.1844–51.

Nau, R., Sörgel, F. & Eiffert, H., 2010. Penetration of drugs through the blood-cerebrospinal fluid/blood-brain barrier for treatment of central nervous system infections. *Clinical microbiology reviews*, 23(4), pp.858–83.

Nelson, C.M. et al., 2013. Tumor necrosis factor-alpha is produced by dying retinal neurons and is required for Muller glia proliferation during zebrafish retinal

regeneration. *The Journal of neuroscience : the official journal of the Society for Neuroscience*, 33(15), pp.6524–39.

Nicklas, W.J., Vyas, I. & Heikkila, R.E., 1985. Inhibition of NADH-linked oxidation in brain mitochondria by 1-methyl-4-phenyl-pyridine, a metabolite of the neurotoxin, 1-methyl-4-phenyl-1,2,5,6-tetrahydropyridine. *Life sciences*, 36(26), pp.2503–8.

Nishimura, K. et al., 2011. Regeneration of dopaminergic neurons after 6-hydroxydopamine-induced lesion in planarian brain. *Journal of neurochemistry*, 119(6), pp.1217–31.

Ogai, K. et al., 2014. Function of Sox2 in ependymal cells of lesioned spinal cords in adult zebrafish. *Neuroscience Research*, 88, pp.84–87.

Ogawa, Y. et al., 2002. Transplantation of in vitro-expanded fetal neural progenitor cells results in neurogenesis and functional recovery after spinal cord contusion injury in adult rats. *Journal of Neuroscience Research*, 69(6), pp.925–933.

Ohnmacht, J. et al., 2016. Spinal motor neurons are regenerated after mechanical lesion and genetic ablation in larval zebrafish. *Development (Cambridge, England)*, 143(9), pp.1464–74.

Orii, H., Sakurai, T. & Watanabe, K., 2005. Distribution of the stem cells (neoblasts) in the planarian Dugesia japonica. *Development Genes and Evolution*, 215(3), pp.143–157.

Padiglia, A. et al., 1997. Modulation of 6-hydroxydopamine oxidation by various proteins. *Biochemical pharmacology*, 53(8), pp.1065–8.

Palumbo, A. et al., 1999. Nitrite- and Peroxide-Dependent Oxidation Pathways of Dopamine: 6-Nitrodopamine and 6-Hydroxydopamine Formation as Potential Contributory Mechanisms of Oxidative Stress- and Nitric Oxide-Induced Neurotoxicity in Neuronal Degeneration. *Chemical Research in Toxicology*, 12(12), pp.1213–1222.

Pan, Y.A. et al., 2013. Zebrabow: multispectral cell labeling for cell tracing and lineage analysis in zebrafish. *Development (Cambridge, England)*, 140(13), pp.2835–46.

Parish, C.L. et al., 2007. Midbrain dopaminergic neurogenesis and behavioural recovery in a salamander lesion-induced regeneration model. *Development (Cambridge, England)*, 134(15), pp.2881–7.

Park, H.-C. et al., 2007. Anolig2 reporter gene marks oligodendrocyte precursors in the postembryonic spinal cord of zebrafish. *Developmental Dynamics*, 236(12), pp.3402–3407.

Park, J. et al., 2006. Mitochondrial dysfunction in Drosophila PINK1 mutants is complemented by parkin. *Nature*, 441(7097), pp.1157–61.

Parmar, M., Torper, O. & Drouin-Ouellet, J., 2018. Cell-based therapy for Parkinson's disease: A journey through decades towards the light side of the Force. *European Journal of Neuroscience*.

Pfriem, A. et al., 2012. A modular, low-cost robot for zebrafish handling. In *2012 Annual International Conference of the IEEE Engineering in Medicine and Biology Society*. IEEE, pp. 980–983.

Pickel, V.M., Joh, T.H. & Reis, D.J., 1975. Immunohistochemical localization of tyrosine hydroxylase in brain by light and electron microscopy. *Brain research*, 85(2), pp.295–300.

Pisharath, H. et al., 2007. Targeted ablation of beta cells in the embryonic zebrafish pancreas using E. coli nitroreductase. *Mechanisms of Development*, 124(3), pp.218–229.

Poli, A. et al., 1990. Effect of 1-methyl-4-phenyl-1,2,3,6-tetrahydropyridine (MPTP) in goldfish brain. *Brain Research*, 534(1-2), pp.45–50.

Pollard, H.B. et al., 1992. A parkinsonian syndrome induced in the goldfish by the neurotoxin MPTP. *FASEB journal : official publication of the Federation of American Societies for Experimental Biology*, 6(12), pp.3108–16.

Van Praag, H. et al., 2002. Functional neurogenesis in the adult hippocampus. *Nature*, 415(6875), pp.1030–1034.

Ramachandran, R. et al., 2010. Conditional gene expression and lineage tracing of tuba1a expressing cells during zebrafish development and retina regeneration. *The Journal of comparative neurology*, 518(20), pp.4196–212.

Reimer, M.M. et al., 2013. Dopamine from the brain promotes spinal motor neuron generation during development and adult regeneration. *Developmental cell*, 25(5), pp.478–91.

Reimer, M.M. et al., 2008. Motor neuron regeneration in adult zebrafish. *The Journal of neuroscience : the official journal of the Society for Neuroscience*, 28(34), pp.8510–6.

Reimer, M.M. et al., 2009. Sonic hedgehog is a polarized signal for motor neuron regeneration in adult zebrafish. *The Journal of neuroscience : the official journal of the Society for Neuroscience*, 29(48), pp.15073–82.

Ren, G. et al., 2011. Disruption of LRRK2 Does Not Cause Specific Loss of Dopaminergic Neurons in Zebrafish M. R. Cookson, ed. *PLoS ONE*, 6(6), p.e20630.

Riachi, N.J. et al., 1988. On the mechanisms underlying 1-methyl-4-phenyl-1,2,3,6-tetrahydropyridine neurotoxicity. II. Susceptibility among mammalian species correlates with the toxin's metabolic patterns in brain microvessels and liver. *The Journal of pharmacology and experimental therapeutics*, 244(2), pp.443–8.

Riachi, N.J., LaManna, J.C. & Harik, S.I., 1989. Entry of 1-methyl-4-phenyl-1,2,3,6-tetrahydropyridine into the rat brain. *The Journal of pharmacology and experimental therapeutics*, 249(3), pp.744–8.

Rink, E. & Wullimann, M.F., 2002. Development of the catecholaminergic system in the early zebrafish brain: an immunohistochemical study. *Developmental Brain Research*, 137(1), pp.89–100.

Rolls, A. et al., 2007. Toll-like receptors modulate adult hippocampal neurogenesis. *Nature Cell Biology*, 9(9), pp.1081–1088.

Rothenaigner, I. et al., 2011. Clonal analysis by distinct viral vectors identifies bona fide neural stem cells in the adult zebrafish telencephalon and characterizes their division properties and fate. *Development (Cambridge, England)*, 138(8), pp.1459–69.

Ryu, S. et al., 2007. Orthopedia homeodomain protein is essential for diencephalic dopaminergic neuron development. *Current biology : CB*, 17(10), pp.873–80.

Sallinen, V. et al., 2010. Dopaminergic cell damage and vulnerability to MPTP in Pink1 knockdown zebrafish. *Neurobiology of disease*, 40(1), pp.93–101.

Sallinen, V. et al., 2009. MPTP and MPP+ target specific aminergic cell populations in larval zebrafish. *Journal of neurochemistry*, 108(3), pp.719–31.

Samaranch, L. et al., 2010. PINK1-linked parkinsonism is associated with Lewy body pathology. *Brain*, 133(4), pp.1128–1142.

Satou, C. et al., 2013. Transgenic tools to characterize neuronal properties of discrete populations of zebrafish neurons. *Development (Cambridge, England)*, 140(18), pp.3927–31.

Satou, C., Kimura, Y. & Higashijima, S., 2012. Generation of multiple classes of V0 neurons in zebrafish spinal cord: progenitor heterogeneity and temporal control of neuronal diversity. *The Journal of neuroscience : the official journal of the Society for Neuroscience*, 32(5), pp.1771–83.

Schindelin, J. et al., 2012. Fiji: an open-source platform for biological-image analysis. *Nature Methods*, 9(7), pp.676–682.

Schneider, J.S. & Markham, C.H., 1986. Neurotoxic effects of N-methyl-4-phenyl-1,2,3,6-tetrahydropyridine (MPTP) in the cat. Tyrosine hydroxylase immunohistochemistry. *Brain research*, 373(1-2), pp.258–67.

Schütze, S. et al., 1995. TNF-induced activation of NF-kappa B. *Immunobiology*, 193(2-4), pp.193–203.

Seri, B. et al., 2001. Astrocytes give rise to new neurons in the adult mammalian hippocampus. *The Journal of neuroscience : the official journal of the Society for Neuroscience*, 21(18), pp.7153–60.

Seri, B. et al., 2004. Cell types, lineage, and architecture of the germinal zone in the adult dentate gyrus. *Journal of Comparative Neurology*, 478(4), pp.359–378.

Shan, X. et al., 2006. Enhanced De Novo Neurogenesis and Dopaminergic Neurogenesis in the Substantia Nigra of 1-Methyl-4-phyenyl-1,2,3,6-Tetrahydropyridine-Induced Parkinson's Disease-Like Mice. *Stem Cells*, 24(5), pp.1280–1287.

Sheng, D. et al., 2010. Deletion of the WD40 domain of LRRK2 in Zebrafish causes Parkinsonism-like loss of neurons and locomotive defect. *PLoS genetics*, 6(4), p.e1000914.

Shiau, C.E. et al., 2015. Differential Requirement for irf8 in Formation of Embryonic and Adult Macrophages in Zebrafish Z. Wen, ed. *PLOS ONE*, 10(1), p.e0117513.

Shihabuddin, L.S., Ray, J. & Gage, F.H., 1997. FGF-2 Is Sufficient to Isolate Progenitors Found in the Adult Mammalian Spinal Cord. *Experimental Neurology*, 148(2), pp.577–586.

Silva, N.A. et al., 2014. From basics to clinical: a comprehensive review on spinal cord injury. *Progress in neurobiology*, 114, pp.25–57.

Sim, C.H. et al., 2006. C-terminal truncation and Parkinson's disease-associated mutations down-regulate the protein serine/threonine kinase activity of PTEN-induced kinase-1. *Human Molecular Genetics*, 15(21), pp.3251–3262.

Simola, N., Morelli, M. & Carta, A.R., 2007. The 6-hydroxydopamine model of Parkinson's disease. *Neurotoxicity research*, 11(3-4), pp.151–67.

Simone, B.W. et al., 2018. Fishing for understanding: Unlocking the zebrafish gene editor's toolbox. *Methods*.

Singh, S.P., Holdway, J.E. & Poss, K.D., 2012. Regeneration of amputated zebrafish fin rays from de novo osteoblasts. *Developmental cell*, 22(4), pp.879–86.

Sîrbulescu, R.F. & Zupanc, G.K.H., 2011. Spinal cord repair in regeneration-competent vertebrates: Adult teleost fish as a model system. *Brain Research Reviews*, 67(1-2), pp.73–93.

Skaggs, K., Goldman, D. & Parent, J.M., 2014. Excitotoxic brain injury in adult zebrafish stimulates neurogenesis and long-distance neuronal integration. *Glia*, 62(12), pp.2061–79.

Soares Godoy, R., 2015. CHEMOGENETIC ABLATION OF DOPAMINERGIC NEURONS IN THE BRAIN OF LARVAL AND ADULT ZEBRAFISH (DANIO RERIO): PHENOTYPES AND REGENERATIVE ABILITY.

Sofroniew, M. V., 2018. Dissecting spinal cord regeneration. *Nature*, 557(7705), pp.343–350.

Speciale, S.G., 2002. MPTP: Insights into parkinsonian neurodegeneration. *Neurotoxicology and Teratology*, 24(5), pp.607–620.

Spomer, W. et al., 2012. High-Throughput Screening of Zebrafish Embryos Using Automated Heart Detection and Imaging. *Journal of Laboratory Automation*, 17(6), pp.435–442.

Steinbeck, J.A. & Studer, L., 2015. Moving stem cells to the clinic: potential and limitations for brain repair. *Neuron*, 86(1), pp.187–206.

Stoker, T.B., Blair, N.F. & Barker, R.A., 2017. Neural grafting for Parkinson's disease: challenges and prospects. *Neural regeneration research*, 12(3), pp.389–392.

Sumanas, S. & Larson, J.D., 2002. Morpholino phosphorodiamidate oligonucleotides in zebrafish: a recipe for functional genomics? *Briefings in functional genomics & proteomics*, 1(3), pp.239–56.

Suzzi, S. et al., 2017. Loss Of lrrk2 Impairs Cell Proliferation And Neuronal Regeneration In The Zebrafish Brain. *bioRxiv*, p.140608.

Takamori, S. et al., 2000. Identification of a vesicular glutamate transporter that defines a glutamatergic phenotype in neurons. *Nature*, 407(6801), pp.189–94.

Takeda, A. et al., 2008. Adult neurogenesis with 5-HT expression in lesioned goldfish spinal cord. *Neuroscience*, 151(4), pp.1132–1141.

Tay, T.L. et al., 2011a. Comprehensive catecholaminergic projectome analysis reveals single-neuron integration of zebrafish ascending and descending dopaminergic systems. *Nature Communications*, 2, p.171.

Tay, T.L. et al., 2011b. Comprehensive catecholaminergic projectome analysis reveals single-neuron integration of zebrafish ascending and descending dopaminergic systems. *Nature communications*, 2, p.171.

Thirumalai, V. & Cline, H.T., 2008. Endogenous dopamine suppresses initiation of swimming in prefeeding zebrafish larvae. *Journal of neurophysiology*, 100(3), pp.1635–48.

Toda, H. et al., 2016. Update on Deep Brain Stimulation for Dyskinesia and Dystonia: A Literature Review. *Neurologia medico-chirurgica*, 56(5), pp.236–48.

Tsarouchas, T.M. et al., 2018. Dynamic control of proinflammatory cytokines Il-1β and Tnf-α by macrophages is necessary for functional spinal cord regeneration in zebrafish. *bioRxiv*, p.332197.

Turner, D. & Kearney, W., 1993. Scientific and Ethical Concerns in Neural Fetal Tissue Transplantation. *Neurosurgery*, 6(33), pp.1031–1037.

Underhill, D.M., 2003. Macrophage recognition of zymosan particles. *Journal of Endotoxin Research*, 9(3), pp.176–180.

Ungerstedt, U., 1968. 6-hydroxy-dopamine induced degeneration of central monoamine neurons. *European Journal of Pharmacology*, 5(1), pp.107–110.

Valente, E.M. et al., 2004. Hereditary early-onset Parkinson's disease caused by mutations in PINK1. *Science (New York, N.Y.)*, 304(5674), pp.1158–60.

Vijayanathan, Y. et al., 2017. 6-OHDA-Lesioned Adult Zebrafish as a Useful Parkinson's Disease Model for Dopaminergic Neuroregeneration. *Neurotoxicity Research*, pp.1–13.

Wehner, D. et al., 2017. Wnt signaling controls pro-regenerative Collagen XII in functional spinal cord regeneration in zebrafish. *Nature Communications*, 8(1), p.126.

Weinreb, O. & Youdim, M.B.H., 2007. A model of MPTP-induced Parkinson's disease in the goldfish. *Nature Protocols*, 2(11), pp.3016–3021.

Weiss, S. et al., 1996. Multipotent CNS stem cells are present in the adult mammalian spinal cord and ventricular neuroaxis. *The Journal of neuroscience : the official journal of the Society for Neuroscience*, 16(23), pp.7599–609.

Westerfield, M., 2000. The Zebrafish Book, 5th Edition; A guide for the laboratory use of zebrafish (Danio rerio). *Eugene, University of Oregon Press*, p.2000.

White, Y.A.R., Woods, D.C. & Wood, A.W., 2011. A transgenic zebrafish model of targeted oocyte ablation and de novo oogenesis. *Developmental Dynamics*, 240(8), pp.1929–1937.

Wilson, S.G. et al., 2016. Tracking the fate of her4 expressing cells in the regenerating retina using her4:Kaede zebrafish. *Experimental eye research*, 145, pp.75–87.

Winner, B. et al., 2002. Long-term survival and cell death of newly generated neurons in the adult rat olfactory bulb. *The European journal of neuroscience*, 16(9), pp.1681–9.

Xi, Y. et al., 2010. Impaired dopaminergic neuron development and locomotor function in zebrafish with loss of *pink1* function. *European Journal of Neuroscience*, 31(4), pp.623–633.

Xi, Y. et al., 2011. Transgenic zebrafish expressing green fluorescent protein in dopaminergic neurons of the ventral diencephalon. *Developmental dynamics : an official publication of the American Association of Anatomists*, 240(11), pp.2539–47.

Yang, Y. et al., 2006. Mitochondrial pathology and muscle and dopaminergic neuron degeneration caused by inactivation of Drosophila Pink1 is rescued by Parkin. *Proceedings of the National Academy of Sciences*, 103(28), pp.10793–10798.

Yeo, S.-Y. et al., 2007. Fluorescent protein expression driven by her4 regulatory elements reveals the spatiotemporal pattern of Notch signaling in the nervous system of zebrafish embryos. *Developmental biology*, 301(2), pp.555–67.

Yokogawa, T., Hannan, M.C. & Burgess, H.A., 2012. The dorsal raphe modulates sensory responsiveness during arousal in zebrafish. *The Journal of neuroscience : the official journal of the Society for Neuroscience*, 32(43), pp.15205–15.

Youdim, M.B.H. et al., 1992. MPTP-induced “Parkinsonism” in the goldfish. *Neurochemistry International*, 20, pp.275–278.

Zhang, R. et al., 2013. In vivo cardiac reprogramming contributes to zebrafish heart regeneration. *Nature*, 498(7455), pp.497–501.

Zhao, M. et al., 2003. Evidence for neurogenesis in the adult mammalian substantia nigra. *Proceedings of the National Academy of Sciences of the United States of America*, 100(13), pp.7925–30.

Zhou, W. & Hildebrandt, F., 2012. Inducible podocyte injury and proteinuria in transgenic zebrafish. *Journal of the American Society of Nephrology : JASN*, 23(6), pp.1039–47.

Zupanc, G.K., 2001. Adult neurogenesis and neuronal regeneration in the central nervous system of teleost fish. *Brain, behavior and evolution*, 58(5), pp.250–75.

Zupanc, G.K.H., 2009. Towards brain repair: Insights from teleost fish. *Seminars in Cell & Developmental Biology*, 20(6), pp.683–690.

Zupanc, G.K.H., Hinsch, K. & Gage, F.H., 2005. Proliferation, migration, neuronal differentiation, and long-term survival of new cells in the adult zebrafish brain. *The Journal of comparative neurology*, 488(3), pp.290–319.

Zupanc, G.K.H. & Sîrbulescu, R.F., 2011. Adult neurogenesis and neuronal regeneration in the central nervous system of teleost fish. *European Journal of Neuroscience*, 34(6), pp.917–929.